

AD-A037 860

UNIVERSITY COLL LONDON (ENGLAND) DEPT OF PHYSICS AND--ETC F/G 4/1  
DETERMINATION OF AIR DENSITY, TEMPERATURE AND WINDS AT HIGH ALT--ETC(U)  
JAN 77 G V GROVES

UNCLASSIFIED

AFGL-TR-77-0068

NL

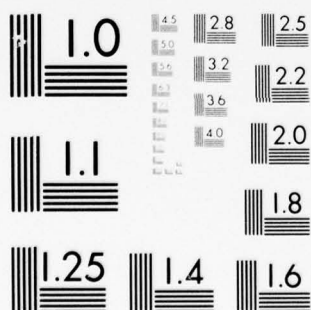
1 OF 2  
AD  
A037860



OF

2

037860



MICROCOPY RESOLUTION TEST CHART  
NATIONAL BUREAU OF STANDARDS-1963-A



ADA037860

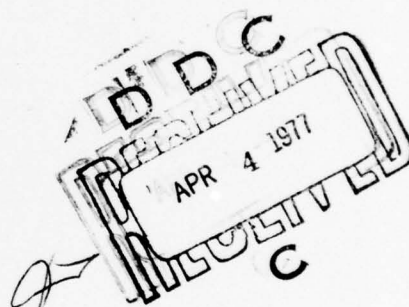
AFGL-TR-77-0068

12

DETERMINATION OF AIR DENSITY, TEMPERATURE AND WINDS AT HIGH ALTITUDE

G. V. Groves  
Department of Physics and Astronomy,  
University College London,  
Gower Street, London WC1E 6BT,  
England.

31 January 1977



Final Report, 1 February 1972 - 31 December 1976

Approved for public release; distribution unlimited.

Prepared for:

Air Force Geophysics Laboratory,  
L.G. Hanscom Field, Bedford, Massachusetts 01730, USA.

and

European Office of Aerospace Research and Development,  
London, England.

COPY AVAILABLE TO DDC PERMIT FULLY LEGIBLE PROTECTION

COPY AVAILABLE TO DDC PERMIT FULLY LEGIBLE PROTECTION

ADU NO. \_\_\_\_\_  
DDC FILE COPY

UNCLASSIFIED

SECURITY CLASSIFICATION OF THIS PAGE (When Data Entered)

19 REPORT DOCUMENTATION PAGE		READ INSTRUCTIONS BEFORE COMPLETING FORM	
1. REPORT NUMBER	2. GOVT ACCESSION NO.	3. RECIPIENT'S CATALOG NUMBER	
18 AFGL-TR-77-0068		9	
4. TITLE (and Subtitle)	5. TYPE OF REPORT & PERIOD COVERED		
6 DETERMINATION OF AIR DENSITY, TEMPERATURE AND WINDS AT HIGH ALTITUDE.	FINAL REPORT. 1 Feb 1972 - 31 Dec 1976		
7. AUTHOR(s)	8. CONTRACT OR GRANT NUMBER(s)		
10 GERALD V. GROVES	AFOSR 72-2264		
9. PERFORMING ORGANIZATION NAME AND ADDRESS	10. PROGRAM ELEMENT, PROJECT, TASK AREA & WORK UNIT NUMBERS		
DEPARTMENT OF PHYSICS AND ASTRONOMY UNIVERSITY COLLEGE LONDON GOWER STREET, LONDON, WC1E 6BT, ENGLAND	61102F 8605-10-01		
11. CONTROLLING OFFICE NAME AND ADDRESS	12. REPORT DATE	13. NUMBER OF PAGES	
AIR FORCE GEOPHYSICS LABORATORY, L.G. HANSCOM FIELD, BEDFORD, MA, MASSACHUSETTS 01730, USA.	11 31 Jan 1977	9	
14. MONITORING AGENCY NAME & ADDRESS (if different from Controlling Office)	15. SECURITY CLASS. (of this report)		
EUROPEAN OFFICE OF AEROSPACE RESEARCH AND DEVELOPMENT, BOX 14, FPO, NEW YORK 09510, USA	UNCLASSIFIED		
16. DISTRIBUTION STATEMENT (of this Report)		15a. DECLASSIFICATION/DOWNGRADING SCHEDULE	
THIS DOCUMENT HAS BEEN APPROVED FOR PUBLIC RELEASE AND SALE; ITS DISTRIBUTION IS UNLIMITED.			
17. DISTRIBUTION STATEMENT (of the abstract entered in Block 20, if different from Report)			
15 ✓ AF-AFOSR-2264-72			
16 8605 17 10			
18. SUPPLEMENTARY NOTES			
19. KEY WORDS (Continue on reverse side if necessary and identify by block number)			
TROPOSPHERE, STRATOSPHERE, MESOSPHERE, TIDAL OSCILLATIONS.			
20. ABSTRACT (Continue on reverse side if necessary and identify by block number)			
<p>The research performed is described in ten papers published by the Principal Investigator <del>between January 1973 and January 1977</del> on the subjects of tidal and quasi-biennial oscillations. The report includes copies of these papers and a review of the analyses which have been carried out on the observation and theory of tidal oscillations and the conclusions reached.</p>			

DD FORM 1 JAN 73 1473

EDITION OF 1 NOV 65 IS OBSOLETE

UNCLASSIFIED

SECURITY CLASSIFICATION OF THIS PAGE (When Data Entered)

361070

YB

ACCESSION for	
NTIS	White Section <input checked="" type="checkbox"/>
DOC	Buff Section <input type="checkbox"/>
UNANNOUNCED	<input type="checkbox"/>
JUSTIFICATION	
BY	
DISTRIBUTION/AVAILABILITY CODES	
DIST.	MAIL ROOM/SPECIAL

*PA*

Qualified requestors may obtain additional copies from the Defense Documentation Center. All others should apply to the National Technical Information Service.

Determination of air density, temperature and wind  
at high altitude

1. Tidal oscillations

On a global scale the Earth's atmosphere may be regarded as a thin spherical shell of rotating fluid capable of periodic oscillations. Few opportunities arise for studying the dynamic response of this system to a given excitation apart from tidal excitations by the Sun or Moon. Gravitational excitation has the advantage that the source function is accurately known, whereas thermal excitation can only be approximately calculated and is subject to change with changes in the distribution of the absorbing gases, notably water vapour. Attention must primarily be given to thermal sources as they excite oscillations that exceed gravitationally excited ones by more than an order of magnitude.

Over many years barometric pressure has provided the main observational data on the atmospheric response at the various tidal component frequencies. In spite of sparse data in ocean areas, it has been possible to compile global distributions of average surface-pressure amplitudes and phases (the time of maximum value) and sometimes of their seasonally averaged values. These investigations leave the vertical structure of the response virtually unexplored, as pressure only gives a measure of the integrated gas density in a vertical column.



With increasing height, amplitudes of tidal oscillations may be expected to increase to compensate for the decrease of density. At the meteor ionization level of 80 to 100 km, tidal components are found to be responsible for the main wind variation. As a consequence of the larger amplitudes, periodic components may be derived from a shorter time series of data extending over perhaps no more than a few cycles.

The possibility of deriving tidal oscillations from a limited time series of data has brought into consideration the use of rocket techniques for which costs severely limit the sampling frequency. The potential advantage offered by rockets is that of good height resolution over a wide altitude range. Wind and temperature measurements may be obtained up to 85 km by the grenade technique and up to about 60 km by meteorological rocket-sondes. The possibility therefore arises of examining the vertical structure of oscillations at stratospheric and mesospheric levels and of making comparisons with values calculated by tidal theory.

Analyses have been carried out under three headings :

- (1) Derivation of diurnal and semidiurnal wind and temperature components from rocket data [1 to 4]
- (2) Calculation of the vertical properties of tidal oscillations generated by assumed heat sources [5, 6]
- (3) Comparisons between observed and theoretical components of oscillation [7, 8].

The first series of data to be analysed was the grenade series from Natal ( $6^{\circ}\text{S}$ ) [1, 2]. The analysis began as an exploratory exercise as the distribution of observing times was rather poor. Residuals of the least-squares fit were analysed and standard deviations were obtained which indicated that amplitudes and phases had been derived with some measure of significance. The appearance in the 24 hourly component of a phase change with height corresponding closely with the theoretical value for the (1,1) Hough mode was evidence that part of a global oscillation was being resolved. Observed phases were however a few hours later than values calculated for the (1,1) mode with assumed tropospheric and stratospheric heat sources, and particular attention has been given to the investigation of this difference by the analysis of further observational data and the detailed calculation of tidal fields. At present no satisfactory explanation for the difference can be given.

When a second set of grenade data became available, this time for Kourou whose latitude ( $5^{\circ}\text{N}$ ) is very similar to that of Natal but in the opposite hemisphere, analysis of 24 hourly wind components gave phases in good agreement with those at Natal [3]. Temperature phases however changed more rapidly with height above 60 km having a gradient which corresponded quite closely with the theoretical value for the (1,2) Hough mode thereby indicating the presence of an equatorially asymmetric component of oscillation.

The presence of (1,2), (1,3) and higher order diurnal Hough

modes has been indicated by the gradients of phase with height observed below 60 km in diurnal series of meteorological rocket launchings at a number of mid and low latitude sites [4]. The source of excitation is considered to be tropospheric water vapour heating and the variations in its distribution that arise as a consequence of tropospheric dynamics. Although no direct relationship has been established between watervapour distribution and the tidal patterns, it is expected that excitation of the (1,1) mode is fairly insensitive to the water vapour variations whereas the higher modes on account of their more rapidly changing horizontal structure, as expressed for example by their Hough functions, are variously excited at different times according to the water vapour distribution. The vertical distribution of a heat source is also a factor upon which the excitation of a particular mode depends, and an analysis of semidiurnal components indicates that this may be more critical than the horizontal distribution. Thus at low latitudes theory shows that the (2,7), (2,8) Hough functions closely match the (1,2), (1,3), whereas observed changes of phase with height in semidiurnal components correspond not with the (2,7), (2,8) but with modes in the region of (2,16). Such modes correspond to the (1,2), (1,3) in terms of their equivalent depths and hence would be excited by heat sources of similar vertical structure.

According to tidal theory the diurnal (1,1), (1,2), ... modes

are confined to low and mid latitudes whereas the higher order semidiurnal modes would propagate at all latitudes. A few sets of stratospheric data from high latitude stations are available and illustrate quite well the presence of propagating semidiurnal modes and the absence of propagating diurnal modes; a diurnal oscillation at high latitude comprising of stratospherically excited trapped modes. At all latitudes, stratospheric semidiurnal oscillations are considered to be strongly influenced by the tropospheric distribution of water vapour and the detailed variations in this distribution which give rise to the generation of high order modes.

By tidal theory the nature of semidiurnal horizontal wind components at high latitude may be simply described as at any height the horizontal wind vector remains approximately constant in magnitude and rotates clockwise in the N. hemisphere and anticlockwise in the S. hemisphere whatever superposition of different modes may be present. Data are available for only a few high latitude sites and unfortunately stratospheric semidiurnal wind magnitudes are small (just a few m/s), but the results obtained are largely in agreement with the theoretical expectation. Such agreement supports the view that the oscillations which are resolved from these short time series of data are of global extent.

Calculations of the vertical properties of tidal oscillations generated by assumed heat sources have been undertaken using the equations of classical tidal theory. The theory neglects



non-linearities and molecular and eddy transport processes and therefore becomes invalid at sufficiently great heights, say at about 90 km according to the details of the calculation. Other assumptions are involved and the theory may not be valid at lower heights, but against these possible shortcomings, a useful description of tidal fields is obtained in terms of separable dependences of latitude and height for prescribed modes of oscillation. Attention has been given to the vertical properties of diurnal and semidiurnal components [5] by the introduction of weighting functions whose application to given tropospheric and stratospheric heat sources leads to an evaluation of the surface pressure oscillation. Such weighting functions provide a simple means of assessing the contribution of heat sources at various levels to the surface pressure oscillation. Another weighting function has been introduced which weights the heat source at any height according to the atmospheric response that it generates at greater heights. These calculations have been extended to obtain the energy fluxes propagating upwards in the (1,1) and (1,3) Hough modes [6]. It is found that tropospheric and stratospheric heat sources excite the (1,1) mode in opposite phases and, as a result of the cancellation produced, the net oscillation and associated energy flux may be particularly sensitive to the individual tropospheric and stratospheric excitations. Attention has therefore been given to the detailed evaluation of the (1,1) modes of tropospheric and stratospheric heating and it is reckoned in these calculations that 38% of the tidal amplitude arising from

the tropospheric excitation is cancelled out by the stratospheric excitation. The energy flux depends on (amplitude)<sup>2</sup> and is correspondingly reduced below what would arise from tropospheric excitation alone. On account of the meridional shift in the global distribution of water vapour into the summer hemisphere a slight reduction at the solstices is to be expected in the (1,1) tropospheric excitation with a possible semi-annual modulation of the tidal energy flux entering the thermosphere. Calculations have shown however that the reduction in January is largely offset by the shorter Sun-Earth distance, while the reduction in July is enhanced. Although more detailed calculations are required, it would appear that the well-known deeper minimum in thermospheric air densities in July compared with January may be accounted for in this way.

As mentioned above, observed diurnal oscillations at Natal and Kourou were found to maximize later by a few hours than those calculated by theory for assumed tropospheric and stratospheric heat sources. A time difference of 3.6 hours was found between the Natal observations and tides calculated for the same latitude (5.9°S) and a maximum heating rate at local noon [7]. In attempting to account for this difference, alternative assumptions have been introduced for the time of maximum heating [8]. The difference could readily be removed by taking the tropospheric heating rate to maximize at 13.3 has instead of 12 noon, but the (1,1) mode of

surface pressure oscillation would likewise be delayed and would then disagree with the observed surface pressure phase. A way of obtaining agreement with both the surface pressure and upper atmosphere data would be to assume that the heating was delayed in the upper troposphere and advanced in the lower troposphere. In the absence of any identifiable process that would give rise to such a variation, no satisfactory explanation for the difference between the observed and calculated upper atmosphere phases can yet be given.

## 2. List of Publications

- (1) Groves, G. V. 1974 'An analysis of grenade-experiment winds and temperatures at Natal ( $6^{\circ}\text{S}$ ) for diurnal and seasonal components', J. Brit. Interplan. Soc. vol.27, pp. 499-511.
- (2) Groves, G. V. 1975 'Diurnal and semidiurnal oscillations of the upper atmosphere derived from grenade experiments at Natal, Brazil', J. atmos. terr. Phys. vol.37, pp. 1133-1138.
- (3) Groves, G. V. 1975 'A comparison of 24-hourly atmospheric oscillations derived from grenade experiments at two low latitude sites', J. Brit. Interplan. Soc. Vol.28, pp.241-244.
- (4) Groves, G. V. 1976 'Rocket studies of atmospheric tides', Proc. Roy. Soc. vol.351 A, pp.437-469.
- (5) Groves, G. V. 1975 'Latitude and height dependences of solar atmospheric tides', J. Brit. Interplan. Soc. vol.28, pp. 797-809.

- (6) Groves, G. V. 1977 'Energy fluxes propagated by diurnal oscillations in the upper atmosphere', J. Brit. Interplan. Soc. vol.30, pp. 32-36.
- (7) Groves, G. V. 1975 'Calculated and observed 24-hourly oscillations of the upper atmosphere at  $5.9^{\circ}\text{S}$  latitude', J. Brit. Interplan. Soc. vol.28, pp.127-133.
- (8) Groves, G. V. 1975 'Propagating modes of the 24-hourly atmospheric tide derived from Natal ( $5.9^{\circ}\text{S}$ ) grenade experiments and global barometric oscillations', Space Research XV, pp.181-189.
- (9) Groves, G. V. 1973 'Zonal wind quasi-biennial oscillations at 25-60 km altitude, 1962-69', Quart. J. Roy. Met. Soc. vol.99, pp. 73-81.
- (10) Groves, G. V. 1975 'Meridional wind quasi-biennial oscillations at 25-60 km altitude, 1962-1969', J. atmos. terr. Phys. vol.37, pp. 1469-1475.



## AN ANALYSIS OF GRENADE-EXPERIMENT WINDS AND TEMPERATURES AT NATAL (6°S) FOR DIURNAL AND SEASONAL COMPONENTS

G. V. GROVES

*Department of Physics and Astronomy, University College London, England.*

Twenty-four grenade experiments carried out in the years 1966-68 are analysed for diurnal and seasonal components at 35-90 km. Results are presented as amplitudes and phases and as time cross-sections in local time and month. The main component of diurnal variation above 60 km is identified as the principal propagating mode with a vertical wavelength of about 31 km. R.m.s. values of the residuals and their variation with height are also discussed.

### 1. INTRODUCTION

IN THE YEARS 1966-68, 24 launchings of Nike-Cajun sounding rockets with grenade payloads were carried out by NASA at Natal, Brazil (6°S, 35°W) as part of the GSFC Meteorological Sounding Rocket Program. Each payload carried 19 grenades, permitting temperatures and winds to be measured at heights between 35 and 95 km with an average vertical resolution of about 3 km [1,2,3].

The data from these launchings have already been used in conjunction with data from 10 grenade and pitot tube experiments at Ascension Island (8°S) to construct seasonal cross-sections of temperature and of meridional and zonal winds for low latitudes [4]. No attempt was made to allow for tidal components either theoretically, because of uncertainties involved in the theory, or observationally. However, tidal and other relatively short-term variations were removed to some extent by the averaging procedures adopted. The distribution of local times of launch was helpful in this respect.

The hourly distribution of launch times for the 24 Natal grenade launchings is shown in Table 1. Although the distribution is not ideally uniform, observations

TABLE 1. Hourly distribution of launch times.

No. of launchings	Local time (hr)													
	00-02	02-04	04-06	06-08	08-10	10-12	12-14	14-16	16-18	18-20	20-22	22-24		
	0	1	2	3	3	3	0	2	0	2	3	5		

extend over a sufficient range of local times to indicate that a formal analysis for diurnal components may give significant results. The procedure followed in this paper is to analyse the Natal data simultaneously for diurnal and seasonal components at heights between 35 and 95 km. Such an analysis involving the simultaneous determination of diurnal and seasonal components does not appear to have been attempted previously.

### 2. SEASONAL AND DIURNAL CHARACTERISTICS OF THE UPPER ATMOSPHERE AT LOW LATITUDE

A low-latitude site has advantages for the resolution of diurnal and seasonal

G. V. Groves

components:

- (i) Certain diurnal modes (the propagating modes) theoretically maximize at the equator and should be more readily detected at latitudes lower than about  $30^\circ$ .
- (ii) Seasonal changes in tidal components can be expected to be small at low latitudes.
- (iii) Month-by-month variations are more regular and can therefore be more readily modelled at low latitudes than at higher latitudes, where winter-time disturbances occur.

The monthly distribution of launch times is shown in Table 2. Although the

TABLE 2. Monthly distribution of launch times.

	Month											
	J	F	M	A	M	J	J	A	S	O	N	D
No. of launchings	0	0	3	0	2	3	0	5	0	8	0	3

distribution is far from ideal, it would appear just adequate to cover the main seasonal variations.

The relative importance of diurnal and seasonal components may be appreciated by comparisons between available reference atmospheres [5] for the seasonal components and the calculations of Lindzen for the diurnal components [6]. The seasonal temperature variation at low latitude increases up to  $15^\circ\text{C}$  at 90 km and is comparable with the diurnal amplitude at most heights. The seasonal and diurnal variations of zonal wind speeds are comparable at 90 km, but at lower heights the seasonal changes exceed the diurnal ones. At 40-55 km the total seasonal change is 70-90 m/s, which exceeds the diurnal variation by an order of magnitude.

### 3. METHOD OF ANALYSIS

Profiles of temperature, W-E and S-N wind components [1,2,3] were first interpolated at 1 km height intervals. Wind components to the east and to the north were taken as positive. Twentyfour values of each parameter,  $V_{\text{Obs}}$ , were available at all heights except near 35 and 95 km, where the number was slightly less. In the case of temperature and W-E wind components, CIRA models [5] were used to interpolate  $V_{\text{model}}$ , a value of the parameter for the particular date of launch. In the case of W-E wind components,  $V_{\text{model}}$  also included a contribution for the QBO, calculated from the formula given in CIRA [5], as values could exceed 10 m/s between 35 and 40 km.

The method of least squares was used to fit the form

$$f(t, M) = A_0 + A_1 \cos \frac{\pi t}{12} + A_2 \sin \frac{\pi t}{12} + A_3 \cos \frac{\pi t}{6} + A_4 \sin \frac{\pi t}{6} \\ + A_5 \cos \frac{\pi M}{6} + A_6 \sin \frac{\pi M}{6} + A_7 \cos \frac{\pi M}{3} + A_8 \sin \frac{\pi M}{3} \quad (1)$$

to the 24 (or slightly less) values of  $V_{\text{Obs}} - V_{\text{model}}$ , where  $V_{\text{Obs}}$  is an observed value,  $A_0, \dots, A_8$  are nine unknowns,  $t$  is local time and  $M$  is the date in months and decimal months reckoned from 1 January as 0.0. The amplitudes and phases

of the 24 hourly, 12 hourly, 12 monthly and 6 monthly components were calculated along with estimates of their standard deviations and those of  $A_0, \dots, A_8$ .

The calculation was repeated with (i) no diurnal terms (i.e.  $A_1$  to  $A_4 = 0$ ) and (ii) no seasonal terms (i.e.  $A_5$  to  $A_8 = 0$ ). Comparisons were made to see whether the seasonal terms calculated in (i) and the diurnal terms calculated in (ii) differed significantly from those found in the original simultaneous calculation of seasonal and diurnal components. In certain limited height regions, 12 hourly and 12 monthly wind components were found to be significantly increased by the inclusion of the other. At these heights their simultaneous resolution was considered unrealistic using the data sample available and they were therefore calculated separately (section 5). Temperature components and all 24 hourly and 6 monthly components passed the test. Similar checks were carried out by setting other combinations of the  $A$ 's to zero and solving for the remaining ones. Although slightly different results were obtained, the differences were not significant in relation to the magnitudes of the calculated standard deviations. It was therefore concluded that with the data available it was realistic to simultaneously evaluate the nine unknowns in Eqn. 1, except in certain limited height regions (section 5).

Another point to consider is whether a value calculated for an unknown at a particular height is significantly different from zero. Amplitudes have been calculated (see below) which differ from zero by amounts less than their estimated standard deviations, indicating with high probability that the determination is not significantly different from zero. No steps were taken to set such unknowns to zero and re-evaluate the others as (i) the situation arose only in certain limited height regions and (ii) the effect of setting certain unknowns to zero had already been investigated and found to be insignificant (even when the unknowns set to zero were significantly non-zero!).

The results presented in this paper were obtained by the least-squares solution of Eqn. 1, with equal weighting of the observations. At first calculations were carried out with the observations weighted according to the observational errors reported by the experimenters. At a few heights the unknowns were determined with improved accuracy, i.e. smaller standard deviations, but at most heights the accuracy was considerably reduced by weighting. This rather surprising result was attributed to the wide range of values reported for the observational errors (sometimes they differed by a factor of ten at the same height) resulting in certain values being too heavily discounted.

All results reported in this paper have been derived from observational data at constant height levels (spaced 1 km apart). At an early stage, similar calculations were carried out with observational data interpolated at constant pressure levels. As the accuracy of the results obtained was not significantly different, it was decided to use constant height levels for convenience.

#### 4. THE 24 HOURLY COMPONENTS

Amplitudes are shown in Fig. 1 and phases in Fig. 2. Each horizontal line is centred at the calculated result and its length is twice the standard deviation associated with this value. A short vertical line is introduced to indicate the centre point when the horizontal line goes off scale.

Below 55 km temperature amplitudes are small, being less than  $2^\circ\text{C}$ . Such values are considerably less than those which have been reported from meteorological rocket measurements (about  $10^\circ\text{C}$ ) and are close to the magnitudes predicted by theory [6]. Fig. 1 shows that amplitudes of  $10^\circ\text{C}$  are first reached near to 80 km and that amplitudes increase to  $30^\circ\text{C}$  just above 90 km.

On classical tidal theory SN wind components due to equatorially symmetric diurnal heating are themselves asymmetric with respect to the equator where zero amplitudes occur. It may therefore seem surprising that, at just  $6^\circ$  latitude, SN tidal components can be resolved with magnitudes which may exceed WE components at certain heights. For propagating modes of the 24 hourly oscillation, the theoretical variation of SN tidal amplitudes with latitude is very rapid

G. V. Groves

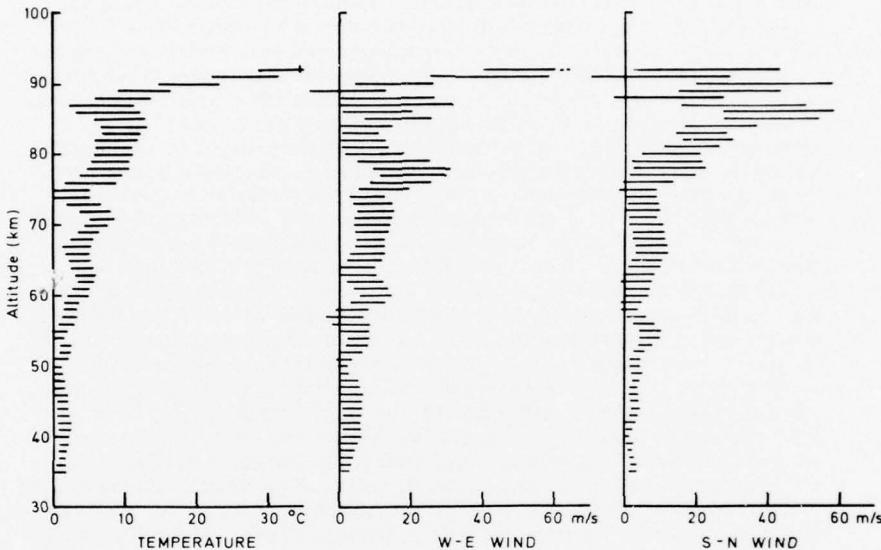


Fig. 1. Diurnal amplitudes.

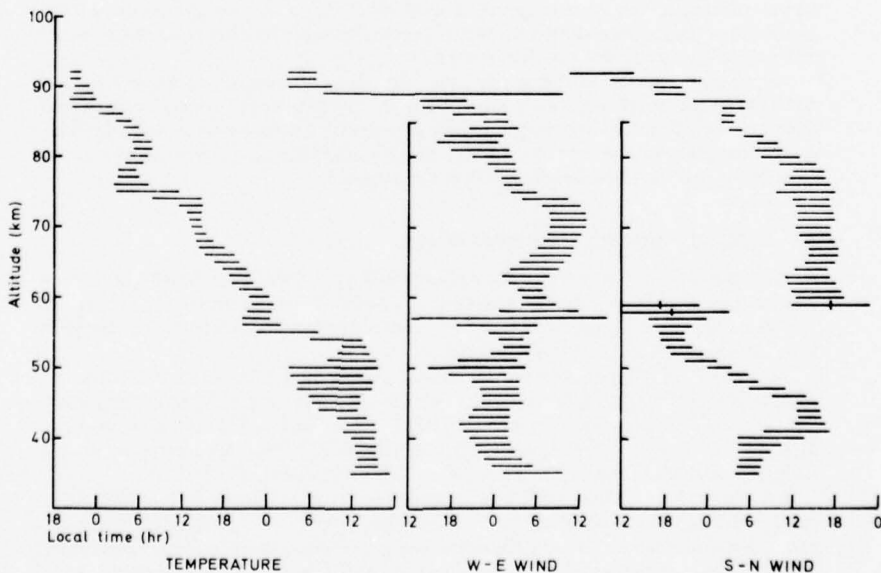


Fig. 2. Diurnal phases.



close to the equator and the magnitude of observations is indeed reasonable. Both WE and SN components reach about 30 m/s close to 90 km above which level accuracy rapidly decreases.

A notable feature of the temperature phase (Fig. 2) is its fairly uniform decrease with height, the mean gradient being about 31 km per 24 hours. The oscillation therefore has a vertical wavelength of 31 km, a value which corresponds closely with that of the principal propagating (1, 1) mode of the 24 hourly tide. Above 80 km, the SN phase changes by 24 hours in about 12 km, a value which corresponds closely with the vertical wavelength of the (1, 3) mode.

From classical tidal theory it can be shown that, if only one mode is present,

$$\text{Phase of SN component} = \text{Phase of WE component} \pm 6 \text{ hr}$$

where, for the (1, 1) or (1, 3) modes, the + sign holds for the S hemisphere and the - sign for the N hemisphere. Comparison between the profiles of WE and SN phase in Fig. 2 shows that this result with the + sign is well supported above 60 km, providing evidence for the predominance of the (1,1) mode or possibly the (1, 3) mode above 80 km.

## 5. THE 12 HOURLY COMPONENTS

Amplitudes are shown in Fig. 3 and are generally less accurately determined than the 24 hourly magnitudes (Fig. 1). In fact, at many heights, the values are not significantly different from zero.

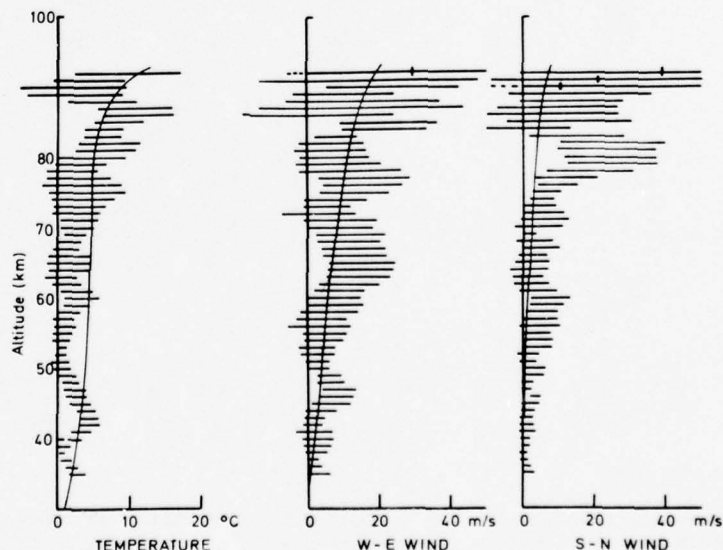


Fig. 3. Semi-diurnal amplitudes with theoretical curves [7, 8].

Small SN amplitudes are to be expected because the latitude is only  $6^\circ$  and the semidiurnal component, unlike the diurnal, does not increase rapidly on moving away from the equator. The curve of Fig. 3 is a theoretical one, interpolated for  $6^\circ$  latitude, from the calculations of Chapman and Lindzen [7]. The observations are consistent with the curve except possibly near 80 km. However, even here the

G. V. Groves

values of 25 m/s are still within  $1\frac{1}{2}$  standard deviations of the curve. At most heights the observed values exceed the calculated ones slightly.

Similar comparisons between temperature and WE wind observations and theory are shown in Fig. 3. The theoretical curves were calculated [7, 8] for the equator but would not be very different at  $6^\circ\text{S}$ . At most heights the observed temperature amplitudes are less than the calculated ones. For WE winds the comparison is closest with roughly equal numbers of observed values falling on either side of the curve.

In certain height regions the semidiurnal components could not be satisfactorily resolved simultaneously with the seasonal components and accordingly the latter were omitted when calculating the former. The regions concerned were 73-83 km for WE winds and 47-55 km and 63-76 km for SN winds.

## 6. THE $A_0$ TERMS

Fig. 4 shows the results obtained for  $A_0$ . For SN winds  $V_{\text{model}} = 0$  and  $A_0$  represents the component of prevailing flow. At most heights this is not significantly different from zero: the difference exceeds  $2\sigma$  only in the region of 50 km where northerly flow of less than 4 m/s is indicated.

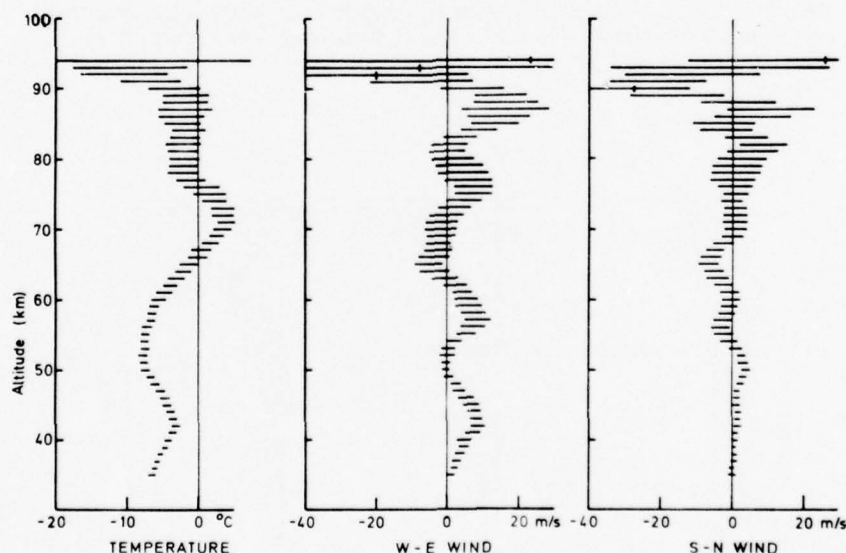


Fig. 4. Values of  $A_0$

For temperature and WE winds  $V_{\text{model}} \neq 0$  and  $A_0$  represents the difference between prevailing components as measured in the atmosphere and as calculated for the model. The most significant deviations from zero are in temperature between 35 and 65 km (up to  $7^\circ\text{C}$ ). At 50 km and below the CIRA temperature models are based predominantly on MRN measurements mostly taken within a few hours of local noon. Diurnal effects are too small (Fig. 1) to account for the difference and a bias is indicated between the MRN and grenade measuring techniques, the MRN (daytime) values being several  $^\circ\text{C}$  higher than the grenade values.

For WE winds significant departures of  $A_0$  from zero are found at the lower heights and amount to at most 9 m/s. This difference may be due to longitudinal

variations in the WE flow between Natal and Ascension Is. ( $8^{\circ}\text{S}$ ,  $14^{\circ}\text{W}$ ) as it is this latter site which provided the main input of data to the CIRA model at low S latitudes below 60 km. Above 60 km  $A_0$  does not differ significantly from zero indicating consistency between observations and the model with regard to the prevailing component.

## 7. TIME CROSS-SECTIONS OF TEMPERATURE AND WIND AT NATAL

Seasonal and diurnal time cross-sections, defined by

$$V_{\text{diurnal}} = A_1 \cos \frac{\pi t}{12} + A_2 \sin \frac{\pi t}{12} + A_3 \cos \frac{\pi t}{6} + A_4 \sin \frac{\pi t}{6} \quad (2)$$

$$V_{\text{seasonal}} = V_{\text{CIRA}} + A_0 + A_5 \cos \frac{\pi M}{6} + A_6 \sin \frac{\pi M}{6} + A_7 \cos \frac{\pi M}{3} + A_8 \sin \frac{\pi M}{3} \quad (3)$$

have been calculated for  $t = 0, 2, \dots, 22$  hr L.T. and  $M = 0, 1, \dots, 11$ , i.e. the first day of each month, and are shown in Figs. 5 and 6. The values of  $A_0, \dots, A_8$  are those upon which Figs. 1 to 4 are based. For SN winds  $V_{\text{CIRA}} = 0$  and for temperatures and WE winds it is the value interpolated from CIRA [5] for the latitude of Natal and the appropriate value of  $M$ .

### 7.1 Diurnal cross-sections (Fig. 5)

Patterns of diurnal variations in upper atmosphere temperatures and winds have previously been constructed from multiple rocket launchings within a 24 hour period and from meteor radar observations. General characteristics of such plots are the detailed nature of the variations from which a downward propagation of phase can often be picked out, i.e. contour patterns move downwards to the right. The contour diagrams in Fig. 5 show similar characteristics, and it may be noted that only diurnal and semidiurnal components have been used in their calculation (Eqn. 2).

If temperature differences of  $\pm 5^{\circ}\text{C}$  are considered significant in any large-scale synoptic study, then Fig. 5 shows that variations with local time should not be ignored above about 45 km. For winds, the diurnal contribution will generally exceed 5 m/s above 45 km. If temperature differences are considered significant when exceeding  $\pm 10^{\circ}\text{C}$ , variations with local time should not be ignored above 80 km.

### 7.2 Seasonal cross-sections (Fig. 6)

Fig. 6 shows that temperatures in the stratosphere and mesosphere are fairly uniform throughout the year, changes at the stratopause being less than  $10^{\circ}\text{C}$ . Above 65 km annual and semi-annual components are apparent and the total variation may reach  $30^{\circ}\text{C}$ . The mesopause is well-defined from December to March and close to 85 km, but for other months there is a double minimum, the upper mesopause being the colder and located above 90 km from June to September.

Harmonic analysis of the WE winds from Fig. 6 into mean + annual + semi-annual components gives the results shown in Fig. 7 (upper diagrams). A strong semi-annual oscillation in the equatorial upper stratosphere with amplitudes exceeding 30 m/s has previously been pointed out by Reed [9]. This oscillation is in the region R in Fig. 7. Above 60 km annual and semi-annual components of WE winds have previously been presented as meridional cross-sections from 0 to  $80^{\circ}\text{N}$  latitude [10]. Max 1, Min 1 and Min 2 in Fig. 7 are features which are traced to higher latitudes in Ref. 10. As certain Natal data were used in constructing the cross-sections in Ref. 10, agreement is not surprising. The phases in Fig. 7

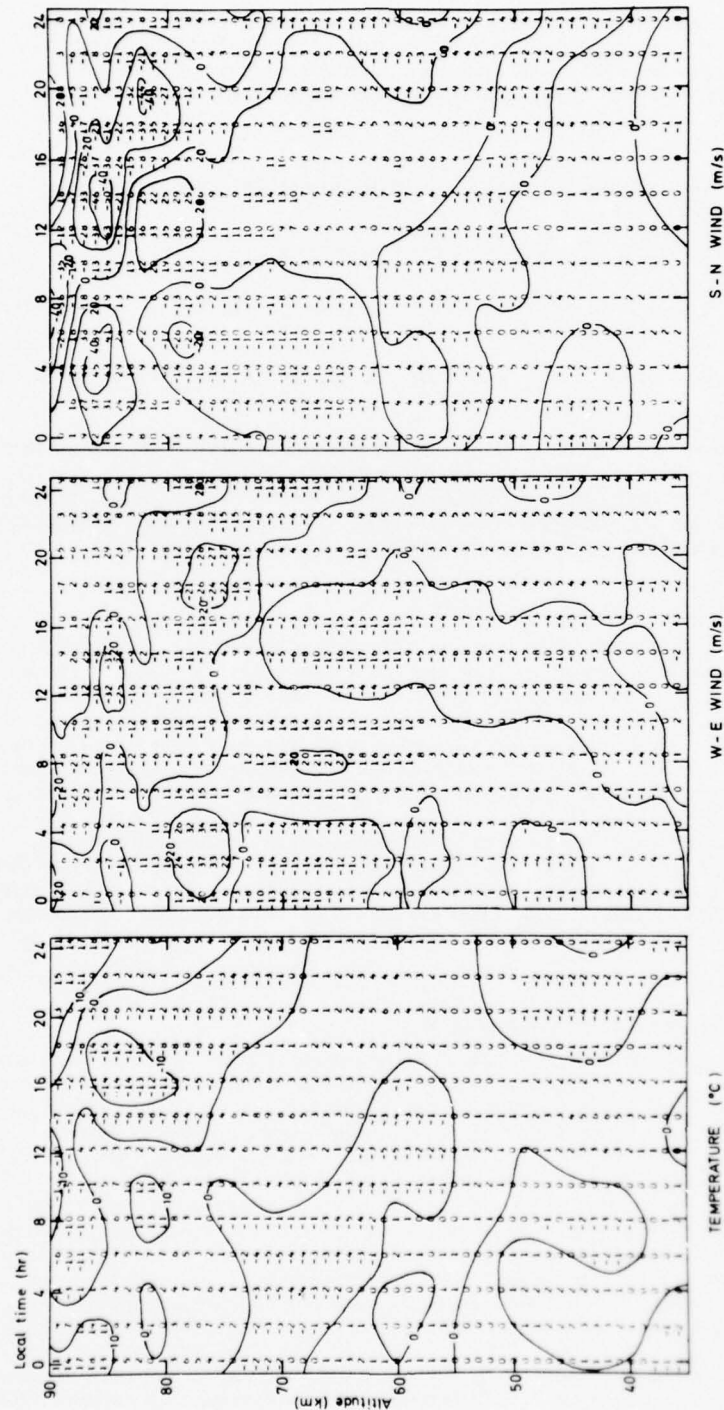


Fig. 5. Local time cross-sections.



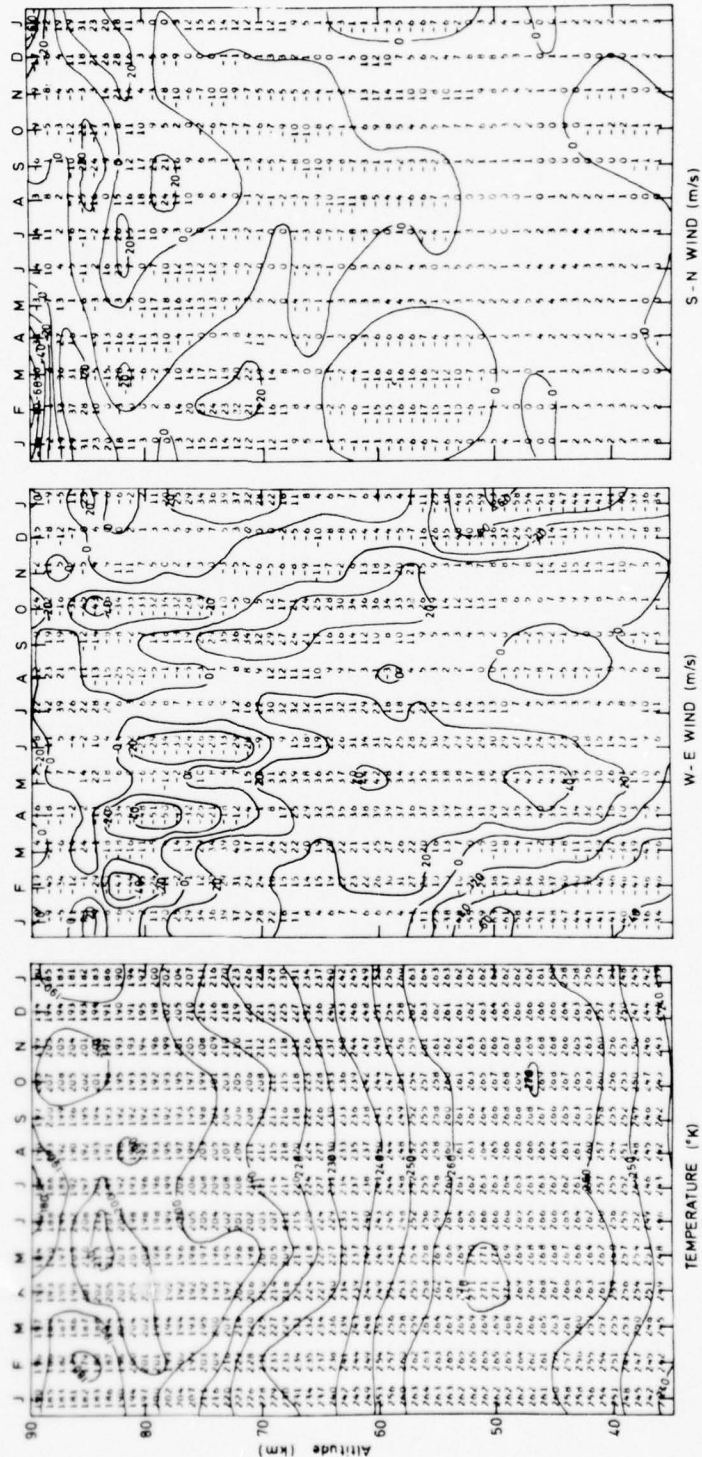


Fig. 6. Monthly cross-sections.

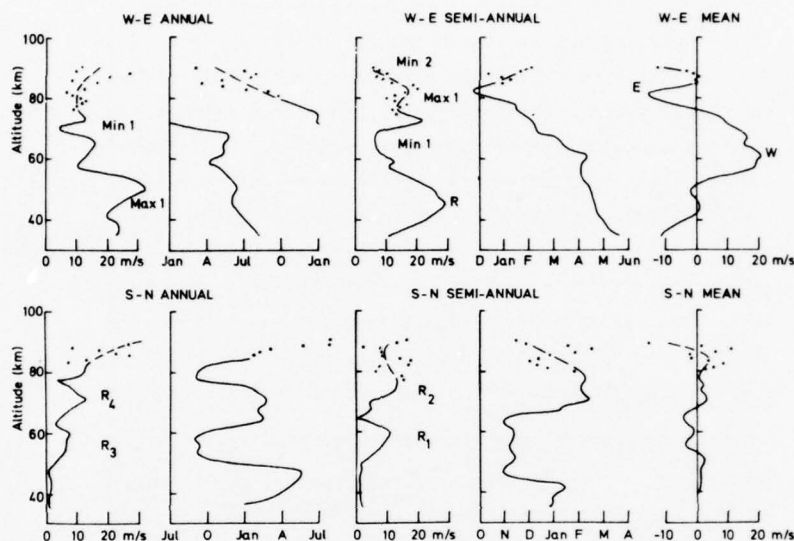


Fig. 7. WE and SN wind components.

also agree with the results in Ref. 10 with a six-month change of date, corresponding to latitude S. The easterlies E in Fig. 7 belong to a belt of easterlies lying within  $20^\circ$  of the equator [10], whereas the westerlies W extend to higher latitude ( $60^\circ$ ).

It should be noted that the temperature and WE wind diagrams in Fig. 6 depend partly on the CIRA models [5] as well as the 24 Natal grenade experiments, having been calculated from Eqn. 3. Table 2 shows an absence of grenade data during parts of the year, the largest gap occurring in January-February, and at these times Fig. 6 is particularly dependent on the CIRA models. In contrast, the SN wind diagram in Fig. 6 is derived solely from Natal data being the sum of the harmonic components shown in Fig. 7 (lower diagrams). The semi-annual component has maximum amplitudes in regions  $R_1$ ,  $R_2$  (with significances of 2 to  $3\sigma$ ). In  $R_1$  the phase for maximum northwards flow is seen to be early November (or May) and for  $R_2$  is early February (or August). In other words the flow directions in  $R_1$ ,  $R_2$  are opposite. For the annual component, amplitudes in regions  $R_3$ ,  $R_4$  are significant (at about the  $2\sigma$  level) and again the flow directions are opposite. Similar results from other sites are needed to enable the nature of the meridional flows to be discussed.

## 8. AN ANALYSIS OF RESIDUALS

The residual of an observed value,  $V_{\text{Obs}}$ , is defined as

$$V_e = V_{\text{Obs}} - (V_{\text{seasonal}} + V_{\text{diurnal}} + V_{\text{QBO}})$$

where  $V_{\text{seasonal}}$ ,  $V_{\text{diurnal}}$  are calculated from (3) and (2) and  $V_{\text{QBO}}$  is zero except for the WE wind for which it is calculated from the relationship in CIRA [5]. Root-mean-square values  $(V_e^2)^{1/2}$  were calculated at each 1 km height interval, where the bar denotes averaging over the number of observations, which was usually 24. The curves in Fig. 8 show the root-mean-square temperatures,  $T_{\text{RMS}}$ , WE winds,  $u_{\text{RMS}}$ , and SN winds,  $v_{\text{RMS}}$ .

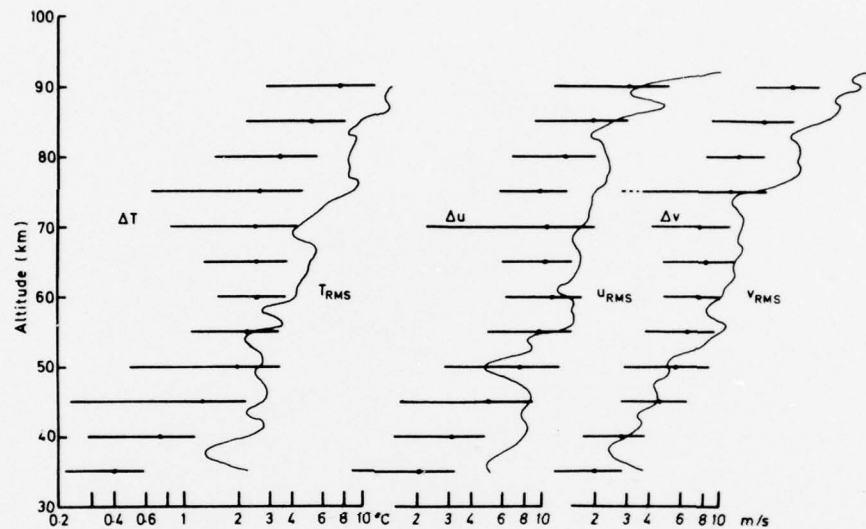


Fig. 8. Mean observational errors ( $\Delta$ ) and RMS values of residuals.

In general a residual is partly instrumental in origin and partly atmospheric. Estimates of instrumental errors have been provided by the experimenters [1,2,3] from which mean errors of observation  $\Delta t$ ,  $\Delta u$ , and  $\Delta v$  have been calculated. These are shown in Fig. 8 with a horizontal bar equal to the standard deviation of the instrumental errors. In general Fig. 8 shows that the RMS values are greater than the mean instrumental errors and can therefore be expected to arise from variations in the atmosphere. Exceptions are at 50-60 km where the two are of comparable magnitude; and also at lower heights for SN winds.

The origin of the residuals is not certain, but possible sources are wave motions (gravity or planetary waves) and small-scale turbulent fluctuations. Both  $u_{RMS}$  and  $v_{RMS}$  generally increase with height by a factor of  $\sim 10$  between 35 and 90 km with  $u_{RMS}$  exceeding  $v_{RMS}$  at most heights below 80 km. The associated kinetic energies/unit volume,  $\frac{1}{2} \rho u_{RMS}^2$ ,  $\frac{1}{2} \rho v_{RMS}^2$ , decrease by a factor  $\sim 20$  between 35 and 90 km on account of the fall of density  $\rho$  with height (Fig. 9). The decrease in  $\frac{1}{2} \rho u_{RMS}^2$  is noticeably rapid below the stratopause (40-50 km), but it then increases just above the stratopause (50-55 km). From calculations of the Richardson number from Natal grenade experiments, there appears to be a region of marginal stability or even turbulence at or slightly above the stratopause [11]. Such a change in atmospheric stability may be responsible for the increase in  $\frac{1}{2} \rho u_{RMS}^2$  just above 50 km. Fig. 9 also shows an increase in  $\frac{1}{2} \rho v_{RMS}^2$  just above the stratopause (50-55 km).

## 9. CONCLUSIONS

From 24 grenade experiments widely separated in time (over 22 months) at Natal it has been possible to resolve diurnal and seasonal components. In a previous analysis of similar data [4] the seasonal component only was obtained. A low latitude site is well situated for resolving tidal motions arising from propagating modes (Section 2). The 24 hourly variations above 60 km are found to have properties characteristic of the (1,1) mode, having a vertical wavelength of about 31 km. Theory [6] has already shown that this mode should predominate at low latitudes. There is evidence of the (1,3) mode predominating in the SN

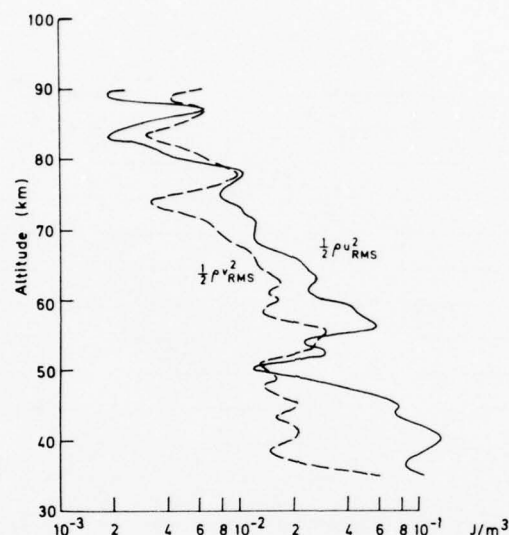


Fig. 9. Kinetic energy/unit volume of WE and SN wind residuals.

wind oscillation above 80 km.

The 12 hourly variations have also been evaluated and amplitudes have been compared with theoretical values (Fig. 3). At most heights the observed temperature amplitudes are less than the theoretical ones. Corresponding 12 hourly phases have yet to be examined in detail and will be reported later.

In classical tidal theory [6], the background atmosphere is taken to be at rest. To some extent, however, tidal patterns will be affected by changes in the transmission characteristics of the atmosphere. Seasonal variations of WE winds at low latitude are quite appreciable (Fig. 6) and have previously been referred to in this respect [12]; the effects of WE winds on the diurnal tide have been estimated and attention drawn to the possible difficulty of obtaining a precise comparison of observations with classical theory. From the observational side, the present analysis now provides strong evidence that low latitude tidal patterns are not seriously influenced by seasonal variations of the background atmosphere, otherwise it would not have been possible to extract significant diurnal components from 24 observations distributed over different seasons. A comparison of observations with theory would not therefore appear unjustified on the assumption that the medium was at rest and such a comparison will be undertaken later.

The second difficulty that seasonal variations may present is that of obscuring an otherwise steadily propagating tidal contribution. Seasonal and diurnal temperature changes at Natal are of roughly the same magnitude, but seasonal wind changes are generally much greater than diurnal ones: the seasonal change in WE winds between 40 and 55 km is 70-90 m/s. Nevertheless, in spite of these apparent difficulties, the data analysis techniques used here have enabled significant results to be obtained for the diurnal components from just 24 observations.

The seasonal variations obtained are shown in Fig. 6. Temperature and WE wind contours partly reproduce features of the CIRA models as well as of the 24 Natal experiments for which launch dates were rather scattered (Table 2). Annual and semi-annual components of WE winds at most N latitudes have previously been calculated (above 60 km) as a means of studying atmospheric structure [10]. The components for Natal (Fig. 7) are consistent with these meridional cross-sections. For SN components (Fig. 7) interpretation is more difficult without



#### *Analysis of Grenade-Experiment*

similar results from other sites as no corresponding meridional cross-sections are available and longitudinal variations may be important.

An analysis of residual temperatures and winds has shown that these are generally greater than the errors of observation and can therefore be expected to be atmospheric in origin. A feature of the wind residuals is the increase of kinetic energy/unit volume just above the stratopause (50-55 km) for which a decrease in atmospheric stability at this level may be responsible.

#### ACKNOWLEDGEMENTS

The assistance of Miss. A. Harris and Miss. B. M. Waters with the preparation of data and presentation of results is gratefully acknowledged. Work at University College London on upper atmosphere structure is supported by the Science Research Council, the Air Force Cambridge Research Laboratories (AFSC) through the European Office of Aerospace Research and Development under Grant AFOSR 72-2264 and by a research grant from the Meteorological Office.

#### REFERENCES

1. W. S. Smith, J. S. Theon, P. C. Swartz, L. B. Katchen, J. J. Horvath, NASA TR R-288 (1968).
2. W. S. Smith, J. S. Theon, P. C. Swartz, J. F. Casey, J. J. Horvath, NASA TR R-316 (1969).
3. W. S. Smith, J. S. Theon, J. F. Casey, J. J. Horvath, NASA TR R-340 (1970).
4. J. S. Theon, W. S. Smith, J. F. Casey, B. R. Kirkwood, NASA TR R-375 (1972).
5. *COSPAR International Reference Atmosphere 1972*, Akademie-Verlag, Berlin (1972).
6. R. S. Lindzen, *Q. J. Roy. Met. Soc.*, **93**, 18 (1967).
7. S. Chapman, R. S. Lindzen, *Atmospheric Tides*, D. Reidel Publ. Co., Dordrecht (1970).
8. R. S. Lindzen, *Proc. Roy. Soc.*, **A303**, 299 (1968).
9. R. J. Reed, *Jrn. Geophys. Res.*, **71**, 4223 (1966).
10. G. V. Groves, *Planet Space Sci.*, **20**, 2099 (1972).
11. S. P. Zimmerman, A. C. Faire, E. A. Murphy, *Space Research*, **12**, 615 (1972).
12. R. S. Lindzen, *J. Atmos. Sci.*, **29**, 1452 (1972).

*(Presented at the Symposium of the British Interplanetary Society on 'Sounding Rockets and Experimental Results' held at University College London, 27 September 1973 and revised for publication 28 March 1974).*

## THE CHARACTERISTICS AND APPLICATION OF AN ON-BOARD COMPUTER FOR USE ON SPACECRAFT

M. A. PERRY

*European Space Research Organisation, European Space Research and Technology Centre, Noordwijk, The Netherlands.*

ESRO requirements for a stored programme general purpose digital computer for use on-board spacecraft are discussed. A machine which is being developed under the ESRO Applied Research Programme is briefly described. This computer has an add time of 2.8 microseconds and uses a 16 bit word. Power consumption is estimated at 10.6 Watts and mass is expected to be below 5 kg.

The interface between the computer and the telemetry and telecommand system is discussed, and problems foreseen in reprogramming the computer in flight via the spacecraft telecommand link are briefly exposed.

### 1. INTRODUCTION

THE LATE SIXTIES brought an interest in the advantages which a stored programme digital computer had to offer scientific satellites. A number of satellite computers are known to have been studied [1 to 7], although not all have finally resulted in hardware as yet.

Table 1 summarizes the characteristics of some typical machines of European origin. Apart from the unanimous choice of a 16 bit word length, these computers are all very different from each other in concept. Against such a background, the ESRO requirements, in terms of on-board computers, were considered and uses to which these machines can be put have been examined.

TABLE 1. *European on-board computers.*

	A	B	C	D	E
Power consumption (Watts)	12	8	5	4	14.5
Mass (kg)	3.5	8	2.8	5	10
Memory capacity	4K ROM 1K RAM	28K RAM	4K RAM	8K RAM	8K RAM
Word length (bits)	16	16	16	16	16
Number of instructions	53	21	23	29	43
Serial or parallel	P	S	S	S	P

### 2. INITIAL CONSIDERATIONS

A satellite computer should not overburden the mass and power budgets of the host vehicle. Tables 2 and 3 compare data for three representative ESRO scientific satellites which have been studied at various times. Note how in Table 2 the on-board electronic systems occupy around 17 percent of the total mass. Table 3 illustrates the typical power budget allocation. On this kind of rough basis, we concluded that a useful satellite computer should consume no more than 10 Watts and should weigh not more than 5 kg with 4096 words of memory.

Additional requirements, derived from the operational constraints, were the

## Diurnal and semidiurnal oscillations of the upper atmosphere derived from grenade experiments at Natal, Brazil

G. V. GROVES

Department of Physics and Astronomy, University College, London

(Received 18 October 1974)

**Abstract**—Results are presented of amplitudes and phases of diurnal and semidiurnal temperature and wind oscillations between 35 and 90 km at Natal (6°S, 35°W) derived from 24 grenade experiments. Eight launchings in October gave diurnal components which were similar to those from ten launchings in May–August, both sets of results having phase profiles characteristic of the (1,1) tidal mode. Semidiurnal components derived from the combined 24 launchings showed rapid changes of phase at certain heights with almost constant phase at intermediate heights. Small numbers of launchings were found to be sufficient to resolve the diurnal oscillation indicating that this was the main component of atmospheric variation on the 24 hr time scale but semidiurnal oscillations could not be satisfactorily resolved with small numbers of launchings.

### 1. INTRODUCTION

Twentyfour Nike-Cajun sounding rockets with grenade payloads were launched at Natal, Brazil (6°, 35°W) by the NASA Goddard Space Flight Center between May 1966 and March 1968 (SMITH *et al.*, 1968, 1969, 1970; THEON *et al.*, 1972). In an earlier analysis (GROVES, 1974) of the wind and temperature data from these experiments seasonal and diurnal components were simultaneously resolved between 35 and 90 km. A notable feature of the diurnal oscillation was a phase change with height characteristic of the (1,1) tidal mode. Twelve-hourly amplitudes were evaluated and compared with theory but phases required a more detailed examination and were not reported.

Analysis of the Natal data has since continued with the following objectives in mind:

(1) To derive diurnal and semidiurnal components for subgroups of the 24 launchings and to compare the results obtained;

(2) To examine the effectiveness of small numbers of launchings in the study of diurnal and semidiurnal variations. The results of this work are presented below.

### 2. DATES AND TIMES OF THE NATAL LAUNCHINGS AND SELECTION OF SUBGROUPS FOR ANALYSIS

From the dates and times of launchings in Table 1, subgroups of launchings were identified which might usefully be analysed for diurnal and semidiurnal oscillations at particular dates or times of the year.

#### 2.1. Five Launchings (1–2 October 1966)

An important factor which limits the resolution of diurnal variations is the variability of background winds and temperatures. If, however, launchings are held within an interval of one or two days, changes due to the seasonal trend are relatively small. A series of five such launchings took place at Natal on 1–2 October 1966. Launch times were evenly spaced over a 30 hr period, but the first and fourth launchings were almost exactly 24 hr apart, providing effectively only four different local times.

To derive both diurnal and semidiurnal components, five unknowns need to be introduced as a prevailing component is involved as well as the amplitudes and phase angles of the two other components. With data at only four different local times a complete analysis was not possible and the semidiurnal component was therefore neglected. The number of unknowns was then three and two degrees of freedom were available for estimating the accuracy of the diurnal component.

#### 2.2. Eight Launchings in Early October (1–2 October 1966; 14–15 October 1967)

By combining the five launchings of 1–2 October 1966 with the three launchings of 14–15 October 1967, a subgroup is formed for which all data relate to the first half of October. The eight launchings provide six effectively different local times and the possibility of deriving both diurnal and semidiurnal variations with estimates of their accuracy based on three degrees of freedom.

Table 1. Dates and local times of Natal grenade experiment launchings

Day	Month	Year	Local Time	Day	Month	Year	Local Time
24	March	1968	1543	28	August	1967	2209
25	"	"	0339	1	October	1966	0602
25	"	"	1539	1	"	"	1818
1	May	1966	2258	1	"	"	2359
3	"	"	2259	2	"	"	0559
24	June	1967	0605	2	"	"	1148
24	"	"	1814	14	"	1967	0859
25	"	"	0613	15	"	"	0854
7	August	1966	0444	15	"	"	2054
7	"	"	2105	18	December	1967	1039
26	"	1967	0918	18	"	"	2239
26	"	"	2118	19	"	"	1049

2.3. *Ten Launchings in May-August (1,3 May 1966; 7 August 1966; 24-25 June 1967; 26-27 August 1967)*

On examining Table 1 for possible seasonal groupings of launchings, it is seen that during the months November-February only three launchings were held (in December), whereas for May-August there were ten. This group was selected as representing solstice conditions (N. hemisphere summer) for which the results might usefully be compared with those from the early October firings representing equinox conditions.

3. DIURNAL VARIATIONS

The results obtained for temperature, W-E and S-N wind components for the different subgroups are compared in Figs. 1-3 with those from the earlier analysis of the combined 24 launchings. The results from the different subgroups are represented by horizontal lines centred on the calculated values and equal in length to twice the corresponding estimated standard deviations. The continuous curves which are repeated on each diagram are from the analysis of the combined 24 launchings. Errors previously estimated

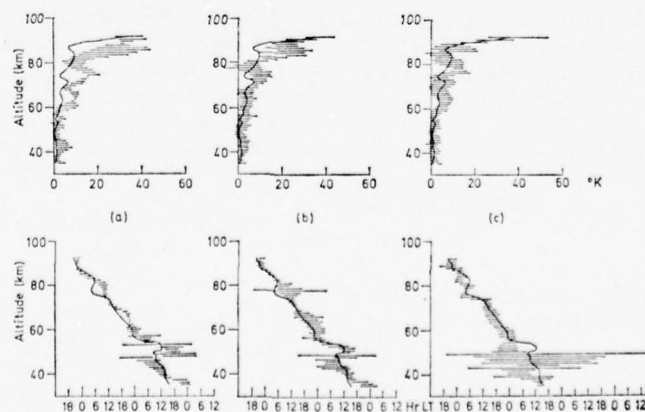


Fig. 1. Diurnal amplitudes (upper diagrams) and times of maximum (lower diagrams) for temperature based on (a) five launchings, 1-2 October 1966; (b) eight launchings in early October; (c) ten launchings in May-August; — 24 launchings.



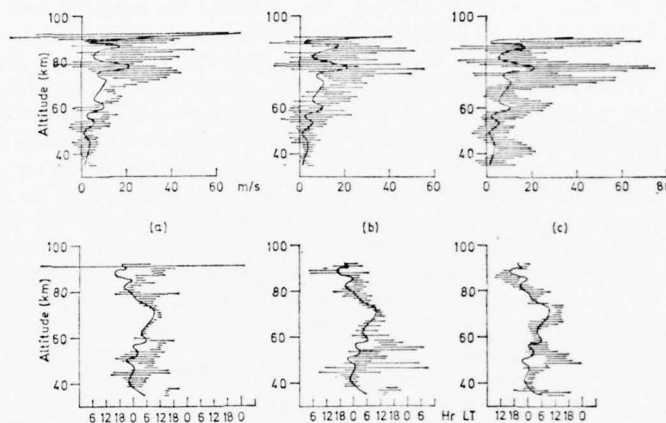


Fig. 2. Diurnal oscillations of W-E wind corresponding to Fig. 1.

(GROVES, 1974) for the continuous curves are not shown here to avoid confusion.

### 3.1. Five Launchings in 30 hr (1-2 October 1966): Figs. 1(a)-3(a)

Although data were available at only four effectively different local times, results were obtained at most heights with no great loss of significance. Only above 70 km in the wind components are error bars much greater than those for the 24 launchings. Possible reasons for this apparent significance are that (i) with the five launchings variations of the background atmosphere were greatly reduced; (ii) the results are not necessarily as accurate as error bars indicate, error estimation itself being subject to considerable uncertainty when only 1 or 2 degrees of freedom are available.

Some indication of the general validity of the results from the five launchings is provided by comparing them with those from the 24 launchings. Agreement between phase angles (i.e. times of

maximum) is remarkably close in both temperature and wind (Figs. 1(a)-3(a)). Agreement between amplitudes is not generally good, the values for the five launchings being greater than those for the 24 at many heights (particularly in temperature) and not as accurately determined. A decrease of accuracy is to be expected with fewer data points and the greater amplitudes are probably a statistical effect arising with the small number of launchings. A check analysis was carried out with decreasing amounts of data from another source and a similar effect developed for a sample size equivalent to that of the five Natal launchings.

### 3.2. Eight Launchings in Early October (1-2 October 1966; 14-15 October 1967): Figs. 1(b)-3(b)

The eight October launchings were first analysed for diurnal and semidiurnal components simultaneously, and then the analysis was repeated with the semidiurnal component neglected to ascertain the effect on the diurnal component.

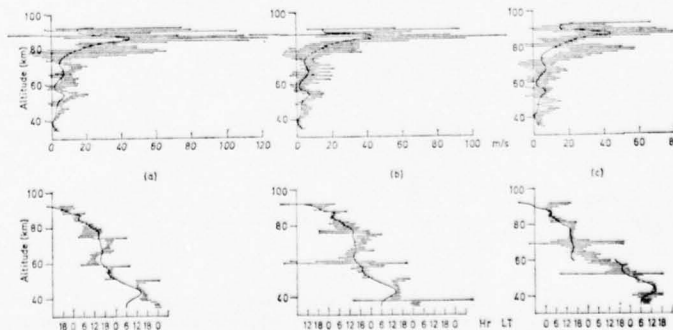


Fig. 3. Diurnal oscillations of S-N wind corresponding to Fig. 1.

Both sets of results are shown in Fig. 1(b)–3(b) by plotting values at even heights with the semidiurnal component included in the analysis, and at odd heights with it omitted. The effect of neglecting the semidiurnal component on the calculation of the diurnal is clearly insignificant.

The results from the eight launchings would not be expected to differ greatly from those of the five launchings as these are included among the eight and, in the main, Figs. 1(b)–3(b) confirm this expectation. Amplitudes (particularly of temperature) tend to be smaller with the eight than the five launchings: a change that may be attributed to the increase of data points. (The check analysis referred to above showed a similar reduction of amplitudes when the data sample was likewise increased.)

At most heights the results from the eight launchings are consistent with those from the 24 launchings (the continuous lines in Figs. 1(b)–3(b)); and the comparison indicates that early October diurnal tidal patterns are not conspicuously different from those at other times of the year when the remaining launchings took place.

### 3.3. Ten Launchings in May–August (1,3 May 1966; 7 August 1966; 24–25 June 1967; 26–27 August 1967): Figs. 1(c)–3(c)

Data were first analysed for diurnal and semidiurnal components simultaneously, but unlike the results from the eight October launchings, the estimated standard deviations were too large for the results to be considered significant and

the analysis was repeated with the semidiurnal component neglected. Results were obtained (Figs. 1(c)–3(c)) which are similar to those from the 24 launchings (the continuous lines) and from the eight October launchings (Figs. 1(b)–3(b)). Agreement between phases is particularly evident: for amplitudes small differences are present but these may not be significant in view of the size of the error bars. From these two independent groups of eight and ten launchings, the diurnal oscillations derived are consistent with regard to their main features for dates representative of equinox and solstice conditions.

## 4. SEMIDIURNAL VARIATIONS

### 4.1. Observational Results for Natal: Fig. 4

Amplitudes and phases of the semidiurnal oscillation derived by analysis of data from the combined 24 launchings are shown in Fig. 4. The amplitudes have been presented previously (GROVES, 1974) together with an account of the method of analysis and a comparison with theory (LINDZEN, 1968; CHAPMAN and LINDZEN, 1970). It was found that observed temperature amplitudes were less than the theoretical ones at most heights. Observed wind amplitudes were generally similar to theory, but observational errors were too large for detailed comparisons to be made.

Results for the corresponding phases are shown in Fig. 4 and are notable for the rapid changes of phase at certain heights with almost constant phase at intermediate heights. In the S–N winds, changes appear at 47–48 km and possibly at other heights in disagreement with

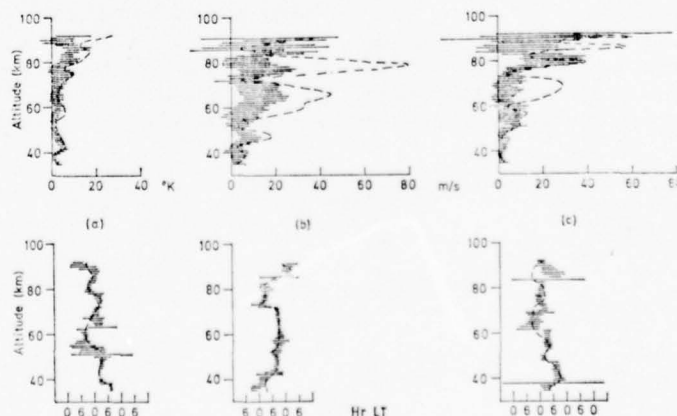


Fig. 4. Semidiurnal amplitudes (upper diagrams) and times of maximum (lower diagrams) based on 24 launchings. (a) temperature, (b) W–E wind, (c) S–N wind. ——— results based on eight launchings in October which show unacceptably large amplitudes but similar phase angles to the 24 launchings.

theoretical results (CHAPMAN and LINDZEN, 1970) which predict a phase reversal at about 28 km and a constant phase at all heights up to about 80 km. These theoretical results have previously been found to disagree with observations at 30° and 37°N (REED, 1972) to which further reference will be made below.

At first the possibility was considered that the rapid changes of phase might be spurious (arising for example in regions of small amplitude) and subgroups of the 24 launchings were therefore analysed to see whether the same phase profiles could be reproduced with independent sets of data. The failure to obtain a significant semidiurnal component with the ten May–August launchings has been referred to already (Section 3.3). The group of sixteen launchings consisting of all but the eight October launchings also failed to provide significant results. The group of eight October launchings gave significant results as mentioned above (Section 3.2) but amplitudes were generally increased. Phases, on the other hand, were remarkably consistent with those of the 24 launchings, reproducing the same rapid changes at the same heights. The comparison is shown in Fig. 4. In summary, the pattern of rapid phase changes found with the 24 launchings was also present with the eight October launchings; but for two groups of ten and sixteen launchings, which excluded these eight, no significant values were obtained.

The foregoing results are taken to indicate that a spurious effect was unlikely to be present on account of the similarity between results for the groups of eight and 24 launchings (although these are not actually independent groups). The failure of the ten and sixteen launching analyses would appear to be due to the extended distribution of their launch dates and associated variations in the background atmosphere or in the semidiurnal oscillation itself.

#### 4.2. Seasonal and Latitudinal Variations

Other sources of information on semidiurnal oscillations in the stratosphere and mesosphere have been considered in conjunction with the Natal results. Meteor trail results provide little opportunity for direct comparison as they only overlap the top end of the height range of the Natal results and relate to higher latitudes. However, from meteor trail observations spread over twelve years a significant seasonal pattern of semidiurnal winds has emerged with the pattern changing most rapidly in October (MULLER, 1966). A seasonal variation is also shown by

drift observations of ionospheric irregularities and both methods have shown minimum amplitudes in northern hemisphere summer (SPRENGER *et al.*, 1971). The failure to extract a significant semidiurnal component from small numbers of Natal launchings distributed over extended periods of time is therefore not surprising.

At lower heights results have been given by REED (1967, 1972) for 30 to 60 km derived from summertime meteorological rocket wind data prior to summer 1966. A notable feature of the results at both 30°N (Cape Kennedy and White Sands) and 37°N (Green River, Wallops Island and Point Mugu) is a rapid change of phase in the S–N wind oscillation near 50 km. At Natal a phase change also occurs near 50 km but the correspondence would appear to be fortuitous as differences of latitude and season are involved. Nevertheless, the rapid phase change in the 30° and 37°N results is well established on the basis of many hundreds of observations and lends support to the view that similar changes in the Natal results are also real features of the atmosphere. As mentioned already, both sets of results fail to confirm previous theoretical results of a constant phase between 30 and 80 km. A possible cause of the disagreement put forward in connection with the 30°–37°N results (REED, 1972) is that the observations were made at the time of summer stratospheric easterlies whereas the theoretical results apply to an atmosphere at rest. Calculations of the semidiurnal tide with zonal circulation included have indeed shown general agreement with the seasonal trend of experimental values from meteor trail drifts and ionospheric irregularities (GRAYZIGER *et al.*, 1971). Comparisons between experiment and theory would provide a more critical test if the vertical profile of the oscillation could also be examined. The meteor technique is effective between about 80 and 100 km and, with a height resolution of  $\pm 1$  km at Garchy (France), observations have led to higher-order modes such as  $(2, n)$ , where  $n > 4$ , being found (FELLOUS *et al.*, 1974). If higher-order modes are present, upper atmosphere semidiurnal tidal patterns can be expected to change rapidly with latitude; this aspect of tidal structure has yet to be investigated.

#### 5. DISCUSSION

Following the earlier analysis of data from the 24 Natal grenade experiments (GROVES, 1974), attention has now been given to the analysis of subgroups of the 24. The earlier analysis proved surprisingly effective, giving significant results,



not only above 60 km where tidal amplitudes show a marked increase with height, but also between 35 and 60 km where diurnal amplitudes are at most a few m/s in wind speed or a few °K in temperature. In the new analyses, with smaller numbers of launchings, results at the lower heights have still remained significant. Clearly a decrease of accuracy occurs with decreasing numbers of data points; and at most heights it would appear that amplitudes in both diurnal and semidiurnal components are affected more seriously than phases.

The relationship between numbers of launchings and results achieved is of practical and economic importance in planning diurnal series of launchings. A sine curve is approximately described by about six equally-spaced points and *a priori* at least this number of launchings in a 24-hr period would appear to be necessary to resolve a diurnal oscillation even when other variations in the atmospheric structure are disregarded. An analysis of five launchings within a 30-hr period was able to resolve the main features of the diurnal phase profile and some features of the amplitude profile. With eight launchings a noticeable decrease (and possible improvement) in the amplitude profile resulted. However, only six of the eight local times were effectively independent and the additional three launchings were for the following year. Therefore with six equally-spaced launchings in the same 24-hr period at least comparable accuracy could be expected. The inclusion of the semidiurnal oscillation as an unknown was not found to have a significant effect on the results for the diurnal oscillation indicating that the latter was the main component of atmospheric variation on the 24-hr timescale.

For the semidiurnal oscillation the amplitudes derived with the eight launchings were considered unacceptable, being considerably greater at many heights than those with the 24 launchings (Fig. 4). The requirements for a satisfactory determination of the semidiurnal component are more demanding than for the diurnal, probably on account of the magnitude of the semidiurnal component relative to other short-period (gravity wave) variations. It is possible that twelve launchings in 24 hr would suffice for a satisfactory determination of the semidiurnal component, but the matter could not be investigated further with the data available.

Results from subgroups of launchings at different times of the year were obtained with some success for the diurnal component but not for the semidiurnal. The diurnal oscillation derived with the eight early October launchings agreed at most heights with that for the ten May–August launchings, the phase profile of both oscillations being characteristic of the (1,1) tidal mode. With the semidiurnal oscillation, a notable feature was the rapid changes of phase at certain heights. Such changes do not appear in theoretical results of the semidiurnal oscillation (CHAPMAN and LINDZEN, 1970). For understanding these differences observations of the upper atmosphere semidiurnal oscillation at different latitudes are considered relevant (Section 4.2).

*Acknowledgements*—The author gratefully acknowledges the assistance of Miss A. HARRIS with the data preparation and computations involved in obtaining the results of this paper. The work has been supported by the Office of Aerospace Research and Development under Grant No. AFOSR-72-2264 and by the U.K. Meteorological Office.

#### REFERENCES

- |                                                                         |      |                                                                           |
|-------------------------------------------------------------------------|------|---------------------------------------------------------------------------|
| CHAPMAN S. and LINDZEN R. S.                                            | 1970 | <i>Atmospheric Tides</i> . D. Reidel, Dordrecht.                          |
| FELLOUS J. L., SPIZZICHINO A., GLASS M. and MASSEBEUF M.                | 1974 | <i>J. atmos. terr. Phys.</i> <b>36</b> , 385.                             |
| GRAYZIGER K. M., SPRENGER K., IVANOVSKIY A. I. and SEMENOVSKIY Yu. V.   | 1971 | <i>Izv. Atmos. and Ocean. Phys.</i> <b>7</b> , 255 (165 in English edn.). |
| GROVES G. V.                                                            | 1974 | <i>J. Brit. Interplan. Soc.</i> <b>27</b> , 499.                          |
| LINDZEN R. S.                                                           | 1968 | <i>Proc. R. Soc. A</i> <b>303</b> , 299.                                  |
| MULLER H. M.                                                            | 1966 | <i>Planet. space Sci.</i> <b>14</b> , 1253.                               |
| REED R. J.                                                              | 1967 | <i>J. atmos. Sci.</i> <b>24</b> , 315.                                    |
| REED R. J.                                                              | 1972 | <i>Mon. wea. Rev.</i> <b>100</b> , 579.                                   |
| SMITH W. S., THEON J. S., CASEY J. F. and HORVATH J. J.                 | 1970 | NASA TR R-340.                                                            |
| SMITH W. S., THEON J. S., SWARTZ P. C., CASEY J. F. and HORVATH J. J.   | 1969 | NASA TR R-316.                                                            |
| SMITH W. S., THEON J. S., SWARTZ P. C., KATCHEN L. B. and HORVATH J. J. | 1968 | NASA TR R-288.                                                            |
| SPRENGER K., GREISIGER K. M. and SCHMINDER P.                           | 1971 | <i>Izv. Atmos. and Ocean. Phys.</i> <b>7</b> , 479 (311 in English edn.). |
| THEON J. S., SMITH W. S., CASEY J. F. and KIRKWOOD B. R.                | 1972 | NASA TR R-375.                                                            |



## **A COMPARISON OF 24-HOURLY ATMOSPHERIC OSCILLATIONS DERIVED FROM GRENADE EXPERIMENTS AT TWO LOW LATITUDE SITES**

**G. V. GROVES**

*Department of Physics and Astronomy, University College London, England.*

---

A comparison is undertaken of two sets of results of 24-hourly oscillations of winds and temperatures at heights between 35 and 95 km altitude in terms of their amplitudes and phases. The first set was derived from 24 grenade experiments conducted in 1966-68 at 5.9°S latitude and the second set was derived from 13 grenade experiments conducted on 19-22 September 1971 at 5.1°N latitude. Good agreement is found between the wind oscillations, but significant differences appear in the temperature oscillations. It is concluded that the wind oscillations were generated chiefly by equatorially symmetrical tidal modes, predominantly the (1,1) with the (1,3) mode contributing appreciably to the S-N wind oscillation. The differences in the temperature oscillations are attributed to a (1,2) mode propagating at the time of the 5.1°N observations. If this interpretation of the temperature results is correct, asymmetrical tidal modes may be a more important feature of atmospheric oscillations than has previously been recognised.

---

### **1. INTRODUCTION**

A DETAILED ANALYSIS of wind and temperature data from 24 grenade experiments conducted by the NASA Goddard Space Flight Center at Natal (5.9°S, 35.2°W) between May 1966 and March 1968 has previously been reported [1] in which attention was given to the resolution of diurnal oscillations as well as seasonal components. Significant amplitudes and phases were derived for the 24-hourly oscillations of temperature, W-E (west-to-east) and S-N (south-to-north) wind components at almost all heights between 35 and 95 km.

In a further analysis of the data from these 24 launchings [2], subgroups of launchings were selected and likewise examined. Significant results were obtained for 24-hourly oscillations with eight launchings on dates in early October and with ten launchings on dates between May and August. Consistent results were derived from the different sets of data, phase versus height profiles showing evidence of an upwards energy propagating (1,1) tidal mode (for which the vertical wavelength is about 30 km).

A further series of grenade launchings has now been conducted by the NASA Goddard Space Flight Center at Kourou (5.1°N, 52.6°W) consisting in the main of 13 launchings between 19 and 22 September 1971 [3]. These observations are particularly suitable for the investigation of diurnal oscillations as launch times fall within a period of just over two days during which background atmospheric changes due to the seasonal trend would be expected to be relatively small. Also, launch times were suitably distributed in local time for a diurnal analysis to be undertaken.

The Kourou data are suitable for direct comparison with the results from Natal which has almost the same latitude in the opposite hemisphere. Upper atmospheric 24-hourly oscillations at low latitudes are generated almost entirely by propagating modes and as these are strongly latitude dependent results from different sites cannot be readily compared unless their latitudes are nearly equal. According to

tidal theory [4], the S-N wind oscillation has a particularly marked latitudinal dependence with the (1,1) mode increasing from zero at the equator approximately in proportion to latitude. An amplitude increase of nearly 14% therefore occurs between  $5.1^\circ$  and  $5.9^\circ$  latitude, but such a change is unlikely to be more than marginally significant and results from the two sites should be comparable provided their N and S hemispherical locations are allowed for.

According to tidal theory, equatorially symmetric modes of generation give rise to equatorially symmetric temperature and W-E wind oscillations and asymmetric S-N wind oscillations. Hence if only symmetrical modes (the (1,1), (1,3), ... modes) are present, observations from sites in opposite hemispheres may be compared by changing the phase of the S-N wind oscillation at one of them by 12 hours. This procedure will be followed below in keeping with previous interpretations of the Natal results as oscillations composed mainly of (1,1) and (1,3) modes [1, 5].

## 2. COMPARISONS OF 24-HOURLY OSCILLATIONS

Winds and temperatures were measured between 35 and 95 km altitude at Kourou on 19-22 September 1971 by 13 grenade experiments with the following local times of launch: 1826, 0000, 0245, 0600, 1115, 1530, 2035, 0120, 0544, 1030, 1510, 2010, 0020 hours [3]. These observations have now been analysed by the author for diurnal oscillations by the procedure previously described for the analysis of data from Natal grenade experiments [1]. The results, in terms of amplitudes and phases (i.e. times of maximum), are shown in Figs. 1(a) to (c) for W-E, S-N wind oscillations and temperature oscillations respectively. Each

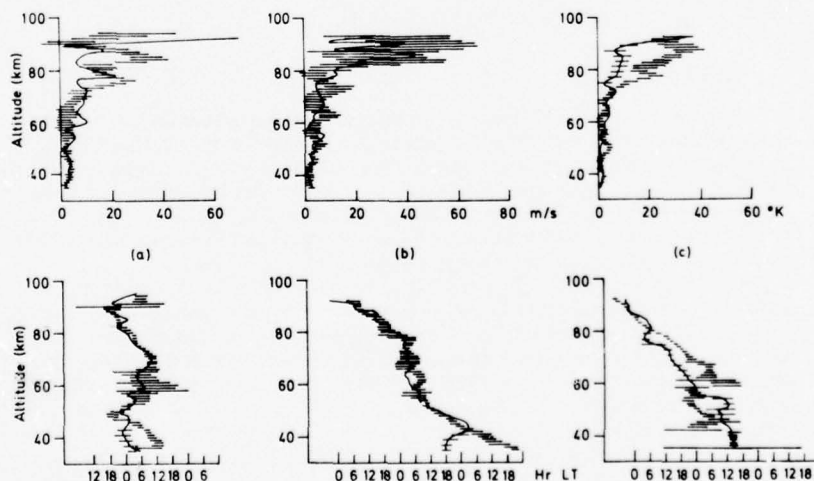


Fig. 1. Diurnal amplitudes (upper diagrams) and times of maximum (lower diagrams) for (a) W-E wind, (b) S-N wind, (c) temperature. Horizontal lines are for Kourou ( $5.1^\circ\text{N}$ ), 19-22 September 1971 [3]. Continuous lines are for Natal ( $5.9^\circ\text{S}$ ), 1966-68 [1], the curve for S-N phases being shifted by 12 hours.

horizontal line is an error bar centred on the value calculated and equal in length to twice the corresponding standard deviation.

The continuous curves in Fig. 1 were derived previously from the 24 grenade experiments at Natal [1], the curve of S-N wind phase being shifted by 12 hours as discussed in Section 1. To avoid confusion, error bars previously estimated for

the Natal results are only shown at 2 km height intervals where there is no overlap with the Kourou results.

### **2.1 Wind Oscillations**

The wind oscillations in Figs. 1(a) and (b) for Natal and Kourou are seen to be in close agreement. Particularly impressive is the agreement between the phase profiles, differences being well within the limits indicated by the error bars (except below 45 km). The agreement between S-N phase profiles after introducing a 12 hour phase change supports the view that the wind oscillation was generated in the main by equatorially symmetrical modes.

In the amplitude profiles, detailed features are present which do not correspond at the two sites, but these differences are not generally significant when regard is taken of the size of the error bars. The high degree of consistency between the two sets of results is quite remarkable when it is recalled that the Natal data originated over a time interval of 22 months in 1966-68 whereas the Kourou data were acquired within 2-3 days in September 1971.

### **2.2 Temperature Oscillations**

In contrast to the wind oscillations, temperature amplitudes and phases show significant differences between the two sets of results at many heights (Fig. 1(c)). Amplitudes differ conspicuously between 70 and 90 km, Kourou values exceeding those for Natal by up to  $25^{\circ}\text{K}$ , whereas standard deviations are  $6^{\circ}\text{K}$  or less.

If the observed oscillations are superpositions of tidal modes, the larger Kourou temperature amplitudes would point to an enhancement of some particular mode or modes. Reference to the Kourou phase profile (Fig. 1(c)) shows a nearly constant gradient from 65 to 92 km indicating the upwards propagation of energy by a single predominant mode. The average gradient of the profile between 65 and 92 km is about 18 km per 24 hours, a value which corresponds closely (within 1 or 2 km per 24 hours) with that of the (1,2) mode.

## **3. DISCUSSION**

Natal and Kourou are the only sites at low latitude at which series of grenade experiments capable of yielding diurnal oscillations have been conducted. By coincidence, their latitudes differ by only  $0.8^{\circ}$  so providing the opportunity for a direct comparison between oscillations that are strongly latitude dependent.

The wind oscillations at Kourou are in close agreement with those previously determined for Natal (Figs. 1(a) and (b)) and are consistent with the assumption that they are generated mainly by equatorially symmetrical modes. This assumption is in keeping with previous theoretical and observational accounts on atmospheric oscillations in which asymmetrical propagating modes have not featured or been treated quantitatively [4, 6]. The principal asymmetrical propagating mode is the (1, 2) and this can apparently be identified in the Kourou temperature oscillation, being the predominant mode above 65 km. The presence of a (1, 2) mode is particularly surprising at the time of the Kourou launchings, i.e. at the equinox, as insolation heating would then be expected to be highly symmetrical with respect to the equator. If the Kourou temperature oscillation is correctly interpreted in terms of a (1, 2) mode, asymmetrical modes may be a more important feature of atmospheric oscillations than has previously been recognised.

The apparent absence of a (1, 2) mode in the W-E wind oscillation is in accord with theory which shows that most of the (1, 2) wind oscillation resides in the S-N component at low latitudes, W-E amplitudes amounting to only 6% of S-N amplitudes at the latitude of Kourou. The apparent absence of a (1, 2) mode in the S-N direction is less readily explained: it could possibly be due to greater contributions from the (1, 1) and (1, 3) modes which are effectively masking it.

G. V. Groves

Calculations have already shown [5] that, at the latitude of these sites, the (1,3) mode (relative to the (1,1) mode) is much greater in the S-N oscillation than in either the W-E wind oscillation or temperature oscillation. Furthermore, in Fig. 1(b), amplitude maxima at 52, 63 and 74 km and minima at 57, 68 and 79 km correspond closely (within 1 km) with the vertical wavelength of the (1,3) mode and indicate the magnitude of the contribution of this mode to the oscillation.

A notable feature of the Kourou S-N wind oscillation is the large scatter in amplitudes above 80 km, standard deviations being about twice those for the Natal results. The stability of propagating tidal modes has previously been investigated theoretically in terms of the Richardson number criterion and it has been shown that turbulence can be expected to be generated within 2 or 3 km of 90 km altitude over the equator [7]. Higher order modes are particularly effective in producing instabilities on account of their shorter wavelengths and associated higher wind shears. The (1,3) mode is therefore a likely agent for generating turbulence particularly in the S-N direction where, by tidal theory, amplitudes are about five times greater than those in the W-E direction at the latitude of these observations. If the scatter shown by the Kourou amplitudes originates from tidal instabilities, an enhancement relative to the Natal conditions of the (1,3) mode, or of a similar mode such as the (1,2) mode which would also be effective in the S-N direction, is indicated.

When Kourou data were first analysed for 24-hourly oscillations, it was expected that smaller standard deviations would be obtained than for the Natal data which were distributed over 22 months instead of just 2-3 days. No real difference is, however, shown by the overall accuracies of the two sets of results, indicating that the scatter probably originates from short-term variations (i.e. on a timescale of 24 hours or less) rather than from the seasonal trend. Another point is that amplitudes and phases of the 24-hourly oscillations must have remained relatively steady during the 22-month period of Natal observations otherwise there would be more scatter in the Natal results than in the Kourou ones. The steadiness of the oscillations implies not only a corresponding steadiness in the thermal sources of tidal generation but also in the transmission characteristics of the atmosphere, which might otherwise be expected to be influenced by, for example, seasonal wind patterns. The close agreement between the Kourou and Natal wind profiles (above 45 km) is further evidence of long-term steadiness, whereas the differences in the temperature profiles are seen as temporary changes at the time of the Kourou observations, the possible nature of which has been discussed above.

Finally, the value of the grenade experiment should be pointed out in providing both wind and temperature data over a wide range of heights from 35 to over 90 km. If wind data alone had been available or if data had been available only up to 60-70 km altitude, much valuable information would have been lost.

#### ACKNOWLEDGEMENTS

The author gratefully acknowledges the assistance of Miss A Harris with the data preparation and computations involved in obtaining the results of this paper. The work has been supported by the USAF Office of Aerospace Research and Development under Grant No. AFOSR-72-2264 and by the U.K. Meteorological Office.

#### REFERENCES

1. G. V. Groves, *JBIS* **27**, 499 (1974).
2. G. V. Groves, *J. Atmos. Terr. Phys.*, in press (1975).
3. W. S. Smith, J. S. Theon, D. U. Wright, Jr., D. J. Ramsdale and J. J. Horvath, NASA TR R-416 (1974).
4. S. Chapman and R. S. Lindzen, *Atmospheric Tides*, D. Reidel Publ. Co., Dordrecht (1970).
5. G. V. Groves, *JBIS* **28**, 127 (1975).
6. B. Haurwitz and Ann D. Cowley, *Pure and Appl. Geophys.* **102**, 193 (1973).
7. R. S. Lindzen, *Proc. Roy. Soc. A* **303**, 299 (1968).



## REVIEW LECTURE

### Rocket studies of atmospheric tides

By G. V. GROVES

*Department of Physics and Astronomy, University College London*

*(Lecture delivered and MS. received 29 April 1976)*

Diurnal and semidiurnal oscillations in the stratosphere and mesosphere as revealed by rocket techniques are reviewed in relation to routine M.R.N. launchings, grenade experiments, and diurnal launch series. Height profiles of phase and amplitude are interpreted as a superposition of modes and feature propagating modes of a higher order than the leading diurnal or semidiurnal modes. Such modes vary between different observing dates and often appear as a dominant part of an oscillation. Their excitation and propagation are discussed with reference to water vapour distribution, correspondence between distribution of heat source and structure of mode (in latitude, longitude and height), and damping. Comparisons are made between observed and theoretical diurnal oscillations at high latitude where negative modes predominate and at low latitude where positive modes predominate. The role of the stratopause region of diurnal heating in opposing the tropospherically generated (1,1) mode of oscillation is discussed and the possible production of variations in heating at the base of the thermosphere is pointed out.

#### 1. INTRODUCTION

Superimposed on the irregular variations of barometric pressure which are related to changes in weather is a small regular daily variation. Towards low latitudes the amplitude of this variation increases to more than 1 mbar (100 Pa) and as other changes generally decrease it becomes a marked feature of the total pressure variation. Barometric oscillations which correlate with the position of either the Sun or the Moon have provided the main observational evidence of atmospheric tides in the lower atmosphere. The analysis of solar components has been undertaken for over 150 years: one of the most extensive compilations is still that of Hann (1889) which covers work dating back to the 1830s.

Subsequent global analyses of barometric oscillations were reviewed in a monograph by Wilkes (1949) together with the developments of dynamical theory which the observational results stimulated. Two short-comings in the theory at that time were the disregard of thermal excitation, only gravitational excitation being reckoned with, and secondly the consequent lack of any treatment of the 24 h component which is plainly of thermal origin. The review by Siebert (1961) rectified the first matter but the 24 h component still remained inadequately accounted for.

Shortly afterwards heating by ozone absorption in the region of 50 km altitude was shown by Butler & Small (1963) to contribute significantly to surface pressure oscillations through particular modes which are strongly coupled in their vertical structure; notably the leading semidiurnal (2, 2) mode. Rather amazingly, a response to a westward moving semidiurnal heating wave in the region of the stratopause is found in the lower atmosphere where the medium has a density  $10^3$  times as great. In general the response to a tidal heat source depends on the correspondence of its vertical and horizontal distribution with the corresponding structure of prescribed modes for the particular frequency of oscillation. In 1966, new theoretical developments enabled the 24 h component to be accounted for with something like reasonable adequacy (see §2).

A wide range of topics has continued to provide observational and theoretical interest in atmospheric tides over the last ten years: these include the smaller lunar tide and the investigation of solar tides in the upper atmosphere. A comprehensive review of the subject has been undertaken by Chapman & Lindzen (1970). The first observations of upper atmospheric tidal winds were made by the meteor-radar technique in the 1950s at Jodrell Bank (Greenhow & Neufeld 1961) and at Adelaide, Australia (Elford 1959). The meteor-radar technique is capable of height resolution (of about 2 km) over the height range 80–110 km, and has now been introduced at several other sites (Webb 1972). Other ground-based methods of wind measurement such as partial reflexions of medium frequency radio waves, lidar and incoherent scatter radar have also been put into operation. These techniques do not however extend good diurnal coverage below 80 km where tidal data have been obtained almost exclusively by rocket techniques.

In the stratosphere and mesosphere wavelike systems of tidal oscillations which relate to conditions in the troposphere propagate upwards with generally increasing amplitude to dissipate their energy in the lower thermosphere: other tidal oscillations couple different height regions of the atmosphere dynamically. Apart from the importance of its intermediate position, the region has its own source of tidal excitation in ozone heating which also attracts investigation. The present review is selective in that attention is confined to the stratosphere and mesosphere notwithstanding the application of rocket techniques for measuring thermospheric winds. The choice reflects the author's own involvement in recent years with the analysis and interpretation of tidal oscillations in the stratosphere and mesosphere, and recent results from this work are included in the review.

## 2. WINDS AND WAVES IN THE UPPER ATMOSPHERE

During the years 1957–65, 28 Skylark rockets were launched at the Woomera range (31.0° S, 136.5° E) as part of the U.K. Space Research Programme for the investigation of seasonal and diurnal variations of winds and temperatures in the upper atmosphere. In these experiments grenades were ejected along the flight path of a rocket and winds and temperatures were measured at various heights by their

effects on the travel times of the resulting sound waves to an array of microphones on the ground (Bowen *et al.* 1964). The feasibility of the 'grenade experiment' had previously been demonstrated in the United States rocket programme, its main attraction being the considerable extension of wind and temperature measurement from the balloon ceiling of 30 km to a limiting altitude of 90–95 km set by the acoustical detection.

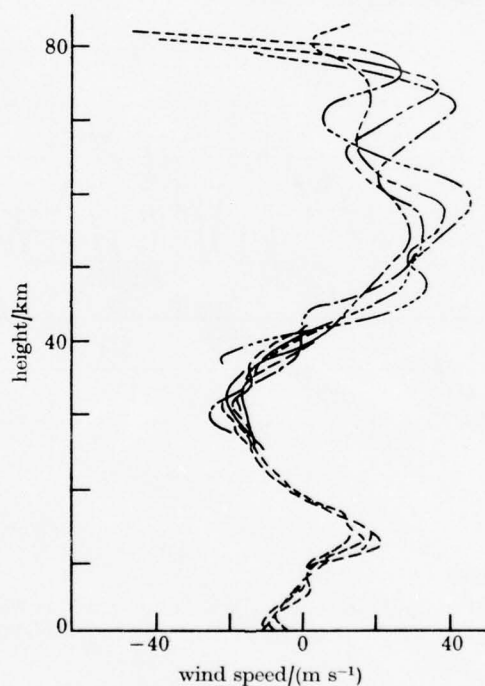


FIGURE 1. W-E wind components, Woomera ( $31.0^{\circ}$  S,  $136.5^{\circ}$  E), 15–16 October 1963. ---, Balloon data; - - - - -, grenade experiments at 19.21 h; - · - · -, 21.18 h; — — —, 00.39 h; - - - -, 04.52 h.

The Woomera experiments showed that seasonal variations of atmospheric parameters generally predominated below 70 to 80 km (Groves 1966) and that variations of a wavelike nature on a time-scale of the order of a day or less became increasingly important above 45 km. The wavelike nature of the wind velocity is apparent in the four profiles in figure 1 (Groves 1965). The downwards progression of the oscillation from one launching to the next corresponds to an obliquely upwards propagation of energy when interpreted as an internal gravity wave (Hines 1960). Amplitudes increase with height as air density decreases in order to maintain the energy flux, but above 100 km dissipation processes become increasingly important, and amplitudes maximize at 110–130 km. Although these experiments admirably revealed details of vertical structure, there were obvious difficulties in

studying variations with time. Results such as those in figure 1 indicated periodicities of the order of several hours but fell short of defining particular frequency components. The limited number of launchings and the restriction to night-time observation meant that adequate time series for the study of diurnal variations were unlikely to be available. By 1965 when the Woomera experiments concluded there were signs that these limitations might be overcome with data collected elsewhere by smaller meteorological rockets.

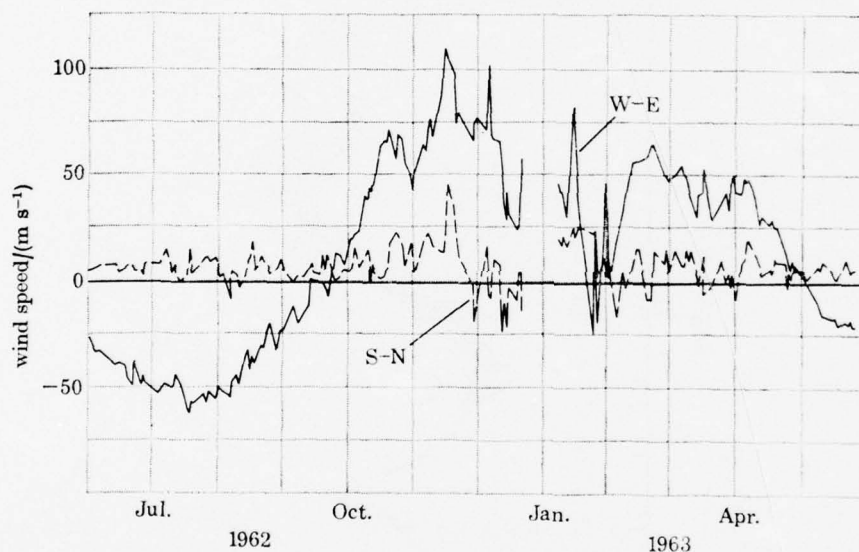


FIGURE 2. Mean wind components for the height interval 45–55 km, White Sands Missile Range (32.4° N, 106.5° W) (Webb 1964).

In October 1959 the Meteorological Rocket Network (M.R.N.) was formed to provide an upwards extension to conventional meteorological observations over N. America and adjacent ocean areas. By the end of 1965 over 5000 launchings had taken place and operations have since continued at some 20 sites with a total launch rate of about 1000 rockets per year. The most frequently used wind sensor has been a parachute package. Tracking by radar enables horizontal wind components to be derived. The wind response of parachute sensors is poor above 50 km (Hyson 1968), but useful results may be obtained to about 65 km by applying a correction which is proportional to the rate of change of horizontal velocity.

Tidal amplitudes at M.R.N. heights amount to only a few metres per second and are therefore very small compared with the seasonal change in the zonal flow which may amount to more than 100 m/s between extreme values. S-N wind components are generally smaller than W-E components but away from the summer months they may increase with displacements of the polar vortex and show wide fluctuations during winter on account of stratospheric warmings. The relative stability during



summer months of the S-N flow between 45 and 55 km was well illustrated by the 1962-3 observations at White Sands Missile Range ( $32.4^{\circ}\text{N}$ ,  $106.5^{\circ}\text{W}$ ) shown in figure 2 (Webb 1964). Unfortunately a serious limitation on the use of M.R.N. data for tidal analysis even during summer months has been their poor distribution in local time, most launch times lying close to local noon. The steady 10 m/s northward flow observed over White Sands during summer (figure 2) was mainly the diurnal component sampled repetitively at times close to 12 noon L.T. ! When 50 km data were plotted against time of day as in figure 3 (Groves 1967*a*), the variation was almost entirely 24 h with maximum northwards flow corresponding (by chance)

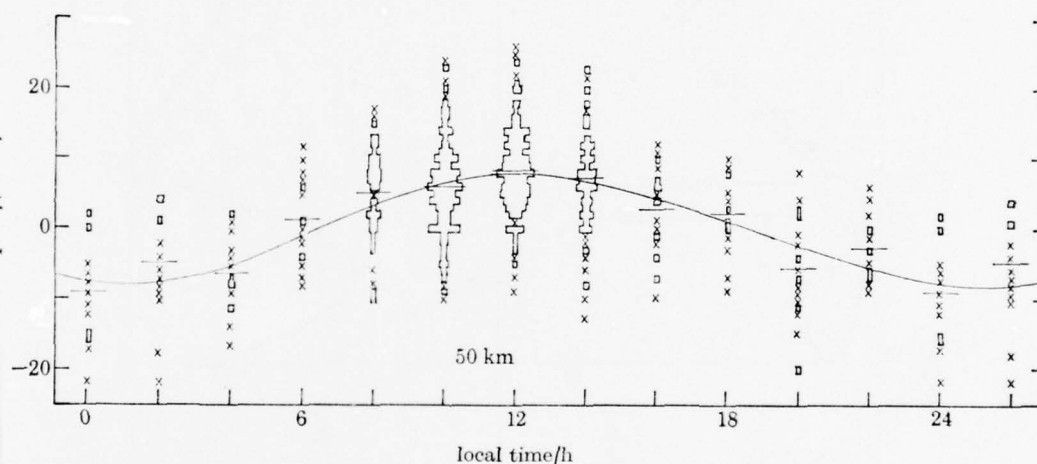


FIGURE 3. Summer S-N wind components at 50 km for sites close to  $30^{\circ}\text{N}$  latitude showing a mainly 24 h variation. x, single observation;  $\boxplus$ , 10 observations; — (horizontal line), mean value of distribution; curve, a least squares fit to the mean values.

with the midday period of maximum launch frequency. Data from other longitudes such as Somniam, Pakistan ( $66.7^{\circ}\text{E}$ ) and Woomera, Australia ( $136.5^{\circ}\text{E}$ ) confirmed a dependence on L.T. rather than G.M.T., i.e. that the variation was a wave moving westward with the Sun. At adjacent heights, similar analyses showed the presence of a semidiurnal component of similar magnitude.

M.R.N. launchings continued to support synoptic studies in subsequent years and the majority of launch times were consequently close to local noon. Nevertheless as with the data in figure 3, a small percentage of launchings took place at other times of day and by combining observations from hundreds of launchings over many years, it was possible to resolve tidal components at latitudes other than  $30^{\circ}$  (Groves & Makarios 1968). Figure 4 shows diurnal amplitudes and phases at two of the sites analysed by Reed, Oard & Sieminski (1969). Results were only obtained for the summer S-N component for the reasons given above except at Ascension Island ( $8.0^{\circ}\text{S}$ ,  $14.4^{\circ}\text{W}$ ), where data were combined from all times of the year. Also

the summer W-E diurnal oscillation could be resolved at  $30^\circ\text{N}$  where more observations were available than elsewhere.

An important feature of the analysis carried out by Reed *et al.* (1969) was a comparison between the observations and the theoretical diurnal winds calculated by Lindzen (1967). In 1966, Lindzen and Kato working independently showed that for

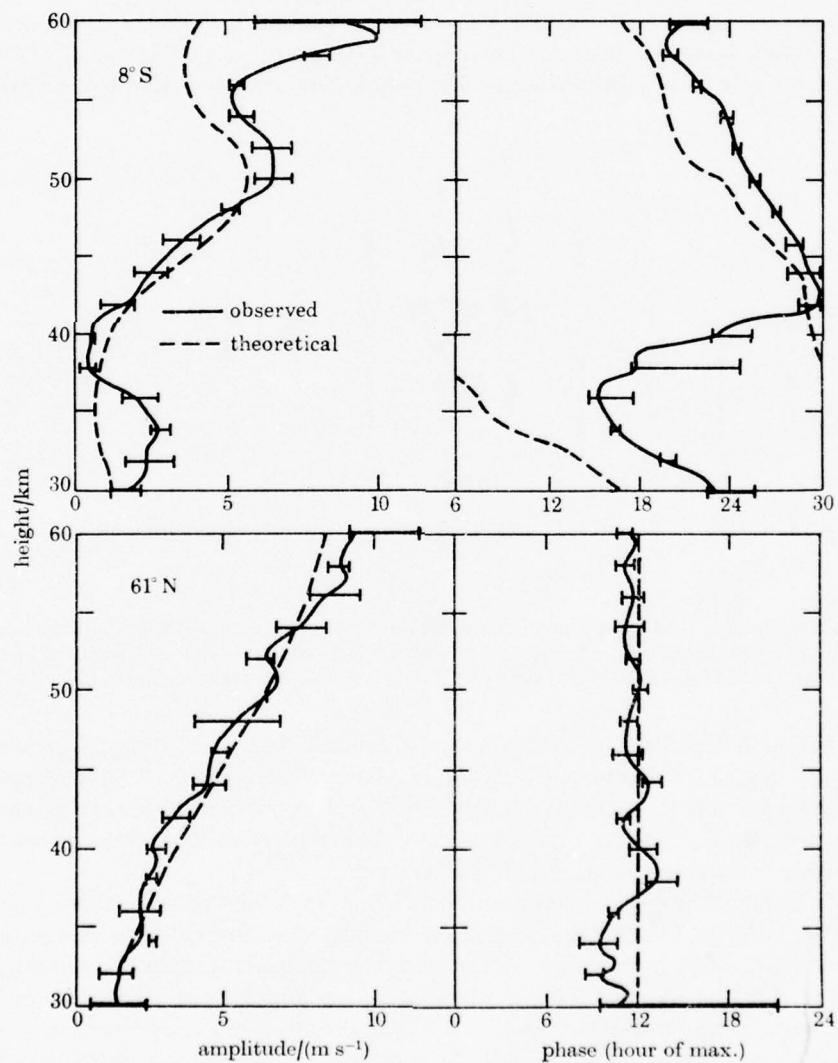


FIGURE 4. Diurnal amplitudes and phases of S-N wind at  $8^\circ\text{S}$  (annual data from Ascension Is.) and  $61^\circ\text{N}$  (summer data from Fort Churchill & Fort Greely), the observed curves being derived from regular M.R.N. launchings and the theoretical curves from Lindzen (1967) (Reed *et al.* 1969).

the diurnal frequency, the solutions of Laplace's tidal equation had a second set of Hough functions which had hitherto been overlooked. 'Positive' modes of oscillation which correspond to the originally known set of functions propagate away from a region of excitation with a rotation of the horizontal wind vector and an increase of amplitude with height in the manner of the wind structures seen in figure 1. Moreover such oscillations are inconsequential at latitudes poleward of  $45^\circ$  latitude. On the other hand, the newly-discovered 'negative' modes of oscillation decay away from the region of thermal excitation without rotation of the wind vector with height and without confinement in latitude.

The observational results in figure 4 and those obtained at intermediate latitudes clearly confirmed the predicted transition from negative modes at high latitude to predominantly positive modes at low latitude. At  $61^\circ$  N, the theoretical results were based on the  $(1, -2)$  and  $(1, -4)$  modes, the main excitation being stratospheric; and their excellent agreement with the observed phases (figure 4) confirmed the assumption of a maximum stratospheric heating rate at local noon. At Ascension Island ( $8^\circ$  S) the slopes of both theoretical and observed phase profiles above 45 km corresponded closely with the 30 km vertical wavelength of the  $(1, 1)$  mode, but observed phases were 2–4 h greater than theoretical values. Small adjustments to the relative roles of water vapour and ozone heating appeared to be all that was necessary to remove the minor discrepancies between observation and theory; and Reed *et al.* (1969) recommended a re-examination of the ozone heating, this being less accurately known than the water vapour heating. Differences between observed and calculated  $(1, 1)$  phases will be discussed again below (figures 5 and 23).

From the same data set, Reed (1972) was able to obtain semidiurnal wind components in summer for two groups of stations lying close to  $30^\circ$  and  $37^\circ$  N. In contrast to the diurnal components, the observational findings were plainly in disagreement with predictions of classical tidal theory (Lindzen 1968; Chapman & Lindzen 1970). Observed amplitudes at 60 km were only half the predicted value of 8 m/s and a very striking difference was the presence of an unexpected reversal of phase at 45–50 km altitude. Reed suggested that the basic atmospheric wind structure which theory ignored may exert an effect on tidal behaviour that would account for these differences. In subsequent calculations of both solar and lunar semidiurnal tides Lindzen & Hong (1974) included zonal winds and horizontal temperature gradients and obtained closer general agreement with observations, the phase reversal previously found at 28 km (without winds) moving up closer to 50 km at mid and high latitudes in summer. Even so, comparisons between observation and theory have yet to be undertaken for the semidiurnal oscillation in the same detail as for the diurnal, present results being limited mainly to  $30^\circ$  N latitude where most launchings have taken place. A possible reason for the difficulty of resolving semidiurnal oscillations from large numbers of routine launchings appears below (§6).

### 3. ATMOSPHERIC TIDES REVEALED BY GRENADE EXPERIMENTS, 35-95 km

Nearly 100 grenade experiments were carried out at the Wallops Island launch site ( $37.8^{\circ}\text{N}$ ,  $75.5^{\circ}\text{W}$ ) between 1960 and 1970. Although this number falls far short of the numbers of launchings combined in the analyses reviewed in §2, grenade experiments have provided data at heights above 60 km where tidal wind amplitudes reach 10-20 m/s and should therefore be more readily detected. At Natal, ( $5.9^{\circ}\text{S}$ ,  $35.1^{\circ}\text{W}$ ) 24 grenade experiments were carried out in 1966-8 by the N.A.S.A. Goddard Space Flight Center and, in spite of the still smaller number of launchings,

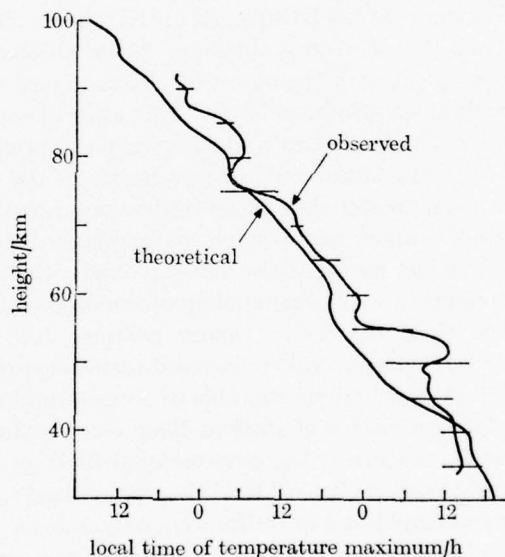


FIGURE 5. Phase (local time of maximum) of diurnal component of temperature at Natal ( $5.9^{\circ}\text{S}$ ,  $35.1^{\circ}\text{W}$ ), the observed curve being derived from grenade experiments in 1966-8 and the theoretical curve from Lindzen (1967).

this site offered several advantages for the resolution of diurnal variations. For example, the month-by-month trend is more regular at low latitude and can therefore be more easily modelled than at higher latitude. Nine unknowns, representing a mean value, diurnal and semidiurnal components and annual and semidiurnal components were fitted to the 24 values at each 1 km of height between 35 and 95 km (Groves 1974). A particular feature of the analysis was the simultaneous solution for diurnal and seasonal components of W-E wind, S-N wind and temperature. Although the 24 launchings were not ideally distributed in local time or season, significant results were obtained at most heights, including heights below 60 km where amplitudes are relatively small. Additional confidence in the results was



provided by the correspondence of diurnal phase profiles with that of the (1, 1) mode, phases changing by 24 h in about 30 km of height.

Figure 5 shows the observed Natal phase (local time of maximum) for the diurnal component of temperature in comparison with that calculated for the same latitude using the tropospheric and stratospheric thermal drives of Lindzen (1967). The systematic displacement between calculated and observed values was estimated as 3.6 (s.d. 0.8) h when account was taken of similar displacements for winds (Groves 1975*a*); the result being in accord with that noted by Reed *et al.* (1969) from analyses of M.R.N. S-N wind data (figure 4).

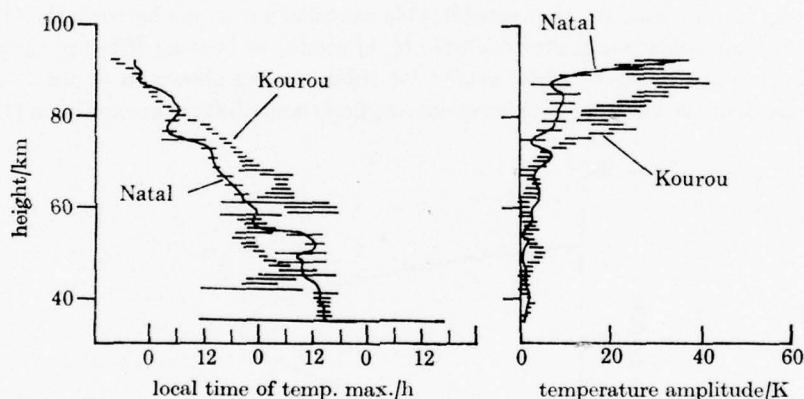


FIGURE 6. Amplitude and phase of diurnal component of temperature at Natal derived by grenade experiments in 1966-8 compared with Kourou grenade experiment results of 19-20 September 1971.

A second set of grenade experiments has provided a valuable opportunity for comparisons with the Natal results being at the same latitude in the opposite hemisphere: on 19-20 September 1971, 13 launchings by the N.A.S.A. Goddard Space Flight Center took place at Kourou ( $5.1^{\circ}\text{N}$ ,  $52.6^{\circ}\text{W}$ ) with an equal distribution in local time for the investigation of diurnal variations (Smith *et al.* 1974). A noteworthy result was the close agreement between the phase profiles of the diurnal wind oscillation at the two sites after introducing a relative 12 h shift of phase between the S-N wind oscillations on account of their location in opposite hemispheres (Groves 1975*b*). In contrast to the wind results diurnal temperature phases at the two sites differed significantly at many heights (figure 6). Whereas the Natal profile had a gradient characteristic of the (1, 1) mode, the Kourou profile had a gradient above 65 km which corresponded closely with that of the (1, 2) mode. The indicated presence of this mode, which is the first member of the set of positive asymmetric modes, was indeed surprising as it called for a low latitude asymmetry in the source of tidal generation corresponding to the (1, 2) Hough function; whereas asymmetries had previously been related to solar declination and depicted by the (1, -1) mode (Lindzen 1967). The corresponding temperature amplitudes also

showed marked differences (figure 6). Between 70 and 90 km, Kourou values exceeded those for Natal by up to 25 K, due it appeared to an enhanced mode, most likely the (1, 2) at the time of the Kourou observations. A (1, 3) mode was apparent in the Kourou S-N wind component and it may be responsible for the temperature amplitude maxima at 77 and 87 km in figure 6, the vertical wavelength of this mode being about 10 km at these heights.

#### 4. SELF-CANCELLATION AND DISSIPATION OF PROPAGATING MODES

Calculations have shown that considerable cancellation occurs between the tidal effects of tropospheric and stratospheric (1, 1) modes of heating (Groves 1975c). On adopting the relative height profile for tidal heating shown in figure 7, the effectiveness of the large stratospheric-mesospheric contribution in exciting a (1, 1)

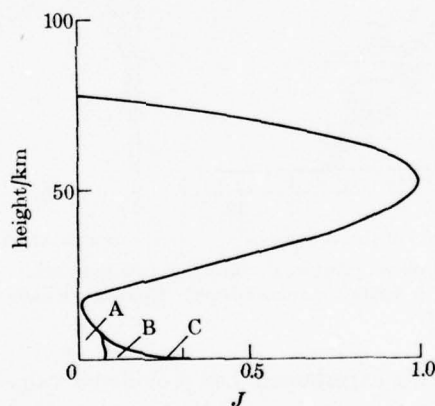


FIGURE 7. A model height profile of the relative amplitude of the diurnal non-adiabatic heating rate per unit mass of atmosphere  $J$ . Contributions are indicated from A, water vapour absorption of solar radiation; B, absorption by particulate matter; and C, energy exchange with the surface.

mode of oscillation was found to be severely reduced by its poor correspondence with the approximately 30 km vertical wavelength of this mode: for the troposphere the correspondence was much closer. By weighting the profile in figure 7 at each level in proportion to its contribution to the (1, 1) tidal amplitudes generated at any given higher level, e.g. at 80 km or above, the curve in figure 8 was obtained, the contribution from any height range of heating being proportional to the area between the curve and the vertical axis over the height range considered. It is seen that the stratospheric-mesospheric region gives rise to four contributions, two positive and two negative, with a net contribution amounting to about 75% of the tropospheric contribution and of the opposite sign; i.e. the net atmospheric response to the (1, 1) mode of heating is about a quarter of that of the tropospheric source alone. The

detailed calculations showed that for higher order modes (i.e. modes of higher meridional wave number), e.g. (1, 2) and (1, 3), the stratospheric cancellation is still greater leaving a net stratospheric contribution which is then small compared with that of the tropospheric source.

A second factor affecting amplitudes is damping. Calculations of thermal tides with the inclusion of dissipative processes have shown that their effect below 100 km is not insignificant for propagating modes (Lindzen & Blake 1971). At 80 km amplitudes were reduced by 13 % when viscosity and conductivity were included and by 26 % when radiative damping using a Newtonian cooling approximation was also included, the mode involved being the (1, 1). Observational evidence of damping would appear to have been provided by the oscillation identified as the (1, 3) mode in the Kourou S-N wind (Groves 1975*b*); the increase in amplitude

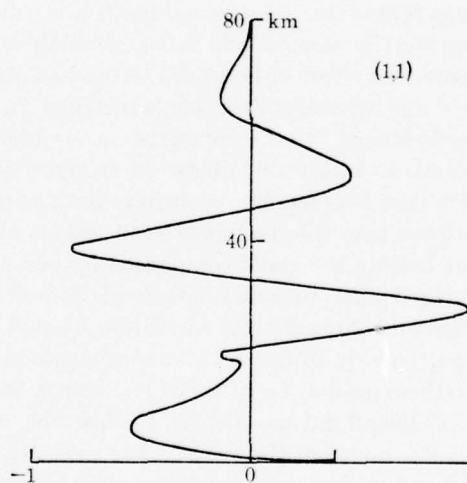


FIGURE 8. Height profile of diurnal heat source (figure 7) weighted according to response at a given higher level.

being less than  $(\text{air density})^{-\frac{1}{2}}$  by a factor of about 2 between 60 and 80 km. That this factor is much greater than the theoretical reductions just quoted may be attributed to the shorter vertical wavelength of the (1, 3) mode (12 km compared with 30 km for the (1, 1) mode). For the (1, 5) and higher order modes with wavelengths of less than 8 km simple extrapolations of the damping factor indicate reductions to less than 20 % of undamped amplitudes at 80 km altitude: such modes would then be unlikely to feature prominently at mesospheric heights.

#### 5. DIURNAL SERIES OF ROCKET NETWORK LAUNCHINGS, 20–60 km

The grenade experiments at Kourou took place just ten years after the introduction of diurnal launch series at Eglin, Florida, in 1961 (Lenhard 1963) when 23 rockets were launched in 23 h and significant diurnal and semidiurnal wind variations were derived at 35, 43 and 64 km altitude. In early 1964 a programme to determine the nature and extent of atmospheric tides in the 30–60 km region was initiated by the U.S. Army Atmospheric Sciences Laboratory and before the end of 1965 four diurnal series of launchings had taken place at the White Sands Missile Range, the last two of which extended over a two-day period so that the recurrence of diurnal motions could be examined (Beyers, Miers & Reed 1966). The advantage of analysing data from concentrated series of launchings in comparison with data from routine launchings (§2) is that no seasonal trend is involved, both W–E and S–N components being equally amenable to harmonic analysis at any time of the year. On the other hand, the effect of non-tidal or random scatter in the data is reduced by combining large numbers of routine launchings. In the experiments at the White Sands Missile Range, wind components showed similar behaviour on consecutive days (30 June to 2 July 1965) between 44 and 56 km, becoming weak and irregular at 40 km and less regular at 60 km. Both components displayed amplitudes of about 12 m/s near the stratopause (52–56 km) with the phase of the meridional component leading the zonal component by about 5–7 h. When this series of data was combined with previous White Sands data, it was concluded that an unmistakable, dominant, diurnal tidal oscillation existed in the stratopause region over this site particularly in the meridional component during most or all seasons. In contrast to these results, a series of 24 launchings over a 2-day period in April 1966 at Ascension Island did not display a consistent, well-defined diurnal oscillation in either wind component (Beyers & Miers 1968). It was concluded that the diurnal variation may have been masked or distorted by some other short-term disturbance at the time of observation or that tidal motion may be inherently more complex at an equatorial station.

Data from series of launchings over a short time interval (1 to 3 days) have been analysed by the author for properties of atmospheric tides between 20 and 60 km. The work is a continuation of that with data from grenade experiments (§3) which showed that even small numbers of launchings, for example 8 or 10, were often sufficient to resolve the diurnal component although accuracies understandably decreased with decreasing numbers of data points, amplitudes being affected more seriously than phases (Groves 1975*d*). Comparisons are made in figure 9 between results at Fort Churchill (58.7° N, 93.8° W) and those at 61.3° N obtained by Reed *et al.* (1969) from routine summer launchings (figure 4). The 19 launchings in 1966 were at 4 h intervals over 3 days and the 18 launchings in 1968 were at 3 h intervals over 2 days. In each case a non-diurnal trend during the interval of observation was allowed for by fitting an expression containing a cubic in time as well as the usual



diurnally and semidiurnally periodic terms, although the modification was not critical to the analysis. In other respects the method of analysis was that previously described (Groves 1967*b*). Figure 9 shows similarities between amplitude and phase profiles for all three sets of observations. Of the 248 summer launchings only 37 were

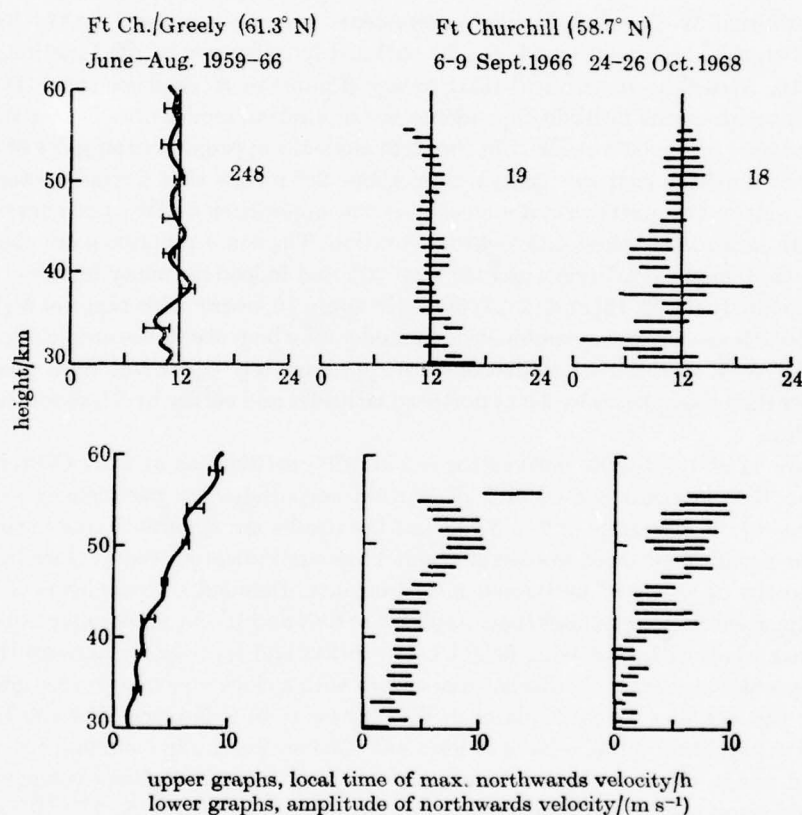


FIGURE 9. Amplitudes and phases of diurnal S-N wind components derived from two series of launchings at Fort Churchill compared with results of Reed *et al.* (1969) for summer data. The number of launchings analysed for each series is shown on the upper diagrams.

outside the hours 08h00 to 16h00 L.T. and therefore the effective number for resolving a diurnal variation was not very much greater than the 18 or 19 multiple launchings. A horizontal line in figure 9 is centred on the most probable value of a quantity and its half-length corresponds to the standard error calculated for this quantity, i.e. there is a 68 % probability that the value lies within the line. As the error bars on the summer data have been calculated by a different method, comparisons between accuracies are probably not meaningful. When comparing the results themselves it should be noted that they are for different dates and that

a seasonal effect could be present. Such changes appear to be small for the months concerned, diurnal oscillations being satisfactorily resolved by the two series of launchings.

#### 6. SEMIDIURNAL OSCILLATIONS

Semidiurnal W-E and S-N wind components may be compared on the basis of a theoretical argument which can be outlined by reference to the functions in figure 10. According to classical tidal theory (Chapman & Lindzen 1970), these functions express the latitude dependence of semidiurnal modes of S-N and W-E wind velocity on a relative scale. For the (2, 2) mode the approximate equality of the curves at northern latitudes greater than about  $20^\circ$  means that a wind vector of almost constant amplitude rotates clockwise. The opposite sign of the two curves at southern latitudes implies anticlockwise rotation. The same properties are shown by the (2, 3) mode at latitudes greater than  $30^\circ$ , and indeed for many higher order modes, namely the (2, 16) and (2, 17) modes in figure 10, over a wide range of higher latitudes. Hence whatever combination of modes may be present, the amplitudes of S-N and W-E semidiurnal oscillations are approximately equal and W-E phases are later than S-N phases by 3 h at northern latitudes and earlier by 3 h at southern latitudes.

Figure 11 shows results derived for semidiurnal oscillations at Fort Churchill. For the 1966 launchings S-N and W-E wind amplitudes are particularly small being mainly in the range of 2 to 3 m/s, but the results are apparently not entirely without significance as accuracies of about 1 m/s are indicated, such values being close to the accuracy of individual measurements. Detailed correspondences are more apparent between phases than amplitudes: S-N and W-E phases move rapidly to earlier times with increasing height below 30 km and less rapidly above 40 km. These profiles are relatively displaced in accord with a clockwise rotation as judged by the vertical lines drawn 3 h later in W-E phase than S-N phase. For the 1968 data, the amplitude profiles have at least one distinct feature in common, a maximum at about 35 km, and phases are again consistent with a clockwise rotation.

Semidiurnal results can also be shown for Wallops Island ( $37.8^\circ$  N,  $75.5^\circ$  W) and Mar Chiquita ( $37.7^\circ$  N,  $57.4^\circ$  W). The data were collected during the Diurnal Tidal Variation Experiment of 19-20 March 1974 (Schmidlin, Yamasaki, Motta & Brynsztein 1975), the comparison being of particular interest as these sites are at the same latitude in opposite hemispheres. The arguments based on figure 10 should still hold at the latitude of these sites with perhaps some enhancement of S-N amplitude relative to W-E amplitude. Figure 12 shows semidiurnal phases and amplitudes derived by the method used for the Fort Churchill data except that the non-periodic terms in the least-squares fit were taken to be linear in time for the Wallops Island analysis and constant for the Mar Chiquita analysis instead of cubic on account of the shorter observing intervals. At Wallops Island S-N and W-E phase profiles show detailed similarity with clockwise rotation. For Mar Chiquita the displacement of the phase profiles corresponds to anticlockwise rotation

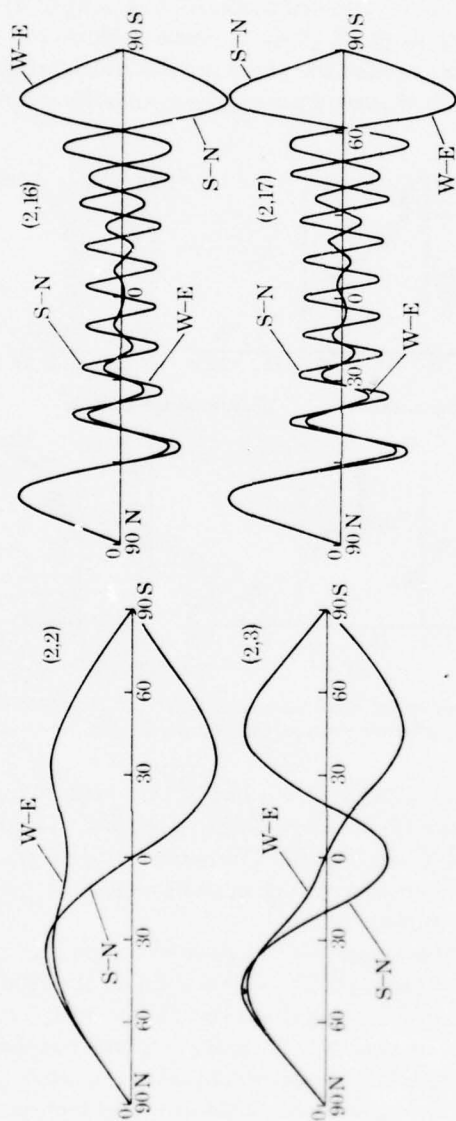


FIGURE 10. W-E and S-N wind functions for various semidiurnal modes in arbitrary units. The approximate equality of the W-E and S-N curves at high northern latitudes corresponds to clockwise rotation of a nearly constant wind vector. The difference of sign at high southern latitudes corresponds to anti-clockwise rotation.

as would be expected for a southern hemisphere site. The W-E profiles at the two sites are generally in phase and the S-N profiles are displaced to an approximately out-of-phase relationship: the interpretation of such comparisons in terms of a superposition of modes is that symmetric modes such as (2, 2), (2, 4) ... predominate over asymmetric ones such as (2, 3), (2, 5) .... Some guide to the order of modes present is provided by the slopes of the phase profiles which are seen to be in the range of 10 to 14 km per 12 h change of phase. The symmetric modes to which such

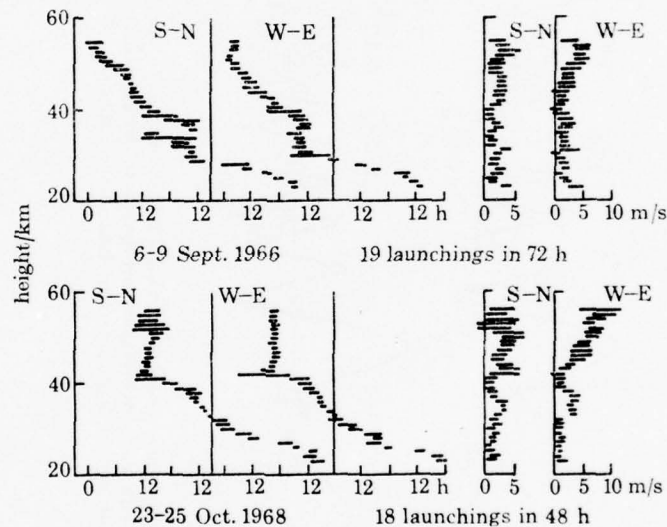


FIGURE 11. Semidiurnal wind components derived from two series of launchings at Fort Churchill.

wavelengths correspond are (2, 14) to (2, 20), but (2, 16) and (2, 20) can be discounted as the wind functions (figure 10) are close to zero at the latitudes of these two sites, leaving mainly (2, 14) and (2, 18). The Mar Chiquita results are remarkable as they derive from only 7 rocket launchings which must be close to the minimum number for any expectation of significant results.

The presence of high order modes is also indicated by the Fort Churchill results (figure 11), the gradients of phase profiles above 40 km in the 1966 data indicating modes of the same order as those just discussed. Below 30 km, modes of a much higher order are indicated by both sets of results, vertical wavelengths being just 3 or 4 km for which corresponding modes would lie in the range (2, 50) to (2, 65)! A transition from shorter to longer wavelengths as height increases could be attributed to dissipative processes which as discussed above (§4) would heavily damp waves of such short wavelengths.

One notable feature of the phase profiles in figures 11 and 12 is their failure to confirm previous theoretical results which present a mainly constant phase arising



from the assumed predominance of the (2, 2) mode. In the classical treatment (Chapman & Lindzen 1970) a rapid phase reversal is obtained just below 30 km between adjacent regions of almost constant phase extending up to the mesopause and down to the surface. In the recent calculations of Lindzen & Hong (1974) with a more realistic atmosphere, the chief modification is to the level at which the reversal occurs. A region of constant phase is present in the 1968 Fort Churchill results at 42–56 km but at lower heights modes of a higher order predominate as discussed above although the (2, 2) and other low order modes are presumably still

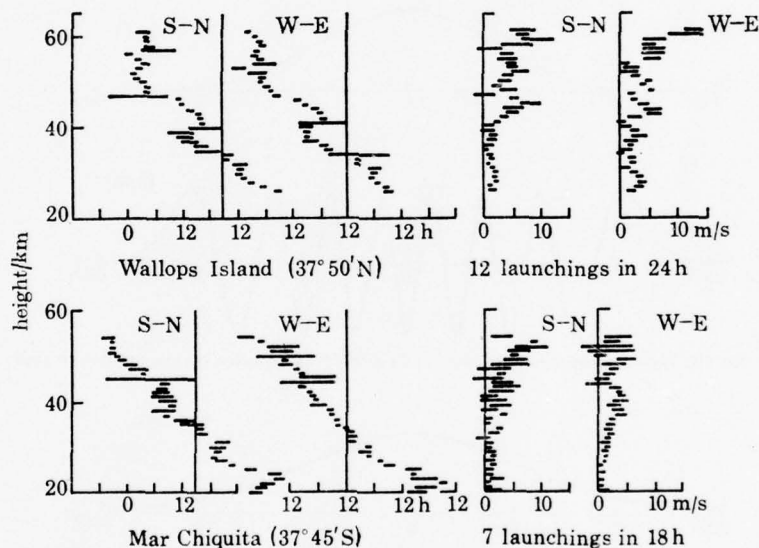


FIGURE 12. Semidiurnal wind components derived from series of launchings at Wallops Island and Mar Chiquita on 19–20 March 1974.

present. The other phase profiles in figures 11 and 12 show a general predominance of high-order modes with near constancy of phase appearing in only very limited height regions if at all. The results are also strikingly dissimilar for the three launch dates, and if such variations between different dates are of general occurrence routine launchings provide a very inhomogeneous set of data. Correspondingly large numbers of profiles are therefore required if any significant analysis is to be achieved, and the results should reveal the contribution of steady modes, the transient ones tending to cancel out. Few semidiurnal results from routine launchings have been published apart from those at 30° N (Reed 1972) which were based on 663 launchings and do indeed show regions of near-constant phase in support of the view that low order modes, e.g. (2, 2), make up the steady part of the oscillation.

## 7. THE GENERATION OF HIGH ORDER TIDAL MODES

The identification of high order semidiurnal modes in stratospheric wind oscillations leads on to the question of their source of generation. The observations themselves show a downward propagation of phase corresponding to an upward propagation of energy and point to a location of the source below 25 km. Also the changing nature of the tidal patterns demands a source of corresponding variability and directs attention to the troposphere.

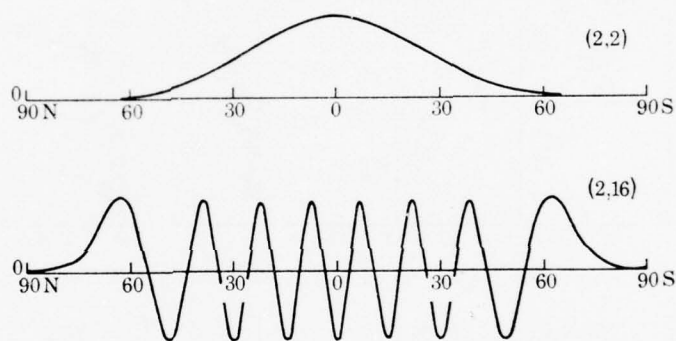


FIGURE 13. Hough functions of the (2, 2) and (2, 16) modes on an arbitrary scale.

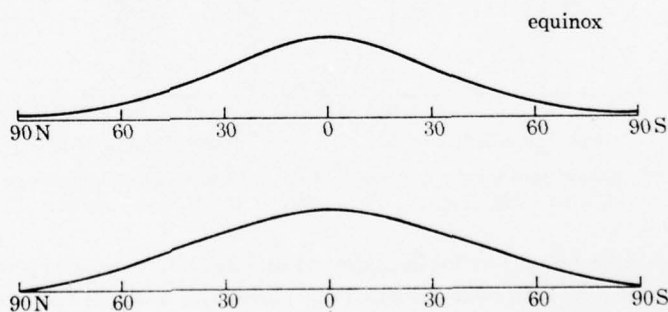


FIGURE 14. Latitude distributions on an arbitrary scale of (top) specific humidity (Siebert 1961) and (bottom) insolational heating by water vapour absorption (Lindzen 1967).

Another consideration is the latitudinal variation required of a source in order to generate the modes observed. This variation is expressed by Hough functions two of which are shown in figure 13, the (2, 16) mode being representative of the range of observed modes. The (2, 2) function has featured prominently in previous theoretical treatments on account of its close resemblance to the adopted latitudinal distribution of insolational heating (figure 14). Also shown in figure 14 is the (equinox) distribution of specific humidity compiled by Siebert (1961), from which the heating distribution is derived with due regard to the change of solar zenith angle with latitude. On the other hand, the (2, 16) function bears no such resemblance

and it is unlikely that any process can be found which more than partially corresponds with such a detailed latitudinal variation: consequently the (2, 16) mode could only be excited as one of a series of modes which add up to a latitude profile departing from the (2, 2) form. Not all such modes would however be significant to the wind oscillation as the tidal effectiveness of a mode depends on the correspondence of its vertical profile with that of the heat source; and modes of wind oscillation would still not be observed at latitudes near the zeros of the corresponding wind functions (figure 10).

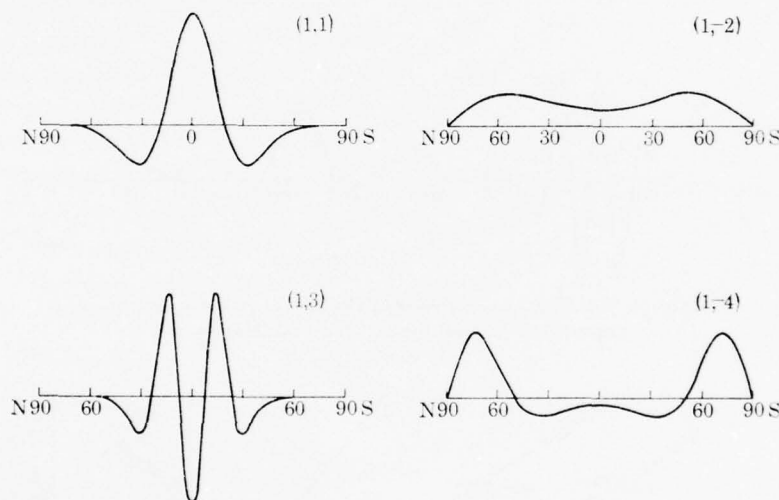


FIGURE 15. The first two members of the sets of positive and negative symmetrical diurnal modes on an arbitrary scale.

Diurnal as well as semidiurnal oscillations would be affected by a modification of the latitude heating profile. The first few members of the sets of symmetric and asymmetric diurnal Hough functions are shown in figures 15 and 16 from which it is noted that a purely high-latitude modification to the tropospheric heating distribution would excite negative modes only. In the vertical direction such modes decay away from the level of thermal excitation and would not generate significant oscillations at stratospheric heights. On the other hand a modification to the latitude profile equatorwards of about  $40^\circ$  latitude would also affect positive modes; and as these propagate vertically with increasing amplitude, upper atmospheric wind oscillations at latitudes less than about  $40^\circ$  latitude would be changed.

Two series of launchings have been held at Cape Kennedy ( $28.4^\circ$  N,  $80.5^\circ$  W) from which the diurnal phases and amplitudes shown in figure 17 have been derived. The phase profiles for 23–25 October 1968 show about  $2\frac{1}{4}$  rotations of the wind vector between 25 and 55 km corresponding to a (1, 3) mode. For 13–15 December 1967 the average gradient of the phase profiles corresponds more nearly with that

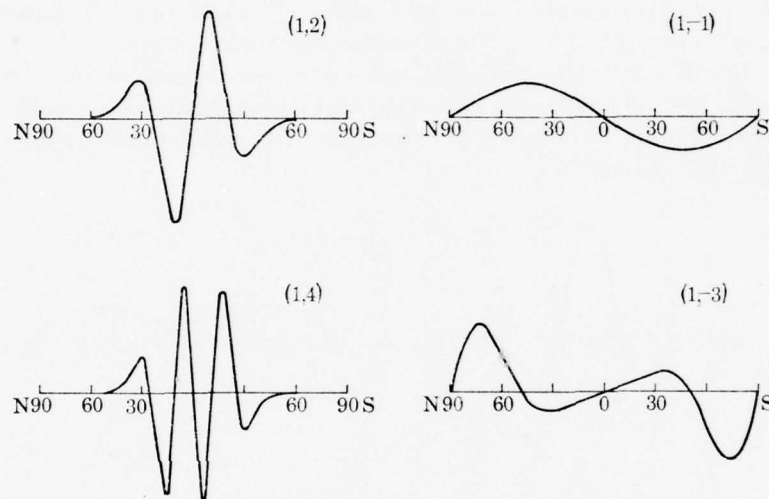


FIGURE 16. The first two members of the sets of positive and negative asymmetric diurnal modes on an arbitrary scale.

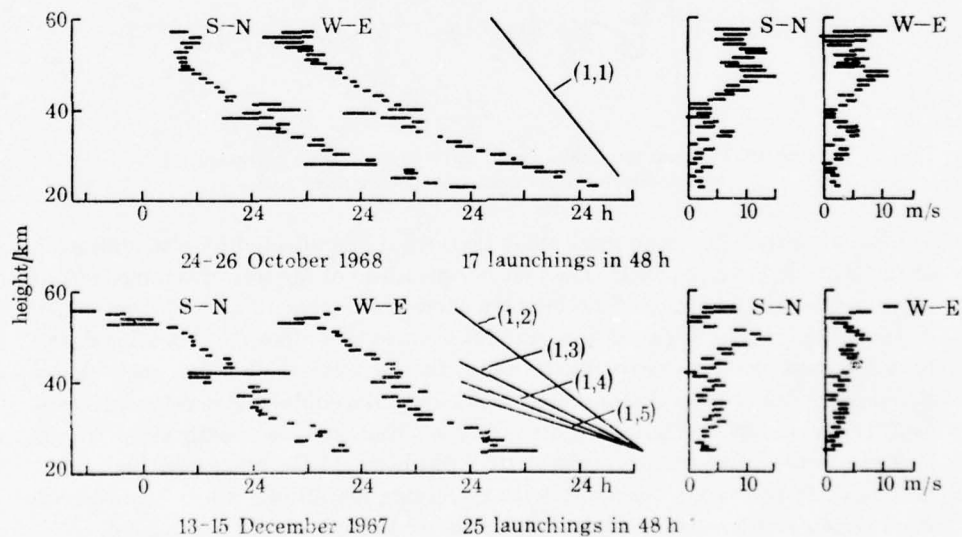


FIGURE 17. Diurnal wind components derived from two series of launchings at Cape Kennedy. The straight lines indicate the approximate theoretical slopes of the phase profiles of the first five positive modes.



of the (1, 2) mode. Such differences between the two sets of results including differences of amplitude could be seasonal but whatever time dependence might be involved it is evident that the wind vectors rotate with height at rates appropriate to modes of a higher order than (1, 1), notably (1, 2) and (1, 3). Figure 18 shows the

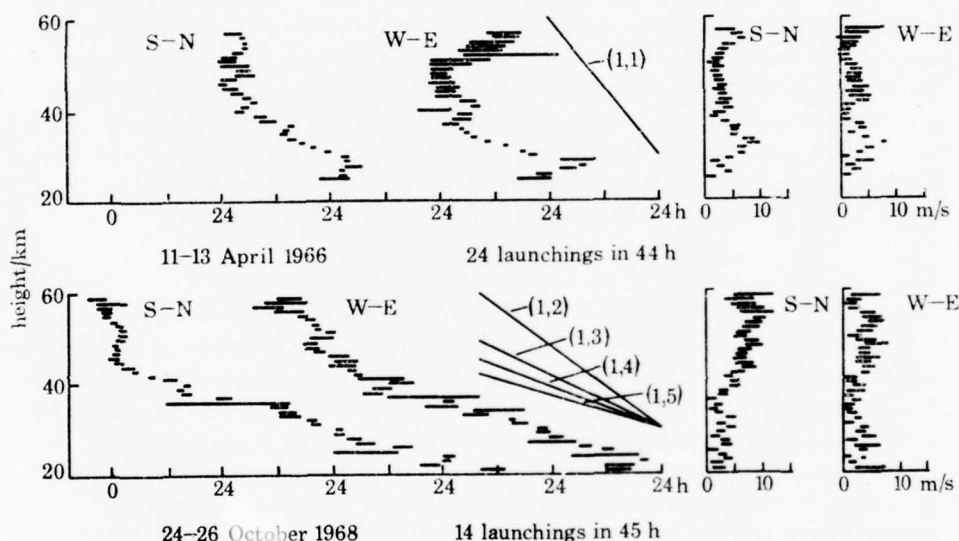


FIGURE 18. Diurnal wind components derived from two series of launchings at Ascension Island. The straight lines indicate the approximate theoretical slopes of the phase profiles of the first five positive modes.

TABLE 1. VALUES OF EQUIVALENT DEPTHS

diurnal modes (1, $n$ )		semidiurnal modes (2, $n$ )	
$n$	km	$n$	km
1	0.691	7	0.706
2	0.238	12	0.243
3	0.120	17	0.121
4	0.072	22	0.072
5	0.048	27	0.048
6	0.035	32	0.035

diurnal winds obtained from two series of launchings at Ascension Island ( $8.0^\circ$  S,  $14.4^\circ$  W) one series being coincidental with the Cape Kennedy series on 24-26 October 1968. The two sets of results again differ considerably and together with the results in figure 17 indicate that variability and high order modes are features of the diurnal as well as the semidiurnal oscillation with the added information that modifications to the source of generation are to be found equatorwards of about  $40^\circ$  latitude.

Whereas the 'higher' order diurnal modes referred to above were the (1, 2) and

(1, 3), being the members adjacent to the fundamental (1, 1), the high order semi-diurnal modes were typically the (2, 16) and were remote from the fundamental (2, 2). A heat source capable of exciting the (1, 2) or (1, 3) modes would be expected to contain important (2, 7) or (2, 8) thermal modes as the Hough functions of these modes are respectively very similar *at low latitudes* to those of (1, 2) and (1, 3). The vertical structure of a mode also plays an important part in determining the tide generating effectiveness of a thermal source, and may account for the presence of modes of order (2, 16) and the relative absence of (2, 7), (2, 8). Table 1 shows equivalent depths (eigenvalues) of leading positive modes and of those semidiurnal modes to which they closely approximate. The equivalent depth is the sole mode-dependent parameter affecting vertical properties, and table 1 shows that semidiurnal modes of order (2, *ca.* 16) do indeed correspond with (1, 2) and (1, 3) on this basis.

#### 8. PROPAGATING MODES AND WATER VAPOUR DISTRIBUTION

The modes to which reference has been made so far in this review have been those associated with *so-called migrating waves*, i.e. waves which move westward with the Sun, having the same dependence on local time at all longitudes. Such modes arise with insolational heating where the absorbing constituent is symmetrically distributed in longitude. Their introduction above has been through observed diurnal and semidiurnal oscillations and the identification of vertical wavelengths in phase and amplitude profiles. No apparent problem has arisen in associating such features with those of particular longitudinally symmetric modes.

Attention nevertheless needs to be given to longitude-dependent modes and their properties as global distributions of water vapour show a marked dependence on both latitude and longitude. Maps of mean January, April, July and October values of specific humidity at 1000, 850, 700, 500 and 400 mbar (100, 85, 70, 50 and 40 kPa) have been presented by Newell, Kidson, Vincent & Boer (1972) for latitudes between 40° N and 40° S. Three regions of maximum values are located in the tropics over Africa, America/Eastern Pacific and SE Asia; and the ratio of maximum to minimum values along the central latitude sometimes exceeds 2 above 700 mbar (3 km) although at the surface the relative difference between maximum and minimum mean values is comparatively small. The 3-wave pattern shifts about 10° of latitude northwards or southwards into the summer hemisphere, the largest excursion being in July at Asian monsoon longitudes. The presence of an  $r$ th harmonic in the longitude dependence of a steady distribution of absorbing constituent and a westward moving Sun results in westward and eastward moving waves of diurnal heating in the  $(r+1)$ th and  $(r-1)$ th harmonics of longitude respectively. Values of east-west (zonal) wave numbers  $s$  of modes arising with  $r = 3$  are then  $s = 4$  and  $-2$ , the negative sign corresponding to an easterly progression of phase. In general the wave numbers  $s_1$  and  $s_2$  of corresponding westward and eastward progressing modes are such that  $s_1 + s_2 = 2$ .

Figure 19 shows equivalent depths of propagating diurnal modes for a range of

low zonal wave numbers. For each westward mode  $(1, s_1, n)$ ,  $s_1 > 1$ , there exists a corresponding eastward mode  $(s_2 = 2 - s_1)$  with an approximately equal equivalent depth. Vertical wavelength depends on atmospheric scale height and gradient of scale height and can therefore be shown only as a range of possible values without reference to a particular height. The predominance of a mode or group of modes having  $s \neq 1$  would give rise to wind oscillations with shorter vertical wavelengths. Figure 19 shows that  $s = 1$  might be observationally distinguishable from the pair  $s_1 = 2$  and  $s_2 = 0$  for the  $(1, s, 1)$  sequence but not for  $(1, s, 2)$ ,  $(1, s, 3)$ , ...; and  $s = 1$  might be observationally distinguishable from  $s_1 = 4$  and  $s_2 = -2$  for the  $(1, s, 3)$

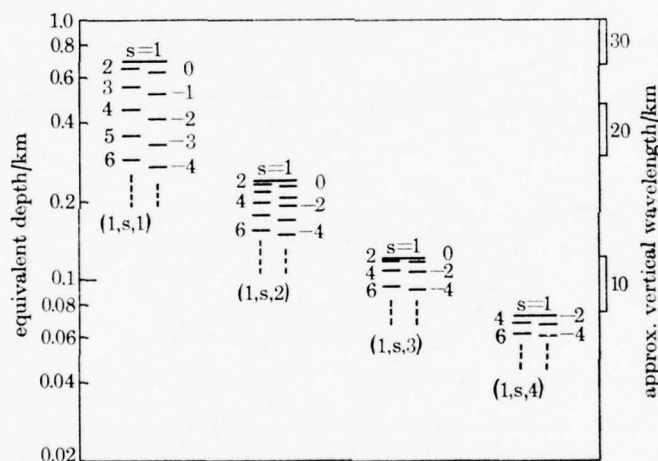


FIGURE 19. Equivalent depths of propagating diurnal modes for a range of low zonal wave numbers. Vertical wavelengths depend on atmospheric scale height and can only be shown approximately.

sequence but not for  $(1, s, 4)$ ,  $(1, s, 5)$ , .... In other words, the vertical wavelength of  $(1, s, n)$ ,  $s > 0$ , might differ from that of  $(1, 1, n)$  with observational significance if  $s > n$ , i.e. if the heating rate and hence the water vapour distribution vary sufficiently rapidly in longitude according to the order of the mode. The evidence available, which is typified by that presented in §§3 and 5, is of a limited nature and so far does not indicate the predominance of any mode with  $s \neq 1$ . The situation could be somewhat analogous to that of diurnal barometric oscillations for which the  $s = 1$  wave (obtained by summing all  $s = 1$  modes) has more than 4 times the amplitude of any other wave (Haurwitz & Cowley 1973). The insensitivity of the vertical structure of propagating modes to longitudinal gradients of heating and the absence of any useful distribution in longitude of observing sites means that almost nothing of an observational nature can be said about the longitudinal properties of upper atmosphere tides at the present time.

Conventional water vapour data are obtained by radiosondes for the standard levels up to 500 mbar and sometimes to 400 mbar (50 and 40 kPa) with less accuracy.

The solid lines in figure 20 have been plotted at two longitudes (approximately those of Ascension Island and Cape Kennedy) from the maps of mean October specific humidity prepared by Newell *et al.* (1972), the values at  $15^\circ$  W being lower than those at  $80^\circ$  W in accord with the 3-wave pattern referred to above. Determinations of water vapour have also been accomplished by satellite observations of the water vapour spectrum and the Tiros 4 results for February to June 1962 confirmed the presence of the three major regions of high moisture content and showed several

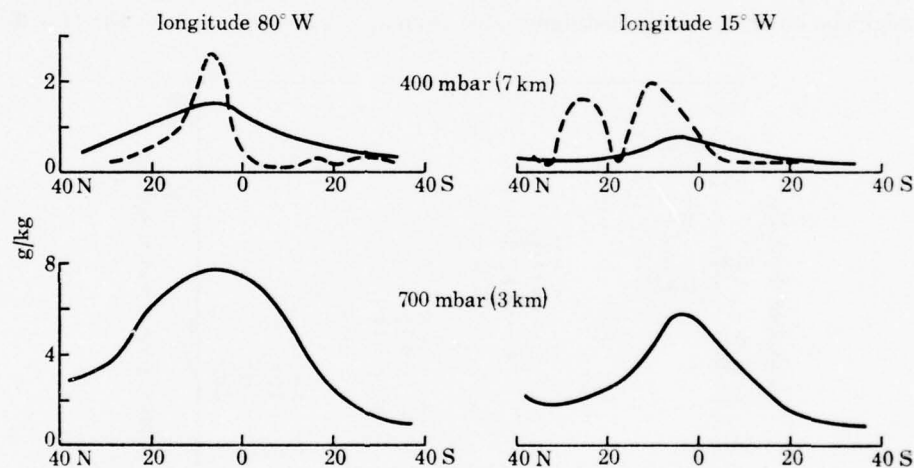


FIGURE 20. Latitude profiles of specific humidity for two longitudes and two levels —, Mean October values; ---, 16-17 October 1970.

other lesser regions near the Intertropical Convergence Zone (Raschke & Bandeen 1967). The distribution of water vapour is however highly dependent upon tropospheric motion and wide deviations can be expected from the monthly mean. The water vapour channel of the Nimbus 4 radiometer receives emissions mainly from an atmospheric layer between 250 mbar and 500 mbar (25 and 50 kPa) with a peak contribution from about 350 mbar (35 kPa): by using both conventional and Nimbus 4 data, a detailed global chart of moisture content at 400 mbar (40 kPa) was prepared for 16-17 October 1970 by Steranka, Allison & Salomonson (1973). As would be expected, considerable changes of moisture content with latitude and longitude are present and it is not immediately obvious what ranges of values of  $s$  and  $n$  would be involved. The  $15^\circ$  W and  $80^\circ$  W profiles shown by broken lines in figure 10 have been read off from this chart and illustrate typical departures from the monthly mean. In particular the changes in latitude now show a closer general correspondence with the Hough functions of the (1, 2), (1, 3) and higher order modes.



## 9. INVERSE TIDAL ANALYSIS

The procedure for calculating tidal fields generated by given gravitational and thermal sources is well described by Chapman & Lindzen (1970) under approximations which lead to separation of height and latitude variables and the so-called classical tidal theory. With the observation of diurnal oscillations over appreciable height intervals the inverse problem of deriving sources of excitation consistent with observed values calls for attention. More specifically, if the amplitudes and phases of the wind and/or temperature oscillations are known for a particular height interval and location, the problem is to investigate the extent to which the properties of the source can be described.

The analysis clearly involves the vertical structure equation, which, when damping is neglected, is

$$\frac{d^2 y_n}{dx^2} - \frac{1}{4} \left[ 1 - \frac{4}{h_n} \left( \kappa H + \frac{dH}{dx} \right) \right] y_n = \frac{\kappa J_n}{\gamma g h_n} e^{-\frac{1}{2}x}, \quad (1)$$

where  $y_n$  is an auxiliary variable from which wind and temperature fields may be derived and  $J_n$  is the non-adiabatic heating rate per unit mass of atmosphere, the suffix  $n$  denoting the mode order and  $h_n$  the equivalent depth.  $H$  is scale height,  $\kappa = (\gamma - 1)/\gamma$ , where  $\gamma$  is the ratio of specific heats of air and  $g$  is acceleration due to gravity.  $x$  is a height dependent variable, being the negative logarithm of the ratio of ambient to surface pressure. When  $h_n$  is such that the coefficient of  $y_n$  is negative,  $y_n$  is exponential and the mode is trapped; when the coefficient is positive,  $y_n$  is oscillatory and the mode propagates. In either case  $y_n$  and derived winds and temperatures depend on  $J_n$  over a range of values of  $x$  which in general will not correspond with the height range of observation.

The inverse problem of deriving  $J_n$  from observed oscillations appears most likely to be tractable when observed winds arise predominantly from trapped modes as there is then an appreciable overlap of the height ranges of heating and observation. In outline, the solution of (1) can be expressed as the sum of a complementary function and particular integral, and the usual boundary conditions of zero vertical motion at the surface and zero downwards energy flux at great altitude can be applied to determine the complementary function. Then by expressing  $J_n$  as a polynomial in  $x$  and relating the particular integral to observed phases and amplitudes, the coefficients of the polynomial can be determined by the method of least squares.

Figure 4 compared the observed summer S-N wind oscillation at 61° N with that calculated by Lindzen (1967) in terms of the (1, -2) and (1, -4) modes. In the inverse problem, one profile would enable only one mode of heating to be derived; however, if profiles of S-N and W-E oscillations are available both the (1, -2) and (1, -4) heating modes may be determined in polynomial form. The analysis has been applied to the Fort Churchill data (figure 9) and the results obtained for 6-9 September 1966 are shown in figure 21. Standard errors derived by the least-squares analysis are shown by cross-lines on the  $J_n$  curves. Accuracy is greatest

near the centre of the height range of observation: towards the lower heights of observation the decrease of accuracy is not too severe as the response to the heating there is biased to higher levels, where observations are available, on account of the decreasing density of the medium with height. Towards the upper heights of observation the same factors lead to a severe loss of accuracy, observations at still greater heights being needed to maintain accuracy.

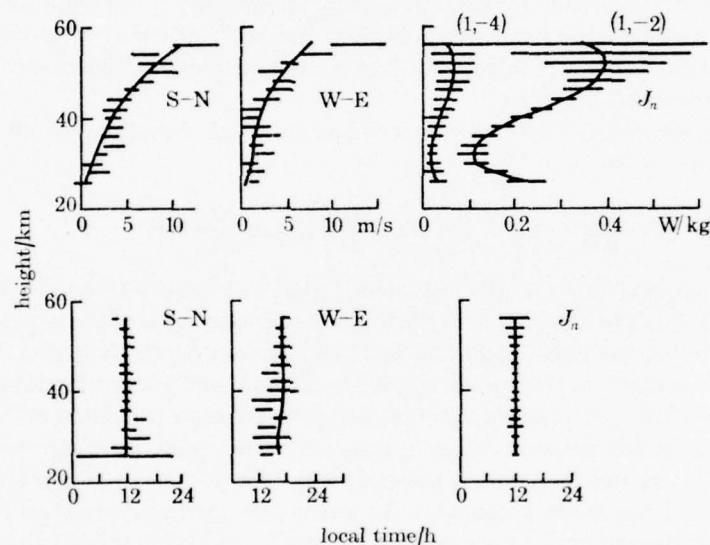


FIGURE 21. Amplitudes (upper diagrams) and phases (lower diagrams) of S-N, W-E diurnal winds at Fort Churchill, 6-9 September 1966 and the derived heating rate coefficients  $J_n$  ( $n = -2, -4$ ) for the (1, -2) and (1, -4) modes. The curves on the S-N and W-E wind diagrams have been calculated from these heating rates.

For both (1, -2) and (1, -4) modes, figure 21 shows that maximum heating is obtained at local noon being governed mainly by the S-N wind phase and to a lesser extent by the W-E. If the oscillation were purely (1, -2) mode, W-E amplitudes would theoretically be 72% of S-N amplitudes; hence as the actual ratio is close to this value, it follows that only a relatively small (1, -4) heating is to be expected. The relative magnitudes of the (1, -2), (1, -4) modes depend on the latitudinal gradient of heating which can be expected to change, for example, with season; and the observational investigation therefore needs to be taken further to enable comparisons to be made. The increase of  $J_n$  amplitude below 30 km would appear to be significant, and this is another feature of the results in figure 21 which needs to be followed up.

A different inverse problem arises with propagating modes as the source of excitation may be in the troposphere and therefore outside the height range of

observation. With the usual surface boundary condition of zero vertical velocity it is found that from observations at heights greater than  $z$  a value may be obtained for the integral  $\int_0^z M_n J_n dz$ , where  $M_n$  is related to solutions of the homogeneous form of (1).  $M_n$  may be regarded as a function which weights  $J_n$  at any height according to its contribution to the tidal fields at a given higher level. Figure 22 shows  $M_n$  for the first six positive modes and their semidiurnal equivalents as listed

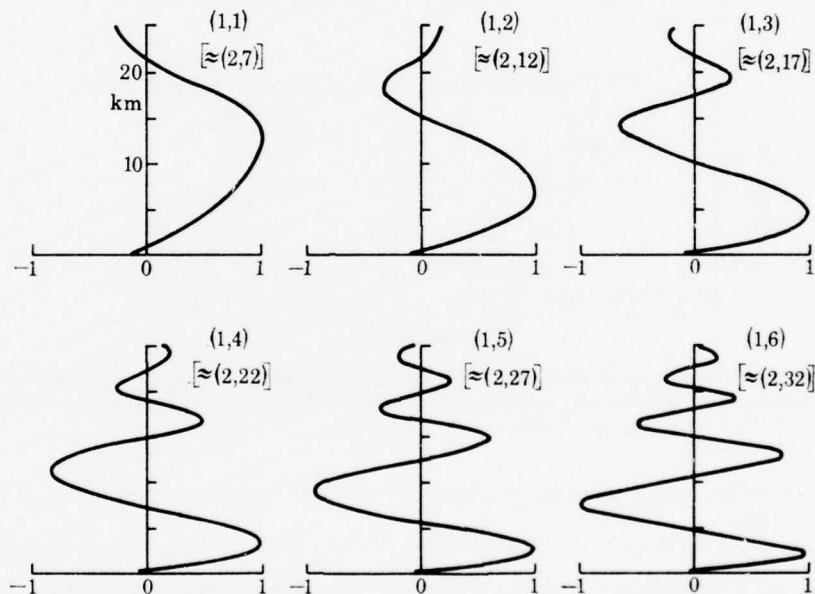


FIGURE 22. Functions  $M_n$  ( $n = 1, \dots, 6$ ) on an arbitrary scale which weight  $J_n$  the coefficient of the  $(1, n)$  mode of heating at any height according to its contribution to the tidal fields at a given higher level.

in table 1.  $M_n$  depends on the basic temperature profile and the curves in figure 22 are appropriate to a low latitude atmosphere. For all modes illustrated a near-surface source is relatively ineffective in generating tides at higher levels; although such a source would be effective in generating barometric oscillations (Groves 1975c). For the generation of upper atmosphere tides each mode has particular heights at which a source would be most effective and intermediate heights at which it would be ineffective. For the  $(1, 1)$  mode, the coupling extends over the whole troposphere and is maximum at about 13 km. The same can be said for the  $(1, 2)$  mode, except for a drop in the level of maximum coupling to about 7 km; and likewise for the  $(1, 3)$  mode, if upper troposphere heating is relatively small, maximum coupling being at about 5 km. On passing to higher order modes, self-cancellation occurs and a broad region of tropospheric heating would become increasingly ineffective as a tidal source.

Apart from these general considerations attention has been given to the application of tidal theory to the evaluation of the integrals  $\int_0^z M_n J_n dz$  from observed diurnal wind oscillations at heights greater than  $z$ . Unless damping is taken into account, it is clear from the evidence of §4 that an underestimate of the magnitude of the integral will result. Attention has therefore been directed to the relation between the phase of the integral and the phase of the corresponding upper atmosphere oscillation as any likely damping can be shown to have an insignificant effect

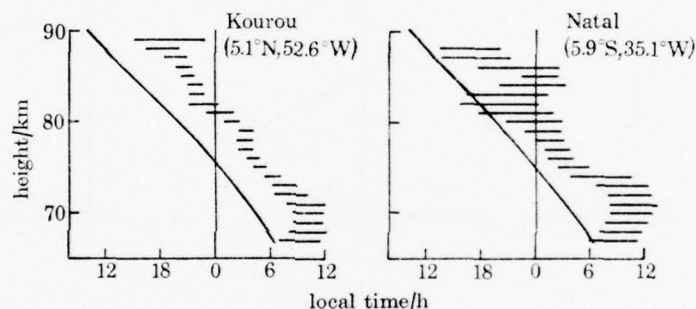


FIGURE 23. Observed phases of diurnal W-E wind (horizontal lines) compared with theoretical values (continuous curves) calculated by classical tidal theory for heating rates at lower levels that maximize at local noon.

on phase. If heating is confined to heights below  $z'$  and has the same phase at all such heights,  $\int_0^{z'} M_n J_n dz$  also has this phase as  $M_n$  is a scalar multiplier; and classical theory then determines the tidal field at heights greater than  $z'$  for the given mode and a given mean temperature profile. A procedure followed has been to take a unit amplitude for  $\int_0^{z'} M_n J_n dz$  and a phase (time of maximum) of local noon, to calculate the corresponding  $(1, n)$  mode of wind oscillation at heights greater than  $z'$  and compare the phase with that of an observed  $(1, n)$  mode of wind oscillation. Generally observed oscillations are a superposition of modes and the feasibility of such a comparison depends on identifying an oscillation or part of an oscillation which comprises a single propagating mode. The W-E diurnal wind oscillations observed by grenade experiments at Natal and Kourou (§3) appear to provide such data above 70 km, the observed gradients of phase identifying closely with that of the  $(1, 1)$  mode.

Figure 23 compares the observed phases with classical theoretical profiles generated by constant phase heat sources (at heights below  $z' \approx 70$  km) which maximize at local noon. Phase differences between observation and theory average 5.5 h for Natal and 6.7 h for Kourou, observed phases being later than the calculated ones. The similarity between these displacements and those in figures 4 and 5



indicate that some common factor is not being adequately taken into account. If the displacement had been one of 12 h, it could be concluded that the net generation of the (1, 1) mode by the stratospheric-mesospheric region of heating was more than sufficient to cancel out that of the troposphere and to actually reverse the phase. However, the displacement is much less than 12 h and one possible approach is to introduce a heating rate which does not maximize at local noon at all heights. Calculations have shown that a 3.6 h displacement would be removed by taking tropospheric heating to maximize only 1 h later, but a difficulty then arose with the (1, 1) mode of surface pressure which could only be removed by the added complication of a height dependent tropospheric heating phase (Groves 1975*e*). As classical tidal theory has been used to calculate theoretical values the discrepancy or a part of it could arise from one or more of the various assumptions on which the theory is based. In particular, the effect of background winds which the theory neglects requires consideration. When these are included however height and latitude dependences cannot generally be expressed in separable form and the analysis becomes considerably more complicated. More detailed calculations need to be undertaken and compared with a larger volume of observational results before a satisfactory basis for the interpretation of propagating modes can be described.

#### 10. DISCUSSION

The principal components of solar tidal variation observed in both surface pressure (Haurwitz & Cowley 1973) and winds at meteor ionization heights (Webb 1972) are diurnal and semidiurnal. Tidal investigations in terms of these two components have been extended over the last ten years into the intermediate regions of the stratosphere and mesosphere by the application of rocket techniques for wind and temperature measurement. Several series of launchings have been specially conducted to investigate tides on an exploratory basis, while other results have been derived as a by-product of launchings conducted for other purposes. In relation to the complex vertical and horizontal structure of atmospheric tides and their seasonal and shorter-term variations observational coverage is at present extremely meagre. In the height range 35–90 km, one of the most effective methods of wind and temperature measurement has been the grenade experiment, and two sets of diurnal results have been provided by this technique at the low latitude sites of Natal and Kourou. These results feature rather conspicuously in this review on account of their unique nature: between 60 and 90 km phase profiles are observed that can be identified with a single predominant mode such as the (1, 1) or (1, 2) and there is evidence of damping in amplitude profiles. In the height range 25–60 km, about 20 diurnal series of launchings have been held of which 8 took place simultaneously during the Diurnal Tidal Variation Experiment of 19–20 March 1974 (Schmidlin *et al.* 1975).

The general picture presented by the available data is that in both diurnal and semidiurnal oscillations major contributions arise from modes of higher order than

the (1, 1) and (2, 2) modes, and that such contributions vary considerably between different observing dates. The origin of the higher order modes is considered to be in the troposphere, where the main source of tidal generation is insolation heating by water vapour absorption. The highest moisture contents occur at low latitudes, their distribution being highly dependent on atmospheric dynamics and showing much greater horizontal gradients than are presented by seasonally averaged distributions. The steeper latitudinal gradients of moisture content shown, for example, by figure 20 would appear to be adequate to generate the observed order of modes, although detailed relations between water vapour distribution and tidal effect have yet to be established.

For diurnal oscillations phase gradients with height are observed in the stratosphere which have values appropriate to the (1, 2) and (1, 3) modes; and still higher order modes may be present with smaller amplitudes. Several factors are expected to operate against the generation of very high order modes: first a time interval of one to two days would be required to set up a steady tidal oscillation and hence oscillations would only be generated for those modes which are present in the moisture distribution after averaging with respect to its spatial movements and temporal changes over this time interval: secondly, a tropospheric heat source with a broad vertical distribution shows little correspondence with the vertical structure of high order modes and would generate them with decreased effectiveness due to self-cancellation as expressed by the source weighting functions (figure 22): thirdly, damping is greater for high order modes on account of their short vertical wavelengths. For semidiurnal oscillations, similar factors would operate with regard to the propagation of high order modes. Modes with an almost identical vertical structure to the (1, 2) and (1, 3) are the (2, 12) and (2, 17) (table 1) and stratospheric phase profiles appropriate to modes of this order are indeed observed. At greater heights dissipation processes preferentially damp out high order modes and a dominant mode in the lower thermosphere could become the (2, 4) as observed by incoherent scatter measurements (Bernard 1974; Salah & Wand 1974).

Polewards of mid-latitudes diurnal oscillations are observed which are consistent with excitation by negative modes of stratospheric heating. Few observations are available at these latitudes, but as indicated in §9, results may be derived by a detailed type of inverse analysis for modes of stratospheric heating. For semidiurnal oscillations there is no confinement in latitude and oscillations at all latitudes appear to be the sum of long vertical wavelength (height coupled) modes, such as the (2, 2) of mainly stratospheric excitation, and short wavelength high order propagating modes of mainly tropospheric origin.

In view of the frequent reference that has been made to a tropospheric origin for oscillations observed at greater heights, it might appear advantageous to have complementary observations at tropospheric heights. For the propagating modes concerned, amplitudes decrease with decrease of height and the task of accurate measurement is correspondingly more difficult. This difficulty is increased in the case of diurnal oscillations by the superposition of trapped modes of tropospheric

heating which are likely to dominate the oscillation. The relatively small amount of available balloon data on diurnal variations has been reviewed by Chapman & Lindzen (1970): results have usually been obtained for annual averages only and show marked regional dependences, probably associated with surface topography: only in the lower stratosphere does a simple oscillation travelling westward with the Sun appear to be dominating. Stratospheric and mesospheric observations therefore enable tropospherically generated positive diurnal modes to be more readily isolated as tropospheric negative mode contributions are absent; to be more conveniently observed on account of their magnified amplitude arising from the lower air density; and to be studied on a much shorter time scale of just one or a few days compared with the seasonal or annual interval used with tropospheric data.

Very little can be said about the longitudinal dependence of stratospheric tides at present as most data relate to the American continent or adjacent longitudes. The effect of longitudinal dependence on the vertical structure of propagating modes is to shorten vertical wavelengths (§8), but the change will only be detectable for sufficiently large wave numbers. This may be the reason why observed profiles could be discussed above in terms of longitudinally symmetric modes with no apparent shortcomings. For stratospherically excited modes, the assumption of longitudinal symmetry should be justified if heating is simply dependent on solar declination and related photochemistry. However, at the time of stratospheric warmings, intense variations in ozone concentration have been shown to correlate with regions of temperature increase, and longitudinal asymmetries could then be expected to be present in the diurnal and semidiurnal heating rates. The consequences for tidal excitation depend on the horizontal and vertical structure of the heat source, and the type of inverse analysis described in §9 is probably no longer feasible. Sufficient rocket data of tidal oscillations are not at present available polewards of  $45^\circ$  latitude for investigating this situation. The semi-diurnal modes introduced by a high latitude heat source would be of a much higher order than the (2, 2), possibly nearer to the (2, 16) (Fig. 13) or an equivalent longitudinally dependent form. Several features observed in wind oscillations at 80–100 km by meteor radar (Fellous, Spizzichino, Glass & Massebeuf 1974) are similar to those discussed here and it would be surprising if a common tropospheric or stratospheric origin were not responsible.

The flux of energy carried upwards by propagating modes is dissipated at various levels according to the vertical wavelength of the mode concerned: for the (1, 1) mode the main dissipation is in the lower thermosphere. The diurnal energy flux has been estimated theoretically by Lindzen (1967) to amount to just less than half the downward flux of solar radiation absorbed above 105 km (taken as  $2.5 \text{ erg cm}^{-2} \text{ s}^{-1}$ ;  $2.5 \text{ mJ m}^{-2} \text{ s}^{-1}$ ). Most of the calculated upward energy flux is carried by the (1, 1) mode and the value at the equator is almost three times the downward flux of absorbable radiation. According to the work reviewed in §4, tropospheric heating alone would generate about 4 times the net amplitude of which 3 parts would be cancelled out by the stratopause region of heating. The point to be made is that the



net flux of energy is sensitive to any change in the (1, 1) mode of heating for one of these regions relative to the other. Changes in solar declination and Sun-Earth distance are common to both regions, but meridional displacements of the water vapour distribution into the summer hemisphere have no obvious counterpart in the stratopause region. At the times of maximum displacement of water vapour, in January and July, the tropospheric (1, 1) mode of heating would be expected to be least, particularly in July on account of the large excursion of water vapour at Asian monsoon longitudes. A simple calculation shows that a 15% reduction in tropospheric heating would approximately halve the amplitude of the net tidal motion; and the upward energy flux which depends on the square of amplitude would then be reduced to about a quarter of its original value! The above numbers are only nominal being chosen to illustrate the appreciable change of upward energy flux that would arise from a small relative change between the two regions of heating. The result emphasizes the need for a more detailed evaluation of tidal heat sources, their contribution to heating in the lower thermosphere and the time variations involved.

In this work on upper atmosphere structure the author has been assisted with numerical analysis and computer programming by Miss A. Harris before April 1975, Miss A. Rawsthorne from April to September 1975 and subsequently by Miss A. M. Yeung; their assistance is gratefully acknowledged. Support has been provided by the Office of Aerospace Research and Development under Grant No. AFOSR-72-2264 and the British Meteorological Office. The diagrams in this paper have been ably prepared by Miss U. Campbell and members of the Departmental Photographic Group. The loan of reports by the British Interplanetary Society Library Service is greatly appreciated.

## REFERENCES

- Bernard, R. 1974 *Radio Sci.* **9**, 295-300.  
 Beyers, N. J. & Miers, B. T. 1968 *J. atmos. Sci.* **25**, 155-159.  
 Beyers, N. J., Miers, B. T. & Reed, R. J. 1966 *J. atmos. Sci.* **23**, 325-333.  
 Bowen, P. J. *et al.* 1964 *Proc. R. Soc. Lond. A* **280**, 170-184.  
 Butler, S. T. & Small, K. A. 1963 *Proc. R. Soc. Lond. A* **274**, 91-121.  
 Chapman, S. & Lindzen, R. S. 1970 *Atmospheric tides: thermal and gravitational*. Dordrecht, Holland: D. Reidel Publishing Co.  
 Elford, W. G. 1959 *Planet. Space Sci.* **1**, 94-101.  
 Fellous, J. L., Spizzichino, A., Glass, M. & Massebeuf, M. 1974 *J. atmos. terr. Phys.* **36**, 385-396.  
 Greenhow, J. S. & Neufeld, E. L. 1961 *Q. Jl R. met. Soc.* **87**, 472-489.  
 Groves, G. V. 1965 *Space Res.* **5**, 1012-1025.  
 Groves, G. V. 1966 *Space Res.* **6**, 1111-1120.  
 Groves, G. V. 1967a *Space Res.* **7**, 986-1000.  
 Groves, G. V. 1967b *Space Res.* **7**, 977-985.  
 Groves, G. V. 1974 *J. Br. interplan. Soc.* **27**, 499-511.  
 Groves, G. V. 1975a *J. Br. interplan. Soc.* **28**, 127-133.  
 Groves, G. V. 1975b *J. Br. interplan. Soc.* **28**, 241-244.  
 Groves, G. V. 1975c *J. Br. interplan. Soc.* **28**, 797-809.



- Groves, G. V. 1975*d* *J. atmos. terr. Phys.* **37**, 1133-1138.  
Groves, G. V. 1975*e* *Space Res.* **15**, 181-189.  
Groves, G. V. & Makariou, S. H. 1968 *Space Res.* **8**, 857-864.  
Hann, J. v. 1889 *Denkschr. Akad. Wiss., Wien* **55**, 49-121.  
Haurwitz, B. & Cowley, A. D. 1973 *Pure appl. Geophys.* **102**, 193-221.  
Hines, C. O. 1960 *Can. J. Phys.* **36**, 1441-1481.  
Hyson, P. 1968 *Q. Jl R. met. Soc.* **94**, 592-597.  
Kato, S. 1966 *J. Geophys. Res.* **71**, 3201-3209.  
Lindzen, R. S. 1966 *Mon. Weath. Rev.* **94**, 295-301.  
Lindzen, R. S. 1967 *Q. Jl R. met. Soc.* **93**, 18-42.  
Lindzen, R. S. 1968 *Proc. R. Soc. Lond. A* **303**, 299-316.  
Lindzen, R. S. & Blake, D. 1971 *Geophys. Fluid Dyn.* **2**, 31-61.  
Lindzen, R. S. & Hong, S. S. 1974 *J. atmos. Sci.* **31**, 1421-1446.  
Newell, R. E., Kidson, J. W., Vincent, D. G. & Boer, G. J. 1972 *The general circulation of the tropical atmosphere*, vol. 1. M.I.T. Press.  
Raschke, E. & Bandeen, W. R. 1967 *Space Res.* **7**, 920-931.  
Reed, R. J. 1972 *Mon. Weath. Rev.* **100**, 579-581.  
Reed, R. J., Oard, M. J. & Sieminski, M. 1969 *Mon. Weath. Rev.* **97**, 456-459.  
Salah, J. E. & Wand, R. H. 1974 *J. geophys. Res.* **79**, 4295-4304.  
Schmidlin, F. J., Yamasaki, Y., Motta, A. & Brynsztein, S. 1975 N.A.S.A. sp-3095, Washington, D.C.  
Siebert, M. 1961 Atmospheric tides. *Adv. Geophys.* **7**, 105-182.  
Smith, W. S. *et al.* 1974 N.A.S.A. TR R-416. Washington, D.C.  
Steranka, J., Allison, L. J. & Salomonson, V. V. 1973 *J. appl. Met.* **12**, 386-395.  
Webb, W. L. 1964 *Astronautics & Aeronautics* **2**, 62-68.  
Webb, W. L. (ed.) 1972 *Stratospheric circulation*. Progress in Astronautics and Aeronautics vol. 27. M.I.T. Press.  
Wilkes, M. V. 1949 *Oscillations of the Earth's atmosphere*. Cambridge University Press.

## LATITUDE AND HEIGHT DEPENDENCES OF SOLAR ATMOSPHERIC TIDES

G. V. GROVES

*Department of Physics and Astronomy, University College London, Gower Street, London WC1E 6BT.*

---

The equations of classical tidal theory have been used to calculate (on a relative scale) certain latitude and height dependences that relate to solar atmospheric tides in the troposphere, stratosphere and mesosphere. The latitudinal dependences are Hough functions which are presented graphically for symmetric and asymmetric diurnal and semidiurnal modes. Two height dependences are developed: one is a function which weights the heating rate at any level in proportion to its response in the surface pressure oscillation; the other is a function which weights the heating rate at any level in proportion to its response in the tidal fields at a given higher level. A typical heating rate profile is adopted to which these weighting functions are applied. The surface pressure oscillation and tidal fields at 80 km are discussed in relation to the levels of heating from which they are mainly excited. Phases of the surface pressure oscillation, expressed as the time of maximum pressure, are calculated for several modes and in view of the various assumptions involved agree well with previously reported observational values for symmetric modes.

---

### 1. INTRODUCTION

THE SUBJECT OF atmospheric tides has been one of long-standing academic interest concerned with the interpretation of barometric oscillations. A major contribution to this study was provided by the first sounding rockets launched in the early 1950's to determine the temperature of the upper atmosphere. The profiles obtained showed that the previously adopted temperatures at 50-60 km altitude were too high and led to the abandonment of the 'resonance theory' which attempted to account for the magnitude of the solar semidiurnal barometric oscillation by resonance magnification of the Sun's gravitational tide. Subsequently tidal theory has been extended to treat thermally generated tides.

In recent years, sounding rocket techniques have contributed further to the study of atmospheric tides by providing stratospheric and mesospheric wind and temperature data at various times of day from which solar tidal components have been resolved. By the grenade experiment technique, diurnal wind and temperature components have been resolved between 35 and 95 km at low latitudes [1]. Observations at these heights are particularly valuable as classical tidal theory is only applicable up to about 90 km due to the onset of dissipation processes and possible non-linearities. Below this level there is therefore the prospect of a comparison between observation and classical theory.

Classical tidal theory neglects non-linearities, molecular and turbulent diffusion, latitude variations of the undisturbed atmosphere, effects of terrain and deviations from hydrostatic equilibrium [2]. Damping due to infrared cooling has been included in an extension of the theory. The above assumptions have been discussed in some detail in Ref. 3 where solutions are obtained for tidal components by the method of separation of variables. Differential equations are obtained for functions of latitude and height respectively, and appropriate

boundary conditions are introduced for their integration.

The latitude dependent functions are solutions of Laplace's tidal equation having zero values at the poles in order to be single-valued. Such solutions, called Hough functions, exist for discrete values of the constant of separation, each value of which defines a possible 'mode' of oscillation. The general solution is then obtained as a summation of such modes.

To each latitude-dependent function corresponds a height-dependent function which is the solution of the 'vertical structure equation' for the same eigenvalue and appropriate boundary conditions. As conventionally defined the eigenvalues have dimensions of length and are referred to as 'equivalent depths'. The lower boundary condition of the vertical structure equation relates to the component of velocity normal to the Earth's surface, the usual assumption being that this is zero. The upper boundary condition relates to the downwards flux of tidal energy across a horizontal surface at the upper boundary level. This is usually taken to be zero by locating the boundary at an adequate height.

## 2. SOLUTIONS OF LAPLACE'S TIDAL EQUATION FOR MIGRATING WAVES

The Hough function  $\Theta_n$  corresponding to an equivalent depth  $h_n$  satisfies Laplace's tidal equation [3]

$$\frac{d}{d\mu} \left[ \frac{1-\mu^2}{f^2-\mu^2} \frac{d\Theta_n}{d\mu} \right] - \frac{1}{f^2-\mu^2} \left[ \frac{s}{f} \frac{f^2+\mu^2}{f^2-\mu^2} + \frac{s^2}{1-\mu^2} \right] \Theta_n + \frac{4a^2 \omega^2}{g h_n} \Theta_n = 0 \quad (1)$$

where  $\mu = \cos \theta$ ,  $\theta$  is colatitude;  $s$  is the longitudinal wave number of the excitation;  $f = \frac{1}{2} m/u_0$ , where  $u_0 = 1.0027$  (the ratio of sidereal to solar angular velocities of the Earth) and  $m = 1, 2, \dots$  for diurnal, semidiurnal .... frequencies;  $a$  is the Earth's radius;  $\omega$  is the Earth's sidereal angular velocity;  $g$  is an average acceleration due to gravity.  $h_n$  is dependent on  $m$  and  $s$  and in general the mode is described as the  $(m, s, n)$  mode with equivalent depth  $h_n^{m,s}$ .

For the particular case of migrating waves,  $m = s$  and the waves move to the west with the Sun. Meteorological elements then have the same dependence on local time at all longitudes and the mode description may be abbreviated to  $(m, n)$ .

Methods of calculating  $h_n$  have previously been described [3, 4] and values from Ref. 3 are shown in Table 1. The corresponding  $\Theta_n$  have been calculated from summations of associated Legendre functions using the tabulated numerical coefficients given in Ref. 3 and are shown on a relative scale in Figs. 1 to 3.

TABLE 1. Values of equivalent depths  $h_n$  in km for  $m = s$  [3].

n	Diurnal modes		Semidiurnal modes	
	(1, n)	(1, -n)	n	(2, n)
1	0.691	803.36	2	7.852
2	0.238	-12.27	3	3.667
3	0.120	-1.81	4	2.110
4	0.072	-1.76	5	1.367
5	0.048	-0.65	6	0.956
6	0.035	-0.64	7	0.706
7	0.026	-0.33	8	0.542
8	0.020	-0.33	9	0.430

# Latitude and Height Dependences of Solar Atmospheric Tides

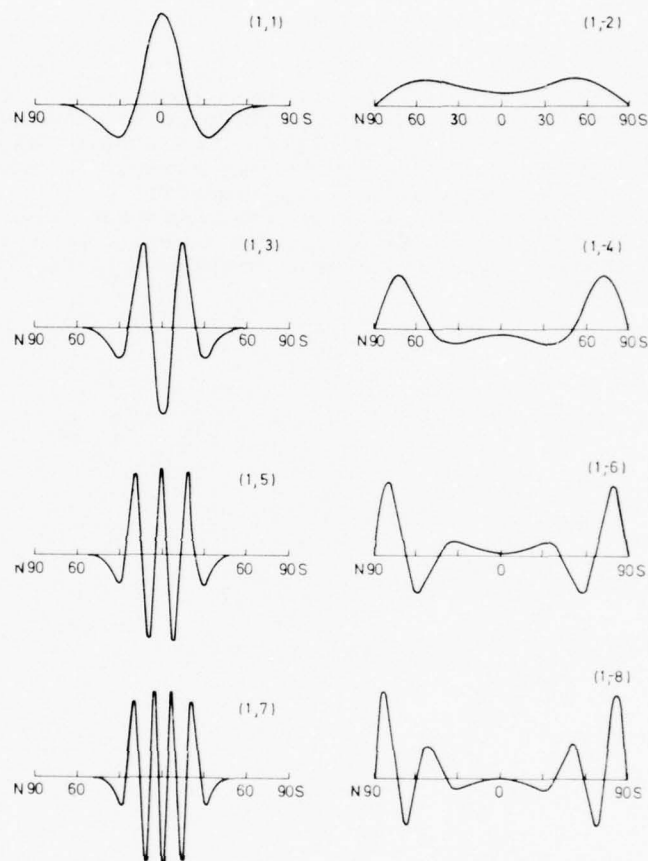


Fig. 1. Symmetric diurnal Hough functions (relative scale).

Any function symmetrical with respect to the equator can be represented by a series of symmetrical Hough functions. For the diurnal frequency there are two sets of Hough functions, whereas for the semidiurnal or higher frequencies only one set arises. The special situation with the diurnal frequency arises because the angular velocity associated with the Coriolis term  $2\omega \sin \phi$ , where  $\phi$  is latitude, becomes equal to the angular velocity of the oscillation at some latitude (namely  $\phi = 30^\circ$ ), whereas for higher frequencies  $2\omega \sin \phi$  is less than the angular velocity of the oscillation at all latitudes. The two sets of diurnal Hough functions relate to latitudinal variations that are confined to latitudes of less than and greater than approximately  $30^\circ$  respectively. For the low latitude set which are denoted by positive values of  $n$  and referred to as positive modes, the equivalent depth  $h_n$  is positive and small (compared with the atmospheric scale height) and the vertical structure is oscillatory with tidal fields propagating to considerable distances from the level of excitation. On the other hand, for the high latitude set, which are denoted by negative values of  $n$  and are referred to as negative modes, the vertical structure is non-oscillatory and tidal fields decay away from a level of heating. The first four symmetric members of each set are shown in Fig. 1. At high latitudes, a given function would be represented almost entirely by negative modes, while at low latitudes positive modes would complete the representation.



The quantity whose latitudinal variation is relevant to the thermal generation of atmospheric tides is the rate of diabatic heating per unit mass of atmosphere. At the equinoxes insolation heating would be expected to maximise at the equator and steadily decrease polewards. Such a variation lacks close similarity with any single Hough function (Fig. 1), but there are partial correspondences with the (1, -2) mode (at high latitudes) and the (1, 1) mode (at low latitudes) and these two modes would be expected to feature prominently in the full Hough function representation of the heating distribution.

At the solstices asymmetric components of heating are likely to be enhanced and Fig. 2 shows the first four asymmetric Hough functions of each set. In this case, the latitudinal variation may be closely approximated by a single Hough

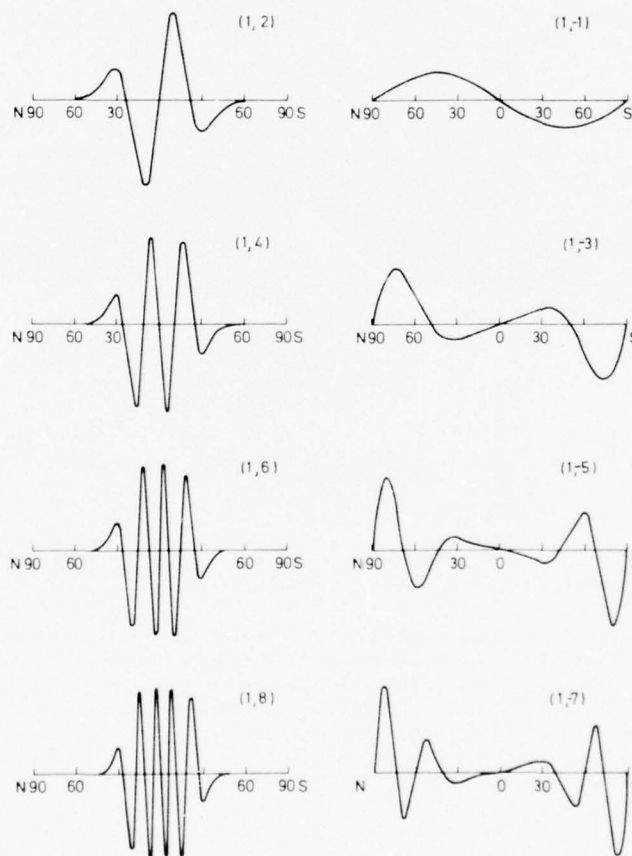


Fig. 2. Asymmetric diurnal Hough functions (relative scale).

function, namely the (1, -1). Such a representation was adopted by Lindzen [5]. On the other hand observations at the low-latitude site of Kourou (5.1°N) have indicated the presence of the (1, 2) mode in the diurnal mesospheric temperature oscillation [1]. It is therefore possible that several Hough functions may be required to represent the asymmetrical as well as the symmetrical latitudinal distribution of diurnal heating.

### Latitude and Height Dependences of Solar Atmospheric Tides

The symmetric and asymmetric Hough functions for the semidiurnal frequency are shown in Fig. 3. In this case, the latitudinal heating profile would be expected to approximate to a single predominant mode, namely the (2, 2) mode.

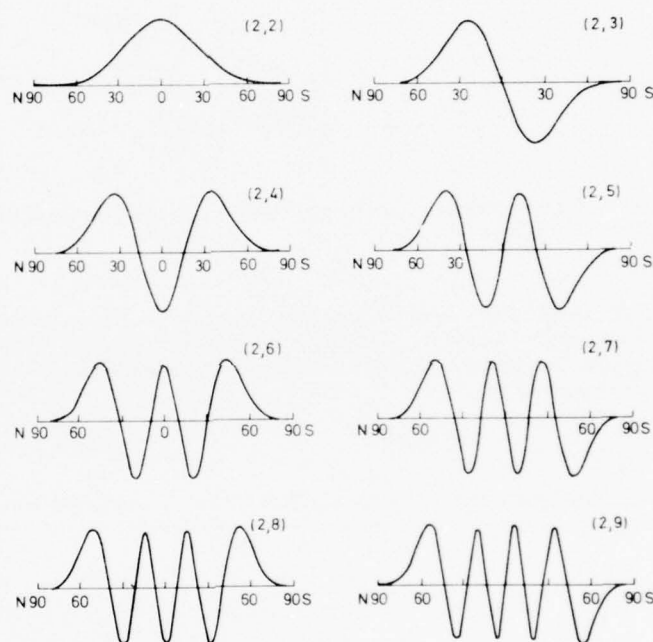


Fig. 3. Semidiurnal Hough functions (relative scale).

### 3. RELATIVE CONTRIBUTIONS TO THE SURFACE PRESSURE OSCILLATION FROM HEATING AT DIFFERENT LEVELS

It is a well-known result [3, 6] that the (2, 2) mode (with an equivalent depth of 7.8 km) is intermediate to the oscillatory propagating modes and the trapped non-propagating modes. Tidal generation by the broad region of stratospheric-mesospheric heating is not self-cancelling for this mode as with oscillatory modes, and tidal fields do not decay away from the region of heating as with trapped modes. Consequently at the surface the main contribution to the semidiurnal pressure oscillation arises from stratospheric and not tropospheric heating.

Global distributions of surface pressure have been analysed by Haurwitz and Cowley [7] into diurnal and semidiurnal Hough function components and their results for annual averages are shown in Table 2. The (2, 2) mode is responsible for the main part of the semidiurnal oscillation, whereas at least three modes make important contributions to the diurnal oscillation.

The calculation of surface pressure is dependent on the integration of the vertical structure equation which for a mode with equivalent depth  $h$  is, when damping due to infrared cooling is neglected, [3]

$$\frac{d^2 y}{dx^2} - \frac{1}{4} \left[ 1 - \frac{4}{h} \left( \kappa H(x) + \frac{dH(x)}{dx} \right) \right] y = \frac{\kappa J(x)}{\gamma g h} e^{-x/2} \quad (2)$$

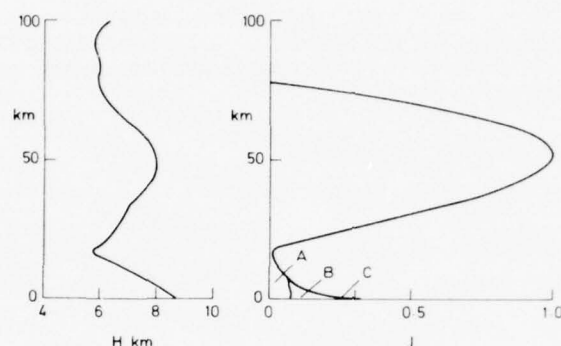


Fig. 4. (Left) Atmospheric scale height  $H$  (km); (Right) Diabatic heating rate per unit mass of atmosphere  $J$  (relative scale).

TABLE 2. Annual amplitudes ( $\mu b$ ) and times of maximum (hours L.T.) of diurnal and semidiurnal modes of surface pressure oscillation [7]. (For asymmetric modes (in brackets) the values are averages of a larger seasonal variation than for symmetrical modes.)

n	Diurnal modes				Semidiurnal modes	
	(1, n)		(1, -n)		(2, n)	
	Amplitude	Time of max.	Amplitude	Time of max.	Amplitude	Time of max.
1	273	5.1	(73	8.0)	-	-
2	-	-	442	5.4	1094	9.7
3	69	17.1	(51	0.4)	(51	0.1)
4	-	-	236	17.1	153	9.5
5	-	-	-	-	(15	1.4)
6	-	-	124	17.1	59	9.5

$y = y(x)$  is an auxiliary function from which the vertical dependence of any meteorological element may be derived for the given mode.  $x$  is the height-dependent parameter

$$x = \int_0^z \frac{d\xi}{H(\xi)}$$

where  $z$  is height and  $H$  is atmospheric scale height.  $J(x)$  expresses the height dependence of a given mode in the expansion of the latitudinal profile of the rate of heating per unit mass; and  $\kappa = (\gamma - 1)/\gamma$ , where  $\gamma$  is the ratio of specific heats of air. In general  $y$  and  $J$  are complex quantities representing both phase and amplitude.

Integrations of (2) have been carried out with the adopted scale height profile shown in Fig. 4 (left) and a heating rate  $J$  whose relative height dependence is shown in the right-hand diagram for all modes. The scale height profile is appropriate to low latitudes and was chosen in preference to one for say mid-latitudes as the integrations of (2) are particularly sensitive to the form of  $H$  in the case of positive diurnal modes which propagate strongly at low latitudes.

The heating rate is assumed to maximise at the same local time  $T$  at all heights for a given frequency of oscillation.  $T$  would be expected to lie close to 12 noon.

In the troposphere three categories of heating are indicated:

- A. Insolation heating by water vapour absorption which has been calculated by the method of Siebert [8] using more recent data on the height variation of specific humidity [9].
- B. Insolation heating by absorption by particulate matter which has been taken as 50 per cent of the heating due to water vapour absorption below 300 mb [10].
- C. Heating by energy exchange with the surface. As no quantitative information appears to be available globally, C has been combined with B and an exponential variation with height adopted.

The contributions of B and C are subject to considerable global variations. C contributes a low altitude 'tail' to the profile which varies between land and sea areas. In the stratosphere, the heating is insolation by ozone absorption and the profile shown is that given by Lindzen [5]. The stratospheric profile has been normalised to unity at its maximum and the tropospheric profile has been scaled accordingly. Although the relative tropospheric and stratospheric contributions are subject to some uncertainty the predominance of the stratospheric contribution is not in doubt and illustrates the effectiveness of the top-side of the ozone layer as an energy absorber per unit mass of atmosphere.

By integrations of (2), functions  $W_p$  have been obtained which weight the heating rate at any height in proportion to its contribution to the surface pressure. Profiles of  $W_p$  and the product  $W_p J$  are shown in Fig. 5 for the (1, 1) mode.  $W_p$  has two components as both phase and amplitude of surface pressure depend on the vertical distribution of heating for positive diurnal modes. One plot relates to

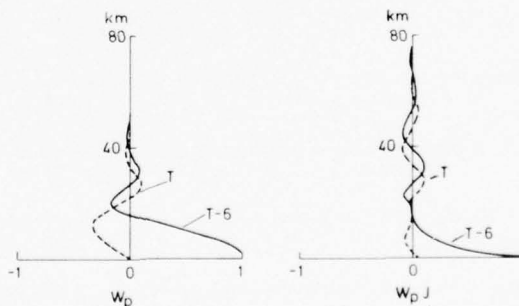


Fig. 5. (Left) The function  $W_p$  which weights the heating rate in proportion to its response in the surface pressure oscillation. Two components of pressure arise, one maximising at T-6 hours L.T. and one at T hours L.T., where T is the time at which the heating rate maximises (provided the product of  $W_p$  and the Hough function value for the heating rate is positive, otherwise these are times of minimum pressure); (Right) The product  $W_p J$  on a relative scale.

a component of pressure which maximises (or minimises) at T-6 hours L.T. if the product of  $W_p$  and the Hough function value is positive (or negative), and the other relates to a component which correspondingly maximises (or minimises) at T hours. The actual pressure variation is the sum of these two components. From the plots of  $W_p J$  the component of pressure maximising (or minimising) at T-6 hours would be reckoned as the positive area between the curve and the vertical axis. As this area is much greater than that for the T hour component,



the (1, 1) mode of surface pressure should therefore maximise (or minimise) close to T-6 hours, i.e. to 6 hours L.T. on taking T to be 12 noon. This result agrees well with the observed value of 5.1 hours L.T. (Table 2) in view of the various assumptions involved.

From Fig. 5, it is seen that the tropospheric heating contribution to the (1, 1) mode of surface pressure is much greater than the stratospheric contribution, for which positive and negative contributions from different levels tend to cancel. The cancelling out of the stratospheric contribution is even more effective with higher-order modes as shown in Fig. 6, and cancelling out also occurs in the troposphere for the (1, 3) and higher modes. As the maximum weight is

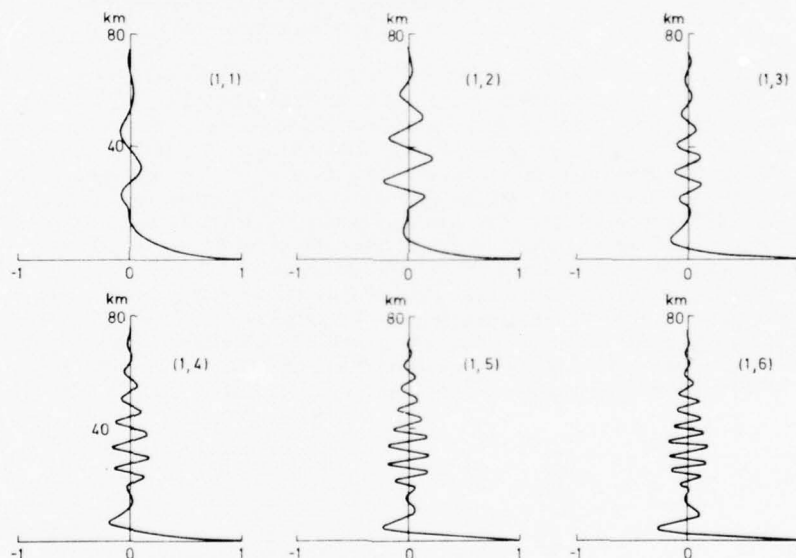


Fig. 6. Plots of  $W_p J$  for the component of surface pressure maximising (or minimising) at T-6 hours L.T. (Positive diurnal modes).

given to heating near the surface, any variation in the low-altitude tail of tropospheric heating can be expected to produce a relatively large response in the surface pressure.

For negative diurnal modes, the T-6 hour weighted heating rate  $W_p J$  is shown in Fig. 7, (the T hour component being zero for trapped modes). In all cases there is increased weighting of the low-altitude heating with practically no contribution from the stratosphere. The (1, -1) mode is exceptional having a corresponding pressure maximum at T + 6 hours L.T. due apparently to its equivalent depth being positive whereas for the other negative modes equivalent depths are negative (Table 1). If the numerical value of the Hough function component of the heating rate is negative, times of heating and pressure maxima are shifted by 12 hours. On taking T to be 12 noon, good agreement is obtained with the observed values in Table 2 for the (1, -2) mode, i.e. 6 hours compared with 5.4 hours L.T. On taking T to be 12 midnight (corresponding to a negative Hough function value) good agreement is also obtained for the (1, -4) and (1, -6) modes, i.e. 18 hours compared with 17.1 hours L.T. Close comparisons are not however obtained for the asymmetric modes. This may be due to their smaller amplitudes and the effect of their greater seasonal variability on the accuracy of an annual average.

# *Latitude and Height Dependences of Solar Atmospheric Tides*

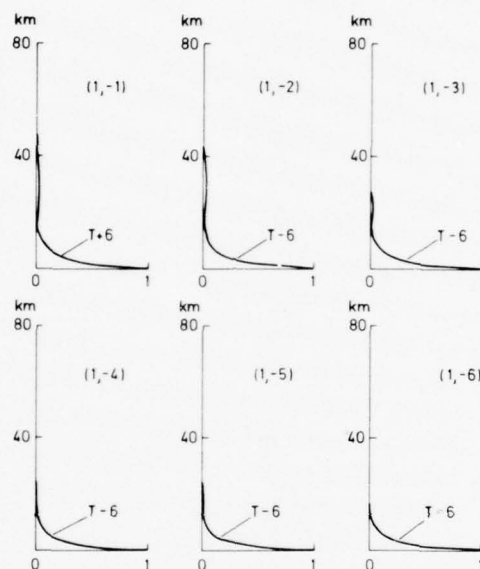


Fig. 7. Plots of  $W_p J$  for negative diurnal modes. There is only one component of surface pressure which maximises (or minimises) at the times shown (for positive or negative Hough function values of the heating rate).

Of the heating processes A, B and C, higher-order modes would be expected to be excited particularly by C, and possibly by B, due to variations between land and sea areas. The diurnal surface pressure oscillation should therefore reflect land-sea distributions through the greater weighting of higher-order thermal excitations at low levels. The global distribution of the diurnal surface pressure oscillation was first evaluated as recently as 1965 [7, 11] due to its detailed dependence on latitude and longitude, and the results do indeed reflect the distribution of oceans and continents.

Figure 8 shows weighted heating rates  $W_p J$  for the first six semidiurnal modes. Only one component arises with the (2, 2) mode corresponding to a maximisation of surface pressure at T-3 hours L.T. On taking T to be 12 noon, maximum pressure for the (2, 2) mode would then occur at 9 hours L.T. In comparison the observed maximum occurs at 9.7 hours L.T. (Table 2). Surface friction would act in the required sense to delay the maximum: on the other hand the discrepancy would disappear if T were taken to be 12.7 hours L.T. instead of 12 noon. A characteristic feature of the (2, 2) mode is the important contribution to surface pressure from stratospheric heating, which by these calculations amounts to 2/3 of the total contribution. For higher-order modes the stratospheric contribution is much reduced due to self-cancelling contributions. For the (2, 7) mode, profiles become almost identical with those of the (1, 1) as the (2, 7) equivalent depth (0.706 km) lies very close to that of the (1, 1) (0.691 km). Since all modes higher than the (2, 2) are of the oscillatory propagating type there is a second component of pressure which maximises (or minimises) at T hours L.T. The results in Fig. 8 show that this component is small compared with the T-3 hour component and hence higher-order modes should still be approximately in phase (or 6 hours out of phase) with the (2, 2). The observational values in Table 2 confirm this prediction for the (2, 4) and (2, 6) modes, but not for the asymmetric (2, 3) and (2, 5) modes which are again smaller in amplitude and subject to greater seasonal variability.

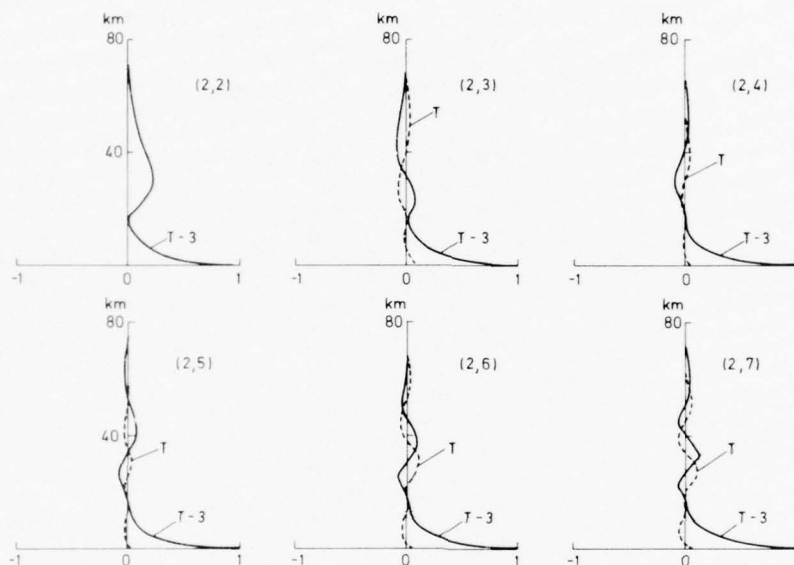


Fig. 8. Plots of  $W_p J$  for semidiurnal modes. There are two components except for the (2,2) mode which maximise or minimise at the times shown (for positive or negative products of  $W_p$  and the Hough function value of the heating rate).

As with the diurnal modes, the greatest weight is given to heating near the surface for producing a semi-diurnal surface pressure response. Nevertheless, the case for a correlation between surface pressure amplitudes and the distribution of land and sea areas does not follow for the semi-diurnal component as it does for the diurnal, because the main contributor to the surface pressure is stratospheric heating (through the (2,2) mode) which is remote from topographical effects.

#### 4. RELATIVE CONTRIBUTIONS TO ATMOSPHERIC TIDAL OSCILLATIONS AT A GIVEN HEIGHT FROM HEATING AT LOWER LEVELS

Reference was made in Section 1 to the use of rocket techniques for observing tidal winds and temperatures in the stratosphere and mesosphere. In the upper mesosphere, tidal winds may be derived from ground-based observations by the meteor-radar and other radio techniques. In all cases, a significant part of the observed oscillation can be expected to arise from thermal excitation at lower levels. In this section the relative contributions of the heating at different lower levels to the tidal oscillation at a given height are presented for various modes and the heating rate profile in Fig. 4.

It follows from the linear nature of the classical theory that the oscillation at any given height may be regarded as a superposition of contributions arising from different levels of heating. Functions  $W_T$  have been calculated which for a given mode weight the heating rate in proportion to its contribution to the tidal oscillations at a given higher level. Graphs of  $W_T J$  are presented which may be regarded as complementary to those in the previous section of  $W_p J$  which showed the relative contributions to the surface pressure oscillation from heating at different levels, the net contribution from any selected height range of heating being proportional to the area between the curve and the vertical axis of the graph. In Figs. 9 to 11, the net contribution from any selected height range of

heating to the tidal oscillation at a given higher level is again proportional to the area between the curve and the vertical axis of the graph.

If we take the given level of observation at 80 km or above, Fig. 9 shows that contributions from stratospheric heating will tend to cancel out for the (1, 1) mode and that the cancellation becomes even more severe for high-order modes.

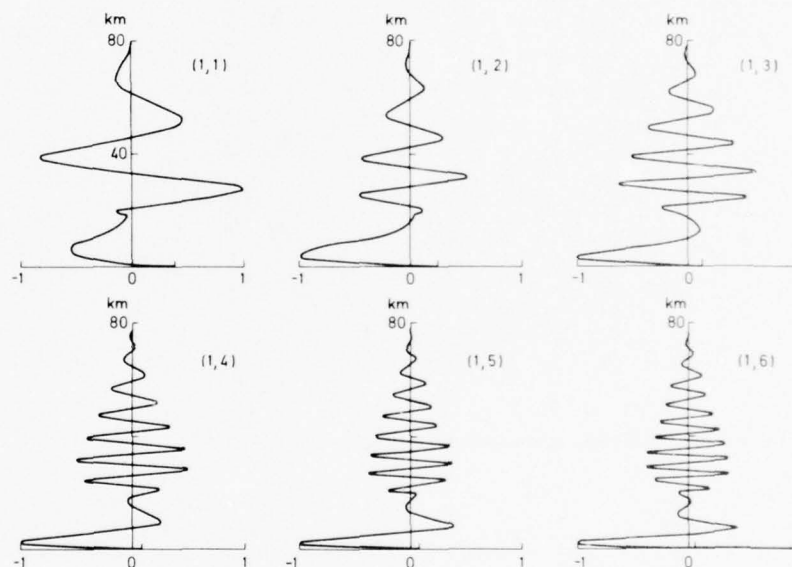


Fig. 9. Plots of  $W_T J$  for positive diurnal modes, where  $W_T$  is the function which weights the heating rate in proportion to its response in the tidal fields at a given higher level.

On the other hand for several low-order modes there are tropospheric contributions which suffer little self-cancellation. For example the main contribution of the (1, 2) mode is from the troposphere where the maximum weighting is at 6 km and the product of weighting and heating rate maximises at 4 km as seen in Fig. 9. The corresponding values for the (1, 3) mode are 4 km and 3 km; and for the (1, 4) mode are 3 km and 2 km (to the nearest km).

In contrast, Fig. 10 shows that if negative modes were observed at 80 km or above their excitation would be from stratospheric heating, which for the low-order modes extends over a very wide height range. From Fig. 11 we see that both stratospheric and tropospheric excitation would in general give rise to semi-diurnal tidal fields at 80 km and above. For the low-order modes the stratospheric contribution is the greater, but for the (2, 7) the situation has reversed and the tropospheric contribution has become slightly greater. Again the (2, 7) and (1, 1) profiles are similar due to the approximate equality of their equivalent depths.

## 5. DISCUSSION AND CONCLUSIONS

Historically the subject of atmospheric tides has been concerned with the interpretation of barometric oscillations excited by the Sun or Moon. In recent years the subject has become one of renewed interest through the observation of tidal fields by rocket and radio techniques over wide ranges of height. The observational results show detailed and complicated variations of meteorological elements



G. V. Groves

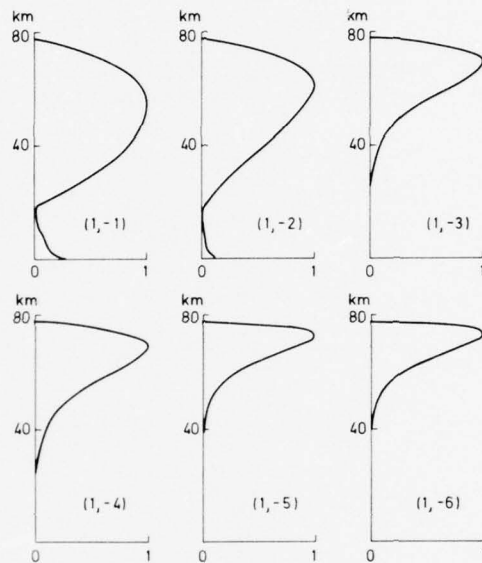


Fig. 10. Plots of  $W_{TJ}$  for negative diurnal modes.

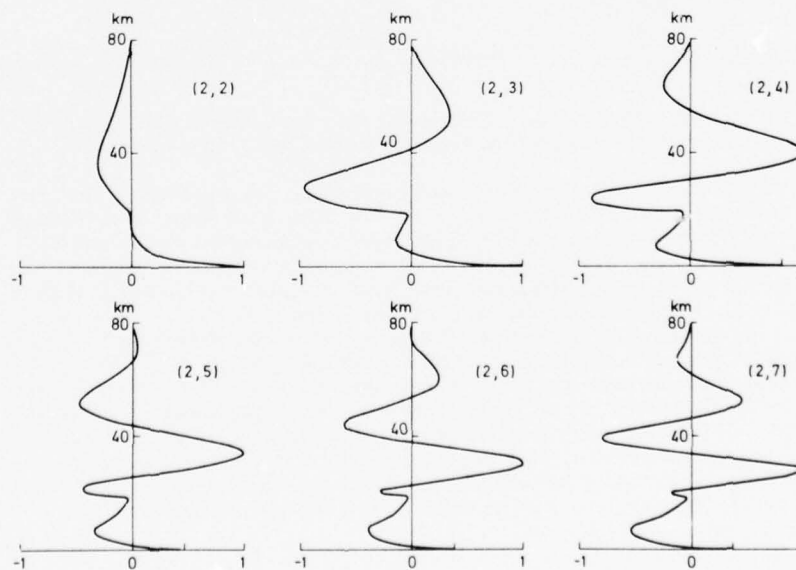


Fig. 11. Plots of  $W_{TJ}$  for semidiurnal modes.

with latitude and height, and the need is apparent for an analytical method of description. Classical tidal theory offers such a description in terms of independently propagating modes provided its application is valid. At 90 km, dissipation processes and possible non-linearities are likely to become significant effects, but

below this height the theory may provide at least a first-order description of practical value.

The calculation of Hough function solutions of Laplace's tidal equation has been reviewed elsewhere [3] and the intention here has been to show the results graphically for the solar diurnal and semidiurnal frequencies and the first few modes. The next step would be to expand the latitudinal distribution of the diabatic heating rate as a series of Hough functions and thereby quantify the thermal excitation of each mode. In this account, we have been content to note the similarity or dissimilarity between the expected latitudinal heating distribution and the Hough functions, and to include the asymmetric functions as these have previously been given less attention than the symmetric ones.

Although calculations have previously been undertaken of the surface pressure oscillation arising from tropospheric and stratospheric heating, the relative contributions from different levels of heating have been lost in the final result. In Section 3, an attempt is made to remedy this situation and the results are shown in Figs. 6 to 8. The contribution of stratospheric heating to the semidiurnal surface pressure oscillation through the (2, 2) mode is apparent in Fig. 8. Any attempt to derive pressure magnitudes is foregone by working in terms of relative quantities. Nevertheless, the results yield the phase of the surface pressure oscillation for any mode, expressed by the local time at which pressure maximises, and comparisons between these phases and those derived observationally are strikingly good for both diurnal and semidiurnal symmetric modes in view of the various assumptions involved.

The investigation presented in section 4 has been motivated by recent extensions of tidal observations to greater heights. The results (Figs. 9 to 11) have been discussed for a level of observation at 80 or so km, and it is pointed out that for certain diurnal modes, namely the (1, 2) (1, 3) and (1, 4), the main part of the observed oscillation would relate to tropospheric heating with levels of maximum excitation at approximately 4, 3 and 2 km respectively. From these remarks and from Figs. 9 and 11 in general, tidal fields at 80 km are likely to be significantly dependent on thermal excitations within the lowest few kms of the atmosphere.

Finally it should be noted that the results presented in sections 3 and 4 are dependent on the heating rate profile in Fig. 4. As far as this is typical of the height variation of the thermal excitation of a given mode, the results should usefully illustrate the tidal response.

#### ACKNOWLEDGEMENTS

The assistance of Miss A. Harris and Miss A. Rawsthorne with computations and the presentation of results is gratefully acknowledged. The work has been supported by the Office of Aerospace Research and Development under Grant No. AFOSR-72-2264 and the U.K. Meteorological Office.

#### REFERENCES

1. G. V. Groves, *JBIS*, **28**, 241-244 (1975).
2. R. S. Lindzen, *Proc. Roy. Soc.*, **A303**, 299-316 (1968).
3. S. Chapman and R. S. Lindzen, *Atmospheric Tides*, D. Reidel Publ. Co. 1970.
4. M. S. Longuet-Higgins, *Phil. Trans. Roy. Soc.*, **A269**, 511-607 (1967).
5. R. S. Lindzen, *Quart. J. Roy. Meteorol. Soc.*, **93**, 18-42 (1967).
6. S. T. Butler and K. A. Small, *Proc. Roy. Soc.*, **A274**, 91-121 (1963).
7. B. Haurwitz and A. D. Cowley, *Pure and Appl. Geophys.*, **102**, 193-221 (1973).
8. M. Siebert, *Atmospheric Tides*, in *Advances of Geophysics*, Vol. 7, Academic Press, New York, 1961.
9. R. E. Newell, J. W. Kidson, D. G. Vincent and G. J. Boer, *The General Circulation of the Tropical Atmosphere*, Vol. 1. MIT press, 1972.
10. Remote Measurement of Pollution, NASA SP-285, p. 188 (1971).
11. B. Haurwitz, *Arch. Meteorol. Geophys. und Bioklimat, A*, **14**, 361-379 (1965).

## ENERGY FLUXES PROPAGATED BY DIURNAL OSCILLATIONS IN THE UPPER ATMOSPHERE

G. V. GROVES

*Department of Physics and Astronomy, University College London, Gower Street, London WC1E 6BT, England.*

For mean January, April, July and October conditions profiles are presented of (1,1) and (1,3) Hough function modes of heating rate per unit mass of atmosphere due to water vapour and ozone absorptions of solar radiation. Tidal response weighting functions are calculated for a typical low latitude basic atmosphere and applied to the heating rates to illustrate the relative effectiveness of heating at different heights in generating tidal fields at 80 km and above. Global averages of the energy fluxes propagated upwards by these modes at 80 km are evaluated; and the results support a value of  $\sim 0.1 \text{ mW/m}^2$  for the tidal energy flux entering the thermosphere by the (1,1) mode when an allowance is made for dissipation at lower heights. For July the flux is 30% lower than for the other months considered and this decrease may be relevant to the July minimum observed in thermospheric air densities.

### 1. INTRODUCTION

IN A DETAILED EVALUATION of diurnal tides below 100 km, Lindzen [1] calculated the flux of energy which propagates upwards above 78 km, the assumed upper limit of the region of ozone heating. The flux arises from positive Hough function modes, the main contributor under assumptions of longitudinal and equatorial symmetry being the (1,1) mode. The calculated flux is therefore latitude dependent having zeros close to those of the (1,1) Hough function  $\Theta_1$  (Fig. 1) at  $19^\circ\text{N}$  and  $19^\circ\text{S}$  latitude with maxima at the equator and at  $32^\circ\text{N}$  and  $32^\circ\text{S}$  latitude where  $\Theta_1$  has extreme values. Being dependent on the square of wave amplitude, the energy flux is proportional to  $[\Theta_1]^2$  and therefore arises mainly at low latitudes, 50 per cent of the flux lying within  $6^\circ$  of the equator. On averaging globally, a mean flux was found [1] which amounted to about half the downward flux of solar radiation absorbed above 105 km (taken to be  $2.5 \text{ mW/m}^2$ ): the dissipation of tidal energy would therefore appear to contribute significantly to heating of the thermosphere. Calculations by Lindzen and Blake [2] show that due to molecular dissipation processes the amplitude of the (1,1) mode reaches a maximum close to 108 km: the main part of the (1,1) mode energy flux would therefore be lost to atmospheric heating below this level.

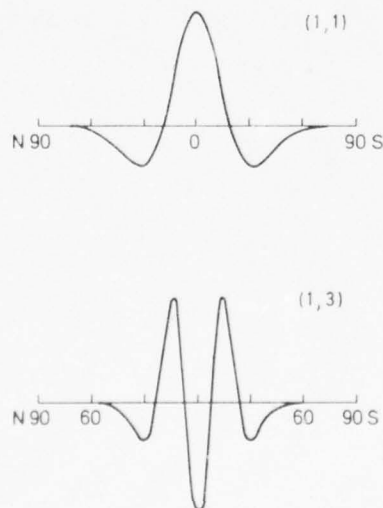


Fig. 1. Hough functions  $\Theta_1$  (upper diagram) and  $\Theta_3$  (lower diagram) of the (1,1) and (1,3) modes on an arbitrary scale.

The present paper is concerned with further evaluations of upward energy fluxes propagated by diurnal oscillations, classical tidal theory being applied to the atmospheric region from the surface to 80 km where fluxes are evaluated by the formula given by Wilkes [3]. Calculations are undertaken for four different months (January, April, July and October) in order to assess the likely variations of flux during the course of the year.

### 2. HEATING DUE TO WATER VAPOUR ABSORPTION

For atmospheric heating by the direct absorption of insolation by water vapour, Siebert [4] derived a simple form of height dependence expressed by the cube root of atmospheric pressure; and this was subsequently adopted by Lindzen [1]. As more detailed data for specific humidity are now available, a re-evaluation of heating rates with regard to both vertical and horizontal dependences would appear to be in order.

If  $q(z, \theta, \phi)$  is the specific humidity at height  $z$ , colatitude  $\theta$  and longitude  $\phi$ , the equations given by Siebert [4] enable the amplitude of the diurnal harmonic of the heating rate per unit mass of atmosphere  $J_O(z, \theta, \phi)$  to be calculated for a given solar declination. The height dependence of the (1,n) mode of heating is then

$$J_n(z) = \frac{1}{\cos \theta} \int_{-\pi}^{\pi} [J_O(z, \theta, \phi)] \Theta_n(\theta) d(\cos \theta) \quad (1)$$

where  $[\ ]$  denotes the longitudinal average and  $\Theta_n$  is the Hough function of the (1,n) mode.

Specific humidity data have been taken from the maps presented by Newell, Kidson, Vincent and Boer [5] at the 1000, 850, 700, 500 and 400 mbar levels for mean January, April, July and October values. Unfortunately at greater tropospheric heights no comparable sets of data are available. A constant water vapour mixing ratio of  $2.5 \times 10^{-6}$  has therefore been adopted for all latitudes, longitudes and heights above the 100 mbar level and values between 400 and 100 mbar have been interpolated by a cubic in pressure which fits the data tangentially at these end points. According to measurements by Mastenbrook [6], stratospheric mixing ratios increased from  $2 \times 10^{-6}$  to  $3 \times 10^{-6}$  between 1964 and 1969 and there was some indication of a small annual cycle.

In evaluating (1), high latitudes may justifiably be excluded from the range of integration as  $\Theta_n$  tends rapidly to zero polewards of mid-latitudes and  $J_O$  also decreases at higher latitudes: the maps of specific humidity [5] which

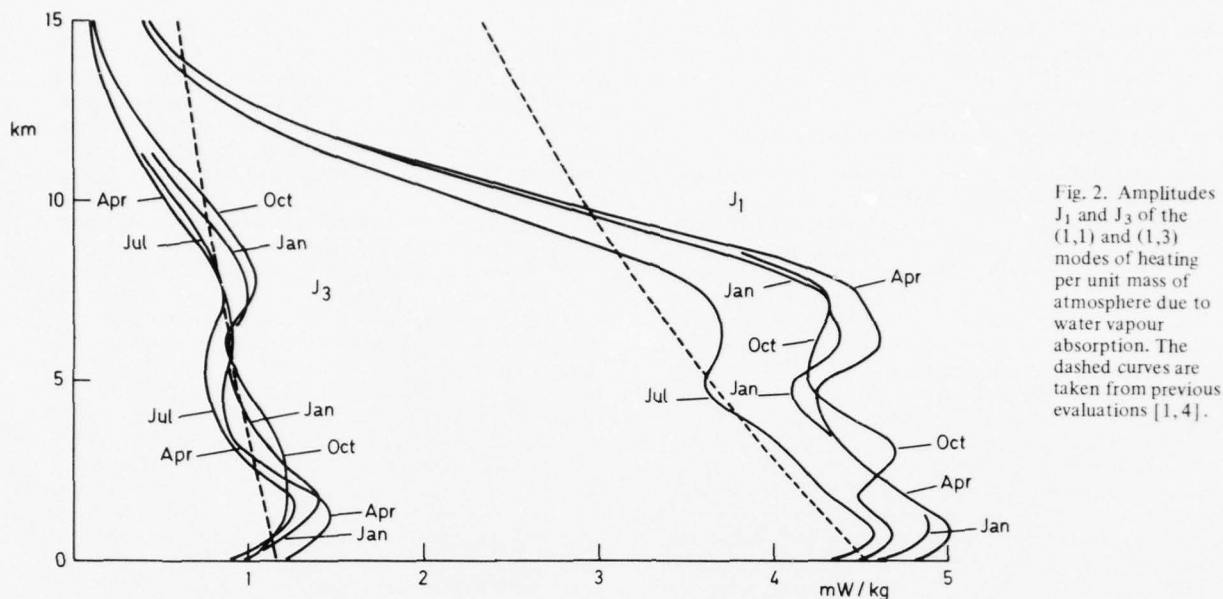


Fig. 2. Amplitudes  $J_1$  and  $J_3$  of the (1,1) and (1,3) modes of heating per unit mass of atmosphere due to water vapour absorption. The dashed curves are taken from previous evaluations [1, 4].

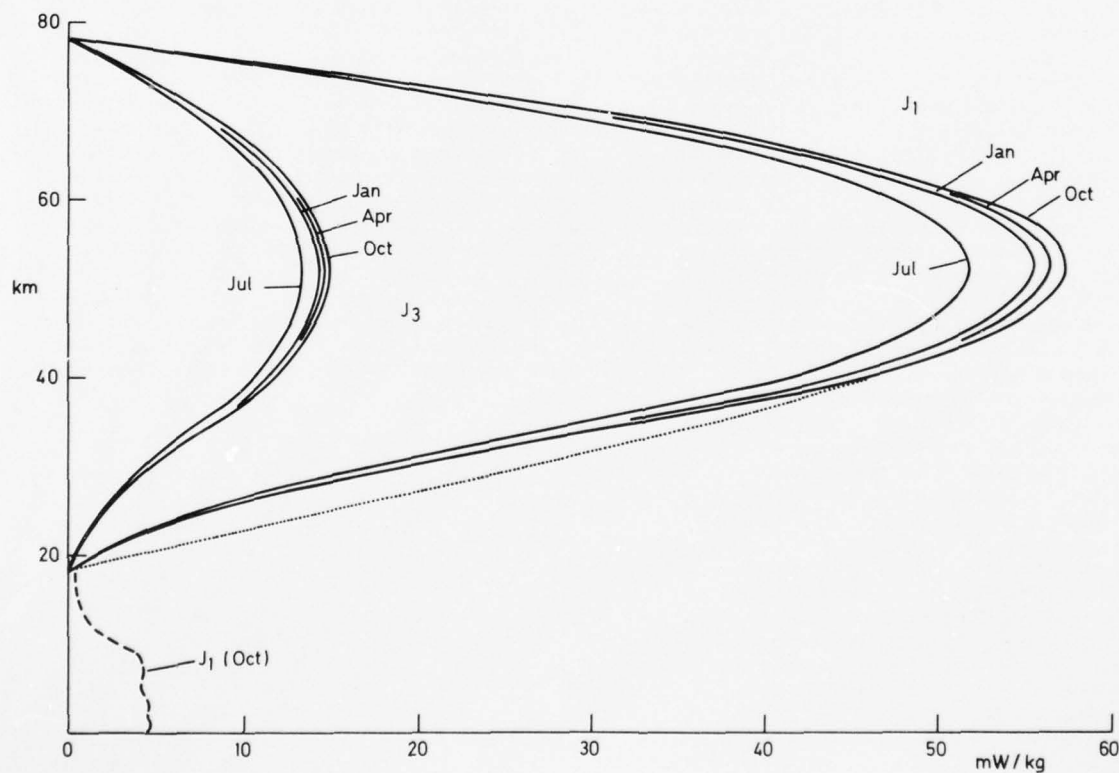


Fig. 3. Amplitudes  $J_1$  and  $J_3$  of the (1,1) and (1,3) modes of heating per unit mass of atmosphere due to ozone absorption. The dotted curve is for October radiative-photochemical equilibrium below 40 km. The dashed curve is taken from Fig. 2.

cover  $40^\circ\text{S}$  to  $40^\circ\text{N}$  latitude were therefore extrapolated to  $55^\circ\text{S}$  and  $55^\circ\text{N}$  latitude, and the integral was evaluated over this range of latitude. Another approximation in the evaluation of (1) has been to replace  $q(z, \theta, \phi)$  by its longitudinal average  $[q]$  in the evaluation of  $[J_0]$ . The error introduced by this reversal of the order of averaging depends on the variation of  $q$  with longitude and was estimated to amount to the order of 1%.

Figure 2 shows the results obtained from Eq. (1) for  $J_n$  ( $n = 1$  and 3). In calculating these results solar declina-

tion was taken for the middle day of each of the four months and a factor was included to allow for the change of Sun-Earth distance. The results are not conspicuously different for January, April and October, but lower  $J_n$  values are obtained in July at all heights for  $n = 1$  and at certain heights for  $n = 3$ . The dashed curves in Fig. 2 show the values used by Lindzen [1] from which the present values differ markedly above 10 km due to the requirement for moisture contents to tend to a mixing ratio of  $2.5 \times 10^{-6}$  at the 100 mbar level. At heights below 10 km, the earlier



values agree well with the July  $J_1$  results but are lower than those for the other months: for  $J_3$  there is good agreement below 10 km.

### 3. HEATING DUE TO OZONE ABSORPTION

For the stratosphere and mesosphere the equinox heating model devised by Lindzen [1] to fit the radiative-photochemical model of Leovy [7] has been adopted and modified. Departures from radiative-photochemical equilibrium occur at the lower heights as ozone lifetimes increase and atmospheric motion becomes an increasingly effective transport mechanism. Below 40 km, the theoretical heating rates have therefore been reduced to correspond with the lower observed ozone concentrations shown by Park and London [8]: the reductions are to 90% of theoretical values at 35 km and to 55% at 25 km (Fig. 3).

Another effect of transport at lower heights is the production of minimum ozone concentrations at the equator and maximum ones in the regions of 60°N and S latitude, where amounts are greatest in spring and least in early autumn. No allowance has been made for this effect as the maxima are only present in the lower stratosphere (below 25 km) and their high latitude location results in weak coupling with positive diurnal modes for which  $\Theta_n$  tends rapidly to zero polewards of mid-latitudes (Fig. 1). Radiative-photochemical conditions may be disturbed at other heights at the time of stratospheric warmings, but such disturbances will be omitted from present considerations as they are relatively transient and coupling with positive (1,n) modes would again be weak.

Variations in heating rates during the year will arise partly from changes in ozone concentration and partly from changes in the flux of absorbable solar radiation. Seasonal time-crosssections of stratospheric ozone concentration are reasonably well established for a number of mid-latitude stations [9], but towards lower latitudes where coupling with positive modes is strongest there is an absence of any marked change with time of year. Account has therefore been taken only of changes in solar flux during the year (through changes in solar declination and Sun-Earth distance). Calculation of the corresponding seasonal factors for particular Hough function modes involves the dependence of ozone concentration on latitude. Except at lower stratospheric heights where radiative-photochemical equilibrium does not hold, observed ozone concentrations appear to increase or decrease at higher latitudes directly with radiational fluxes. Air densities tend to follow the same trend and the ozone-to-air mixing ratio, which is the quantity relevant to tidal excitation, tends to lack any distinct latitudinal variation. The seasonal factors have therefore been calculated on the assumption that ozone-to-air mixing ratios are independent of latitude, further justification being provided by the rapid decrease of  $\Theta_n$  to zero polewards of mid latitudes (Fig. 1).

Ozone heating rates calculated for January, April, July and October are shown by the continuous curves in Fig. 3. The dotted curve is for October radiative-photochemical equilibrium below 40 km and indicates the extent to which the model has been modified in the light of observed ozone concentrations. The October  $J_1$  curve of Fig. 2 has been added to Fig. 3 to illustrate the comparative effectiveness of the ozone layer as an energy absorber per unit mass of atmosphere. Other factors are involved however in comparing the effectiveness of the two regions of heating in exciting tidal oscillations.

### 4. SELF-CANCELLATION OF PROPAGATING MODES

The relative ineffectiveness of ozone heating in exciting the (1,1) mode (in comparison with the (2,2) mode) was

recognised by Bulter and Small [10] when calculating oscillations of surface pressure. They attributed the difference to the shorter vertical wavelength of the (1,1) mode (in comparison with that of the (2,2) mode), the wavelength of about 28 km being less than the height range over which absorption by ozone is appreciable. The same process of self-cancellation also results in a reduced upward propagating wave [11].

If  $J(z)$  is the non-adiabatic heating rate per unit mass of atmosphere at height  $z$  for a given mode then a tidal response weighting function  $W_T(z)$  may be introduced such that  $W_T(z)J(z)dz$  is proportional to the contribution from heating in the interval  $(z, z+dz)$  to tidal fields at greater heights [11].  $W_T(z)$  depends on the given mode and on properties of the basic atmosphere, notably the profile of scale height  $H$ . For the (1,1) mode and a typical low latitude basic atmosphere,  $W_T(z)$  has zeros at 1, 21, 33, 45, 62, 77, ... km (Fig. 4). The change of sign of  $W_T(z)$  on passing through a zero means that heat sources just above and below the height of a zero are self-cancelling with respect to the generation of oscillations at greater heights. Self-cancellation will occur particularly with a height range of heating that spans several zeros, a situation that is more likely to occur with higher order modes as the zeros are then closer together.

When the tidal response weighting function  $W_T$  of the (1,1) mode is applied to the October heating rate profile in Fig. 3, the product  $W_T J$  is obtained as shown by the continuous curve in Fig. 5 on an arbitrary scale. The net contribution to tidal fields above 80 km from any selected height interval of heating is then proportional to the area between the curve and the vertical axis over the selected height interval. In the stratosphere and mesosphere there are two positive and two negative areas which combine to give a considerably reduced net contribution; whereas for the troposphere the area is almost entirely of one sign. From Fig. 5 it is found that the net contribution from the stratosphere and mesosphere is of the opposite sign to that of the troposphere and cancels out 38% of it. Reference has previously been made to the role of the stratopause region of heating in opposing the upward propagation of

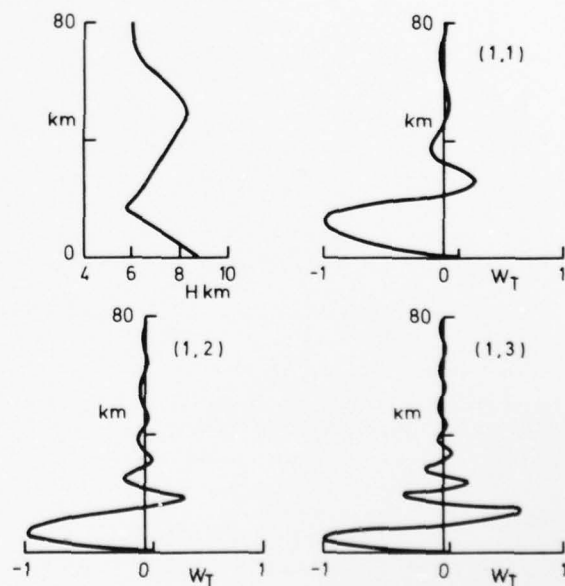


Fig. 4. Plots of scale height  $H$  and the corresponding tidal response weighting functions  $W_T$  for the (1,1), (1,2) and (1,3) modes.  $W_T$  weights the heating rate in proportion to the response of tidal fields at greater heights and is plotted on an arbitrary scale.

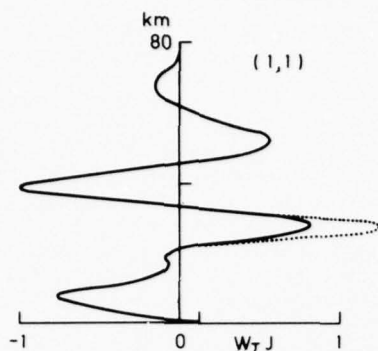


Fig. 5. The weighted heating rate  $W_T J$  for the (1,1) mode on an arbitrary scale.

the tropospherically generated (1,1) mode, even to the extent of a 75% cancellation [12]. This higher percentage cancellation corresponds to ozone heating based on radiative-photochemical equilibrium below 40 km (the dotted curve in Fig. 3) and the dotted curve in Fig. 5 shows how the greater cancellation would arise. The lower percentage cancellation now obtained (38%) is considered to be a more realistic estimate.

When the tidal response weighting function  $W_T$  for the (1,3) mode is likewise applied to the October heating rate profile the product  $W_T J$  shown in Fig. 6 is obtained. In this case the positive and negative areas of the stratosphere and mesosphere almost completely cancel each other out and tidal fields at 80 km are effectively generated by tropospheric heating alone.

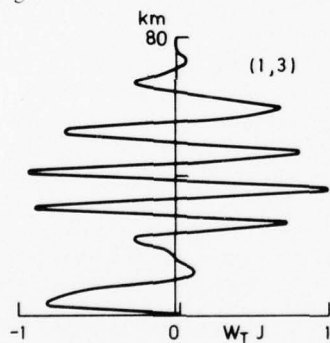


Fig. 6. The weighted heating rate  $W_T J$  for the (1,3) mode on an arbitrary scale.

## 5. UPWARD ENERGY FLUXES AT 80 KM

For the heating rates  $J_1$  and  $J_3$  in Figs. 2 and 3, the upward fluxes of energy at 80 km have been calculated by classical tidal theory [1]. The results obtained for the global averages of these fluxes  $\bar{E}_1$ ,  $\bar{E}_3$  are shown in Figs. 7 and 8.

The most noticeable feature of variation during the year is the lower values of  $\bar{E}_1$  and  $\bar{E}_3$  in July. These lower values are a direct consequence of the lower July values of  $J_1$  and  $J_3$  shown in Figs. 2 and 3. In the stratosphere and mesosphere (Fig. 3) the reduction is due to the factors associated with the greater Sun-Earth distance and solar declination in July. In the troposphere (Fig. 2) the reduction arises partly from these factors and partly from the global displacement of water vapour into the northern hemisphere, the latter effect being responsible for the greater part of the reduction in the middle troposphere. In January there is a meridional displacement of water vapour into the southern hemisphere but the effect of this appears to be largely

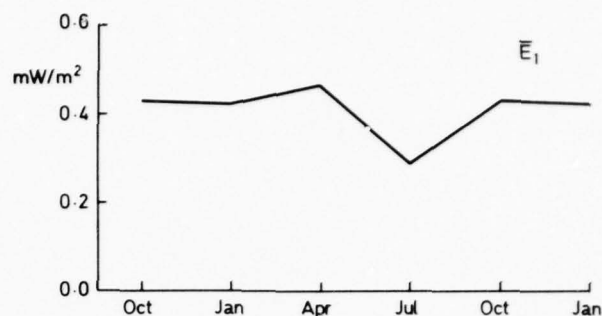


Fig. 7. The global average of upward energy flux  $\bar{E}_1$  of the (1,1) mode at 80 km without dissipation.

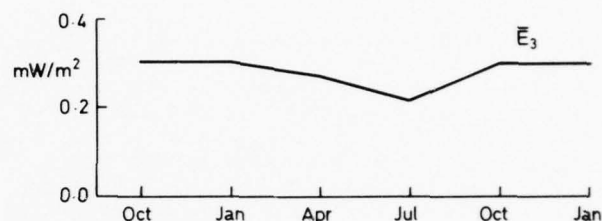


Fig. 8. The global average of upward energy flux  $\bar{E}_3$  of the (1,3) mode at 80 km without dissipation.

counterbalanced by the shorter Sun-Earth distance, January values for  $\bar{E}_1$  being only marginally less than those for April and October.

The results in Figs. 7 and 8 differ from those previously calculated for equinox conditions [1] in two respects: (i) the  $\bar{E}_1$  values in Fig. 7 are only about one-third the previous values and (ii) the  $\bar{E}_3$  values (Fig. 8) are comparable with  $\bar{E}_1$  (Fig. 7) whereas previously  $\bar{E}_3 \ll \bar{E}_1$ . These differences have been investigated by replacing the basic atmospheric scale height (Fig. 4) by  $H = 7.61$  km, the value adopted previously [1], and evaluating the corresponding profiles of  $W_T$  and  $W_T J$  with  $J$  equal to the previously adopted (1,1) mode heating rates (the dashed curve in Fig. 2). Two positive and two negative areas are obtained on the  $W_T J$  graph at stratospheric and mesospheric heights as in Fig. 5, but their net contribution is found to slightly augment the areal contribution for the troposphere instead of subtracting from it. In addition the tropospheric contribution is greater than in the present calculations as much higher water vapour heating rates were adopted for the upper troposphere as shown in Fig. 2. Differences between the present and earlier values of  $\bar{E}_1$  may therefore be satisfactorily accounted for by the revisions that have been made of basic atmospheric scale height and water vapour heating rate.

In the case of the (1,3) mode, the previous relative smallness of  $\bar{E}_3/\bar{E}_1$  arises partly from the larger value obtained for  $\bar{E}_1$  and partly from  $\bar{E}_3$  itself being smaller. In the present calculations the positive areal contribution between 10 and 17 km on the  $W_T J$  graph (Fig. 6) gives rise to only a small subtraction from the main tropospheric contribution between 0 and 10 km; whereas with  $H = 7.61$  km, the zero of  $W_T$  is lowered from 10 to 6 km and greater cancellation occurs between the negative area from 0 to 6 km and a positive area from 6 to 11 km. The detailed representation of  $H$  at tropospheric heights therefore significantly affects the calculation of  $\bar{E}_3$ . This is not the case at stratospheric and mesospheric heights as excitation of the (1,3) mode by ozone heating is subject to considerable self-cancellation due to the great depth of the region of heating in comparison

with the ( $\sim 12$  km) wavelength of this mode irrespective of the detailed representation of basic atmospheric scale height.

## 6. DISSIPATION OF ENERGY FLUXES IN THE UPPER ATMOSPHERE

As mentioned in §1, calculations [2] have shown that the main part of the energy of the (1,1) mode is dissipated below 108 km. The same calculations show that even below 80 km dissipation may not be entirely insignificant: calculated amplitudes at 80 km were reduced by 13% by the inclusion of eddy viscosity and conductivity and by 26% when radiative damping was also included. As energy fluxes depend on the square of amplitude, they would accordingly be reduced at 80 km to 55% of values without dissipation; and this factor of reduction should be applied to the values of  $\bar{E}_1$  in Fig. 7 as these were calculated by classical theory which neglects dissipation.

Of particular interest is the possibility of significant tidal heating of the thermosphere by upward propagating energy fluxes. For the (1,1) mode, energy fluxes entering the thermosphere at say 105 km may be roughly estimated from the results in Fig. 7 by applying a further factor of reduction to allow for dissipation below this level. From the calculations of Lindzen and Blake [2], (1,1) mode amplitudes would appear to be reduced by a factor of 2 at 105 km due to viscosity, conductivity and radiative damping with respect to undamped values; and hence  $\bar{E}_1$  (Fig. 7) would be reduced by a factor of 4, i.e. to  $\sim 0.1$  mW/m<sup>2</sup>. This value agrees with that given by Volland [13] following a different line of argument: he attributed the residual exospheric temperature of about 500°K at zero level of solar activity to an upward energy flux and estimated from Jacchia's temperature profiles that a rate of heat input above 100 km of 0.1 mW/m<sup>2</sup> would be necessary to maintain a 500°K exospheric temperature.

The amount by which the flux of (1,1) mode energy entering the lower thermosphere is depleted in July compared with other times of the year is seen from Fig. 7 to be about 0.03 mW/m<sup>2</sup> on applying the factor of 4 reduction to allow for dissipation at lower heights. By examining the requirements of a lower thermosphere heat source capable of generating the observed semi-annual variation of air density at 400 km altitude, Volland [14] obtained an upward energy flux of 0.03 mW/m<sup>2</sup>. On this basis the July minimum of energy flux obtained in the present calculations would appear to be relevant to the interpretation of the July minimum of thermospheric air densities.

In comparison with the (1,1) mode, the (1,3) mode is unlikely to contribute significantly to thermospheric heating on account of greater dissipation at lower heights. It is estimated on the basis of the shorter wavelength of this mode that dissipation below 80 km would reduce  $\bar{E}_3$  at 80 km to 25% of the values shown in Fig. 8; and the flux would be further dissipated before reaching the lower thermosphere.

## 7. DISCUSSION

In the present paper an attempt has been made to estimate as realistically as possible the upward flux of energy of the diurnal tide above the region of ozone heating. A scale height profile for the basic atmosphere has been adopted (Fig. 4) which is typical of the low latitude atmosphere where positive (1,n) modes propagate most effectively, and attention has been given to refining the calculation of water vapour and ozone heating rates and their variation during the year. Compared with earlier estimates [1, 4], water vapour heating rates in the upper troposphere are considerably reduced (Fig. 2) and ozone heating rates below 40 km have been lowered to allow for the departure from radiative-

photochemical equilibrium indicated by observation (Fig. 3). The adopted variation of ozone heating during the year relates to changes in Sun-Earth distance and solar declination, whereas that of water vapour heating is additionally affected by meridional movements of water vapour into the summer hemisphere. In July these effects combine to produce the lowest heating rates in the (1,1) mode and the lowest upward energy fluxes (Figs. 2, 3 and 7); in January no distinct minimum is formed partly on account of the Sun being at its nearest to the Earth.

No account has been taken of atmospheric heating by surface energy exchange or by absorption of radiation by dust: in the first place their latitudinal distributions are not closely coupled with the (1,1) or (1,3) modes being influenced mainly by land and ocean areas and secondly their vertical distribution is confined mainly to heights near the surface where the tidal response weighting functions  $W_T$  for these modes are small (Fig. 4).

A particularly interesting aspect of the upward tidal energy flux is its contribution to heating of the thermosphere. Dissipation processes remove an appreciable part of the energy before the thermosphere is reached and estimates of upward energy fluxes at 105 km can only be given approximately without more detailed calculation of the loss. Wind systems in the stratosphere which may also affect propagation characteristics and energy fluxes have not been considered. Nevertheless results are obtained which support the value of 0.1 mW/m<sup>2</sup> previously given by Volland [13] to account for a residual exospheric temperature of 500°K at zero level of solar activity. It is also reasonable that the July minimum in the calculated energy flux is relevant to the well-known July minimum in thermospheric air densities. Results are given in this paper for globally averaged fluxes: the fluxes occur however predominantly at low latitudes, the equatorial values for the (1,1) mode being about 5.5 times greater.

## ACKNOWLEDGEMENTS

In the preparation of this paper the author has been ably assisted by Miss A. M. Yeung who undertook the data analysis and computer programming for the results on water vapour heating. The assistance of Miss U. Campbell and members of the Departmental Photographic Group with production of illustrations is gratefully acknowledged. The work has been supported by the Office of Aerospace Research and Development under Grant No. AFOSR-72-2264.

## REFERENCES

1. R. S. Lindzen, *Quart. J. Roy. Meteorol. Soc.*, **93**, 18-42 (1967).
2. R. S. Lindzen and D. Blake, *Geophys. Fluid Dyn.*, **2**, 31-61 (1971).
3. M. V. Wilkes, *Oscillations of the Earth's atmosphere*, Cambridge University Press 1949.
4. M. Siebert, 'Atmospheric tides', *Adv. Geophys.*, **7**, 105-182 (1961).
5. R. E. Newell, J. W. Kidson, D. G. Vincent and G. J. Boer, *The general circulation of the tropical atmosphere*, Vol. 1, MIT Press 1972.
6. H. J. Mastenbrook, *J. Atmos. Sci.*, **28**, 1495-1501 (1971).
7. C. Leovy, *J. Atmos. Sci.*, **21**, 238-248 (1964).
8. J. H. Park and J. London, *J. Atmos. Sci.*, **31**, 1898-1916 (1974).
9. H. U. Dütsch, *Adv. Geophys.*, **15**, 219-322 (1971).
10. S. T. Butler and K. A. Small, *Proc. R. Soc. Lond.*, **A274**, 91-121 (1963).
11. G. V. Groves, *JBIS*, **28**, 797-809 (1975).
12. G. V. Groves, *Proc. R. Soc. Lond.*, (in press).
13. H. Volland, *Planet. Space Sci.*, **17**, 1581-1597 (1969).
14. H. Volland, *Planet. Space Sci.*, **17**, 1709-1724 (1969).



## CALCULATED AND OBSERVED 24-HOURLY OSCILLATIONS OF THE UPPER ATMOSPHERE AT 5.9°S LATITUDE

G. V. GROVES

*Department of Physics and Astronomy, University College London, Gower Street, London WC1E 6BT.*

---

A comparison is undertaken between observed upper atmosphere tidal oscillations at 5.9°S and results calculated by classical tidal theory. The two sets of results are generally in good agreement. Attention is drawn to certain small significant differences, in particular to an average phase difference of 3.6 (s.d. 0.8) hours between the observed and calculated oscillations. The difference is associated with the (1,1) tidal mode and observed amplitudes maximize later than the calculated ones.

---

### 1. INTRODUCTION

COMPARISONS BETWEEN THEORETICAL and observed upper atmosphere tidal winds have previously been undertaken, notably by Lindzen for 30°N latitude [1] and by Reed *et al* [2] for 30°N and other latitudes. Agreement has been very satisfactory, particularly at high latitude, while small differences at low latitude would appear to call for only relatively minor adjustments to the adopted thermal excitations.

Oscillations of temperature and horizontal wind components between 35 and 95 km have recently been derived from an analysis of 24 grenade experiments conducted by the Goddard Space Flight Center at Natal (5.9°S, 35.2°W) over the years 1966-68 [3]. These results are of particular interest for comparison with theory, being at low latitude and including the oscillation of temperature as well as that of wind. Also they extend the height to which comparisons can be made from 60 to nearly 95 km. The purpose of the present paper is to undertake such comparisons using classical tidal theory and previously formulated thermal excitations [1].

### 2. MODES OF TIDAL OSCILLATION CALCULATED FOR 5.9°S LATITUDE

In Ref. 1 24-hourly components of thermal excitation are formulated for the troposphere using a previous model of Siebert for insolation heating by water vapour absorption. For the stratosphere, the excitation is formulated on the basis of a numerical model of Leovy for ozone heating. The continuous lines in Fig. 1 show the height dependence in these two regions of heating on an arbitrary scale in terms of the rate of heating per unit mass of air. (The broken lines will be referred to in section 5.) The same height dependence is taken to apply to all modes.

Numerical coefficients that are associated with the (1,1), (1,3) and (1,5) modes in Ref. 1 are 0.062, -0.016 and 0.008°K for tropospheric heating and 0.5447, -0.1411 and 0.0723°K for stratospheric heating. These are the three main equatorially symmetric modes, the notation used for mode description being that of Ref. 4. Although the stratospheric coefficients are about 10 times greater than the tropospheric ones, a factor equal to atmospheric density enters into the cal-



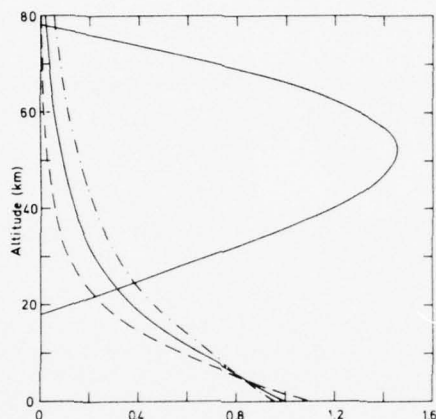


Fig. 1. Height dependence of tropospheric and stratospheric thermal excitations of the 24-hourly tide (on an arbitrary scale). Key: — values taken from Ref. 1; --- variation as  $(\text{pressure})^{1/2}$ ; - · - variation as  $(\text{pressure})^{1/4}$ . The scale of the broken lines has been evaluated by the theory in Ref. 12.

culution, so that heating rates per unit volume in the troposphere are the greater. The time of maximum heating rate is taken to be 1200 LT for both sources. (A negative value for a numerical coefficient such as that of the (1,3) mode above represents a maximum at 2400 LT.) Units of  $^{\circ}\text{K}$  are shown because on multiplication by the height functions (Fig. 1) and the appropriate latitude functions (Hough functions) both of which are of order unity or less, the amplitude of the diabatic temperature change due to radiational heating is obtained. Actual temperature changes will differ in amplitude and phase on account of adiabatic and other processes. Propagating modes, such as the (1,1), (1,3) or (1,5) are responsible for a general increase of temperature oscillation with height; so that at 80 km, for example, an amplitude of the order of  $20^{\circ}\text{K}$  is predicted without any heat input at this level.

Trapped modes are represented in the formulation of the thermal excitations in Ref. 1 by the (1,-2) and (1,-4) symmetrical modes. (A seasonal contribution is represented by the (1,-1) asymmetrical mode but this will not be introduced here.) For trapped modes, there is no progressive increase of amplitude with height: tropospheric heating generates a mainly tropospheric oscillation and in the upper atmosphere the oscillation is generated mainly by stratospheric heating. On account of their different forms of latitudinal dependence (Hough functions), propagating modes are dominant at low latitudes and trapped modes at high latitudes.

Whereas in Ref. 1 tidal components were calculated over a range of latitudes for an isothermal atmosphere, the calculations presented here are for  $5.9^{\circ}\text{S}$  latitude and a temperature profile (Fig. 2) based on the following data appropriate to this latitude: 0-32 km — balloon data [5, 6, 7]; 34-86 km — grenade data [7, 8, 9]; above 86 km — CIRA 1972 [10].

Fig. 3 shows the amplitudes of the individual modes calculated at  $5.9^{\circ}$  latitude for temperature, WE and SN wind oscillations. It is seen that the  $(1,1)_L$  mode arising from tropospheric heating (subscript L for lower) and the  $(1,1)_U$  mode arising from stratospheric heating (subscript U for upper) provide the two largest contributions. The  $(1,3)_L$  mode gives the next largest contribution which almost approaches that of the  $(1,1)_U$  in the SN (i.e. from south to north) wind component. The  $(1,5)_L$  is generally the next largest contributor, its temperature amplitude being almost equal to that of  $(1,3)_L$ , whereas its WE (i.e. from west to east) wind amplitude is smaller than  $(1,3)_L$  and only exceeds  $(1,-2)_U$  above 90 km.

### Calculated and Observed 24-Hourly Oscillations of the Upper Atmosphere

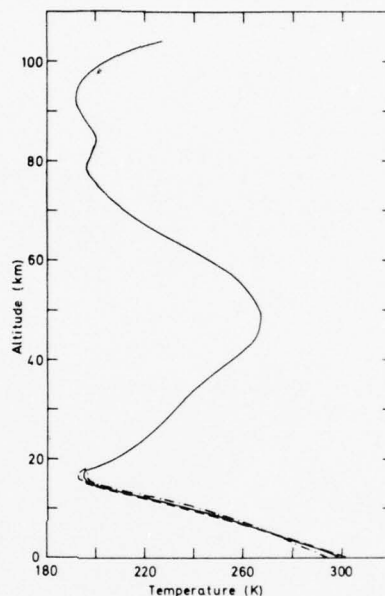


Fig. 2. Basic temperature profiles used in tidal calculations. Key: — mean; - - - maximum lapse rate; - · - minimum lapse rate.

The contributions from many of the trapped modes are too small to plot in Fig. 3.  $(1,-2)_L$  and  $(1,-4)_L$  are extremely small at stratospheric heights being less than  $0.016^\circ\text{K}$ ,  $0.06\text{ m/s}$  and  $0.002^\circ\text{K}$ ,  $0.004\text{ m/s}$  respectively above  $35\text{ km}$ . Even the contributions of  $(1,-2)_U$  and  $(1,-4)_U$  are small at stratospheric heights: those of  $(1,-4)_U$  are less than  $0.065^\circ\text{K}$  and  $0.14\text{ m/s}$ , and  $(1,-2)_U$  produces only  $2\text{ m/s}$  in the WE wind and  $1^\circ\text{K}$  in temperature.

The only propagating mode of importance to arise from stratospheric heating is  $(1,1)_U$ . The  $(1,3)_U$  mode is just recordable in Fig. 3 for the SN wind.

To summarise, it is seen from these calculations that the  $(1,1)$  mode dominates the upper atmosphere tidal oscillation at  $5.9^\circ$  latitude and is the only mode for which both tropospheric and stratospheric heating effects are comparable. The next largest contribution is  $(1,3)_L$  which for  $5.9^\circ$  latitude is much greater in the SN wind than in the WE wind or temperature oscillations.

### 3. COMPARISON OF CALCULATED AND OBSERVED OSCILLATIONS

Summations of tidal modes calculated as described in section 2 are compared in Figs. 4 and 5 with the observed 24-hourly oscillations previously reported for Natal [3] in terms of amplitude and time of maximum. The observed values are shown by the continuous lines with bars which indicate previously estimated standard deviations. The calculated values are shown by the continuous lines without bars. (The broken lines will be discussed in section 4.)

Inspection of the differences between observed and calculated amplitudes at  $5\text{ km}$  height intervals in Fig. 4 shows that 27 such differences are less than the estimated  $1\sigma$  value and that the remaining 9 are less than  $2\sigma$ . On this basis, agreement is quite good. Also, for temperature and SN winds, differences are almost equally positive and negative showing no obvious systematic difference between observed and calculated values. This is not so for WE winds where calculated values are systematically less than those observed by  $3.5\text{ (s.d. } 1.2)\text{ m/s}$ .

G. V. Groves

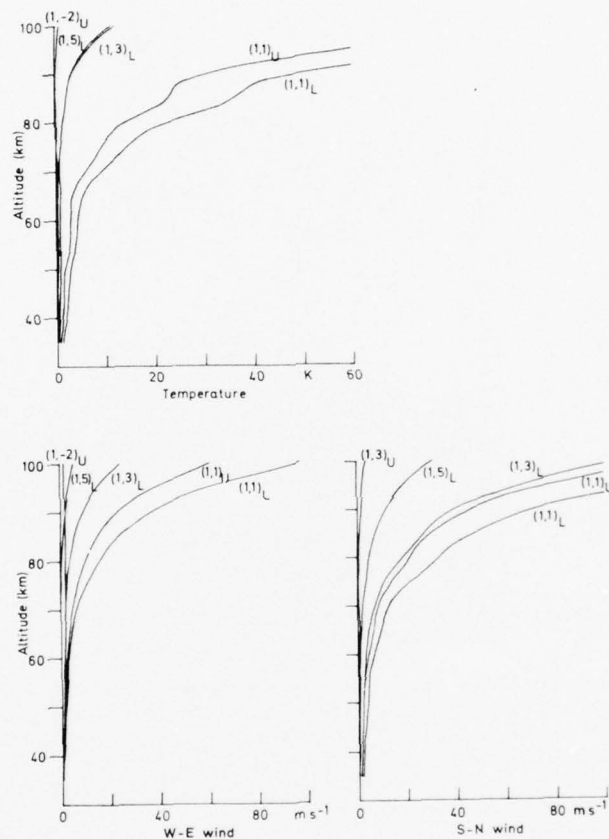


Fig. 3. Amplitudes of individual tidal modes calculated for  $5.9^\circ$  latitude. Suffix L denotes tropospheric excitation, suffix U denotes stratospheric excitation.

Observed and calculated phases are shown in Fig. 5 in terms of times of maximum amplitude. In this case 11 differences out of 36 exceed  $2\sigma$  and 14 lie between 1 and  $2\sigma$ . On average observed values maximize later than calculated ones. A systematic difference stands out clearly on the temperature plot and averages 2.8 (s.d. 1.0) hours. The difference is associated with the (1,1) mode, which for the temperature oscillation dominates other modes at all heights (Fig. 3). For the WE and SN wind plots, calculated contributions from higher order modes are more important than for temperature and tend to obscure the comparison. Crosses have therefore been added to Fig. 5 which represent the calculated contribution from the (1,1) mode alone. In the observed wind oscillation the (1,1) mode dominates over other modes only above 65 km, and at these heights the crosses are located systematically earlier than the observed values. The average difference between observed and calculated phases for the (1,1) mode is found to be 3.4 (s.d. 2.1) hours from the WE wind data and 5.2 (s.d. 1.1) hours from the SN wind data. From combined temperature and wind data, the average difference obtained is 3.6 (s.d. 0.8) hours.

Another notable feature in Fig. 5 is the rapid rate of change of phase of the SN wind oscillation which at many heights is much greater in the calculated curve

# Calculated and Observed 24-Hourly Oscillations of the Upper Atmosphere

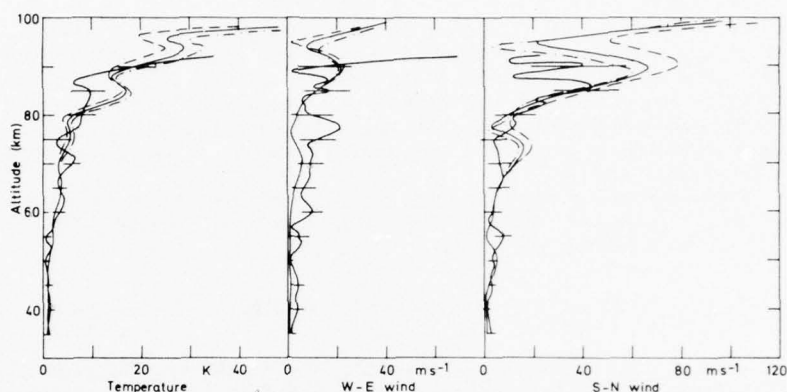


Fig. 4. Amplitudes of observed and calculated oscillations. Key: —|—|—| observed values with bars denoting estimated standard deviations [3]; other curves have been calculated using the basic temperature profiles shown in Fig. 2 (— mean; --- maximum lapse rate; - · - · - minimum lapse rate).

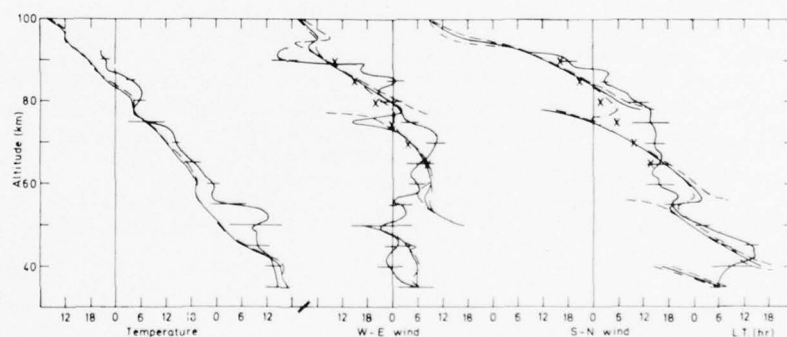


Fig. 5. Time of maximum amplitude for observed and calculated oscillations. For key to curves see Fig. 4. Crosses denote calculated values for the (1,1) mode.

than in the observations. This difference is attributed mainly to the (1,3) mode which appears to be overestimated by the calculation.

## 4. EFFECT OF BASIC TEMPERATURE PROFILE ON UPPER ATMOSPHERE TIDES

Changes in basic tropospheric temperature profile, particularly in the lapse rate, have previously been found to significantly influence computed 24-hourly tidal patterns above about 70 km [11]. The results are noteworthy in that small changes in the troposphere lead to appreciable modifications at the upper levels.

Minimum and maximum lapse rates for the Natal troposphere were therefore devised (Fig. 2) and the tidal calculations repeated. The results are given by the broken lines in Figs. 4 and 5. Only small variations occur in the lapse rate (the temperature decrease between 0 and 16 km ranging from 98 to 108°K), but computed amplitudes are noticeably affected above 70 km. Temperature and WE wind amplitudes decrease with higher lapse rate, but SN amplitudes increase due apparently to the larger (1,3) mode which responds to a change of lapse rate more



G. V. Groves

readily than the (1,1) mode and in the opposite sense.

In Fig. 4 the calculated changes in tidal amplitudes at the upper levels are seen to be within the range of variation indicated by the observational error bars. This is to be expected as variation of the basic temperature profile is just one of several sources of modulation of upper atmosphere tides. For Natal basic temperature variations are fortunately quite small (Fig. 2) otherwise it is unlikely that significant oscillations could have been resolved from observations extending over a period of 22 months.

The broken lines in Fig. 5 show that phases are only very slightly affected by changes of lapse rate. In particular the comparison between observed and calculated phases (section 3) still holds.

#### 5. EFFECT OF HEIGHT DEPENDENCE OF TROPOSPHERIC THERMAL DRIVE ON TIDES

In the above calculated results, the tropospheric thermal drive has the height dependence shown by the continuous line in Fig. 1 which is a plot of  $[p(z)/p(0)]^k$  where  $k = 1/3$  and  $p(z)$  is atmospheric pressure at height  $z$ . This particular value of  $k$  originates from a calculation by Siebert [12] in which the height dependence of specific humidity was  $[p(z)/p(0)]^\alpha$ ,  $\alpha$  being a constant chosen to fit water vapour data. Lower tropospheric observations put  $\alpha$  between 2 and 3 and Siebert chose 2.44 to give  $k = 1/3$ .

To examine the effect of possible uncertainties in  $k$ , the preceding calculations were repeated for  $k = 1/4$  and  $1/2$  (corresponding to  $\alpha = 2\frac{1}{6}$  and 3). The broken lines in Fig. 1 show the height dependences of the thermal excitations for these two cases. Corresponding amplitude changes in the calculated tides only appear above 70 km and are so similar to those shown by the broken lines in Figs. 4 and 5 that separate plots of the results will not be presented here. It is found that an increase in  $k$ , i.e. a more rapid decrease of heating with height, reduces temperature and WE wind amplitudes, but increases SN amplitudes in much the same way as an increase of lapse rate in the basic temperature profile (section 4).

Phases show no change of observational significance when  $k$  changes from  $1/4$  to  $1/2$ ; and the comparison between observed and calculated phases (section 3) still holds.

#### 6. DISCUSSION

A comparison has been undertaken between observed and calculated upper atmosphere oscillations at 5.9°S latitude. For the diurnal tide, earlier calculations [1] have already shown a strong latitudinal dependence in tidal patterns, particularly at low latitudes. For SN wind oscillations the dependence is so marked that a change of 1° latitude is likely to be observationally significant. It was therefore decided to calculate and examine the amplitudes of individual modes at the Natal latitude (Fig. 3). For temperature, the (1,1) mode predominates at 35 to 95 km as shown by calculation in Fig. 3 and by observation in Fig. 5 where there is a nearly uniform rate of change of phase with height. For wind oscillations the (1,1) mode appears to be dominant only above 65 km.

Observed and calculated results are compared in Figs. 4 and 5 and are generally in good agreement. Three features have been pointed out for which the differences, although small, appear to be significant:

1. Amplitudes of the calculated WE oscillation are systematically lower than those observed by 3.5 (s.d. 1.2) m/s.
2. The calculated (1,1) mode reaches maximum amplitude earlier than temperature and wind observations indicate by 3.6 (s.d. 0.8) hours.
3. The calculated (1,3) mode introduces a greater change of phase with height (into the SN wind oscillation) than is actually observed.

### Calculated and Observed 24-Hourly Oscillations of the Upper Atmosphere

To identify the origin of such differences is not easy. Classical tidal theory has limitations, arising from the assumptions on which it is based, and precise comparisons between observation and theory may be difficult to obtain. Such difficulties have previously been pointed out with respect to the effects of zonal background winds on the propagating characteristics of the atmosphere for the (1,1) mode [13]. The Natal observations were, however, distributed over a period of time (22 months) and do not therefore relate to any particular background wind structure. In fact, the successful resolution of significant tidal patterns indicates an absence of appreciable modulation (by background winds or otherwise); and the assumption of a medium at rest appears reasonable in this case.

The basic temperature structure has been taken into account using an annual mean profile as seasonal variations are not marked at the Natal latitude. Attention has been given in section 4 to the effects of possible changes in the tropospheric lapse rate to which the coupling between diurnal heating and upper atmospheric tidal response has been previously shown to be very sensitive [11]. Changes in the height profile of tropospheric heating have also been introduced (section 5) as these also affect the atmospheric tidal response. The effects of such changes have been mainly to amplitudes above 70 km and are not of observational significance within the limits considered.

The three differences listed above are put forward as matters that appear to warrant further investigation. Considerable importance is attached to the second of these as it relates directly to the phases of the (1,1) thermal excitations. Previously these have been taken to maximize at local noon in both the troposphere and stratosphere. A preliminary investigation in which alternative assumptions for the (1,1) thermal drives are considered has recently been completed and is reported elsewhere [14].

### ACKNOWLEDGEMENTS

The author gratefully acknowledges the assistance of Miss A. Harris with the data preparation and computations involved in obtaining the results of this paper. The work has been supported by the Office of Aerospace Research and Development under Grant No. AFOSR-72-2264 and by the U.K. Meteorological Office.

### REFERENCES

1. R. S. Lindzen, *Quart. J. R. Met. Soc.* **93**, 18 (1967).
2. R. J. Reed, M. J. Oard and M. Sieminski, *Mon. Weath. Rev.* **97**, 456 (1969).
3. G. V. Groves, *JBIS* **27**, 499 (1974).
4. S. Chapman and R. S. Lindzen, *Atmospheric Tides*, D. Reidel Publ. Co., Dordrecht (1970).
5. Exametnet Data Report Series, NASA SP-175, Washington D.C. (1968).
6. Exametnet Data Report Series, NASA SP-231, Washington D.C. (1970).
7. W. S. Smith, J. S. Theon, P. C. Swartz, J. F. Casey and J. J. Horvath, NASA TR R-316, Washington D.C. (1969).
8. W. S. Smith, J. S. Theon, P. C. Swartz, L. B. Katchen and J. J. Horvath, NASA TR R-288, Washington D.C. (1968).
9. W. S. Smith, J. S. Theon, J. F. Casey and J. J. Horvath, NASA TR R-340, Washington D.C. (1970).
10. COSPAR Working Group 4, *COSPAR International Reference Atmosphere 1972*, Akademie-Verlag, Berlin (1972).
11. R. S. Lindzen, *Proc. Roy. Soc.* **A303**, 299 (1968).
12. M. Siebert, in: *Advances in Geophysics* **7**, p. 105, Academic Press, New York (1961).
13. R. S. Lindzen, *J. Atmos. Sci.* **29**, 1452 (1972).
14. G. V. Groves, Propagating modes of the 24-hourly atmospheric tide derived from Natal (5.9°S) grenade experiments and global barometric oscillations, *Space Research* **15**, (1975) in press.

(Presented at the Symposium of the British Interplanetary Society on "Sounding Rockets and Experimental Results" held at University College London, 25 September 1974.)

Reprint from:

COSPAR

# SPACE RESEARCH XV

Proceedings of Open Meetings of Working Groups  
on Physical Sciences  
of the Seventeenth Plenary Meeting of COSPAR

São Paulo, S. P., Brazil — June 1974

Organized by

THE COMMITTEE ON SPACE RESEARCH — COSPAR

and

THE "INSTITUTO DE PESQUISAS ESPACIAIS — INPE"  
OF BRAZIL

Edited by

M. J. RYCROFT



AKADEMIE-VERLAG · BERLIN

1975

# **PROPAGATING MODES OF THE 24-HOURLY ATMOSPHERIC TIDE DERIVED FROM NATAL (5.9° S) GRENADE EXPERIMENTS AND GLOBAL BAROMETRIC OSCILLATIONS**

G. V. GROVES

Department of Physics and Astronomy, University College London, London, UK

Calculations based on tidal theory show that the main contributions from equatorially symmetric modes to 24-hourly oscillations of upper atmosphere winds and temperatures at 5.9° S latitude arise from tropospheric and stratospheric thermal excitation of the (1, 1) mode. An average phase difference of about three hours between oscillations observed at Natal and the calculated results is investigated using a recent result for the (1, 1) mode of annual mean surface pressure. It is found that a significant revision of the amplitudes and phases of the thermal excitation is required if observations are to be consistent with classical tidal theory. On limiting the revision to the lower atmosphere (below 20 km), heating rates for the (1, 1) mode are derived which maximize earlier near the surface and later in the upper troposphere instead of at 1200 LT at all heights as previously assumed. Corresponding amplitudes are increased in the lower troposphere and decreased in the upper troposphere compared with previous values.

## **1. Introduction**

Amplitudes and phases of 24-hourly oscillations of temperature and horizontal wind components between 35 and 95 km altitude have recently been derived from an analysis of 24 grenade experiments conducted by the Goddard Space Flight Center at Natal over the years 1966–1968 [1]. The present paper describes a continuation of the analysis of these results in which comparisons are made between observed oscillations and those calculated by tidal theory for particular thermal drives.

Attention is given particularly to the (1, 1) mode of oscillation which is the first of a series of solutions of Laplace's tidal equation corresponding to positive equivalent depths (eigenvalues).

## **2. Observed Oscillations in the Upper Atmosphere**

Diurnal motions between 30 and 60 km altitude have previously been resolved using data from large numbers of Meteorological Rocket Network (MRN) firings. The results of several authors were reviewed in CIRA 1972 [2] and will not be discussed here, except to recall that significant values have been obtained at 30° N